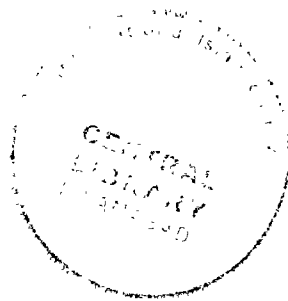


*A dissertation submitted to the
Department of Computer Science
International Islamic University, Islamabad
as a partial fulfillment of the requirements
for the award of the degree of
Doctor of Philosophy in Computer Science.*



TH-27346 $\frac{1}{2}$

PhD
006.32
FAB

Neural networks (computer science)
Artificial intelligence
Neural networks (Neurology)

INTERNATIONAL ISLAMIC UNIVERSITY ISLAMABAD
FACULTY OF COMPUTING AND INFORMATION TECHNOLOGY
DEPARTMENT OF COMPUTER SCIENCE

Date: 19-02-2024

Final Approval

It is certified that we have read this thesis, entitled "Brain Tumor Segmentation and Grading Using Handcrafted Features and Convolutional Neural Network" submitted by **Faizan Ullah** **Registration No. 157-FBAS/PIIDCS/F16**. It is our judgment that this thesis is of sufficient standard to warrant its acceptance by the International Islamic University Islamabad for the award of the degree of PhD in Computer Science.

Committee

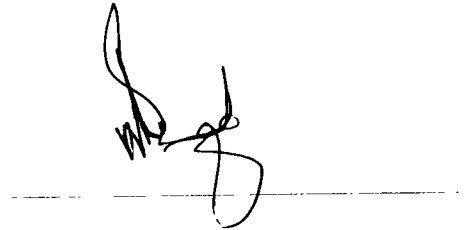
External Examiner:

Dr. Ayaz Hussain,
Professor
Quaid-i-Azam University, Islamabad



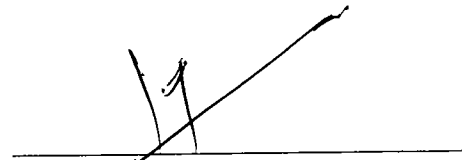
External Examiner:

Dr. Wassem Shahzad,
Professor
FAST University, Islamabad



Internal Examiner:

Dr. Syed Muhammad Saqlain,
Assistant Professor,
Department of Computer Science,
FCIT, IIUI



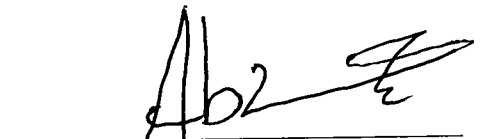
Supervisor:

Dr. Muhammad Nadeem,
Assistant Professor,
Department of Computer Science,
FCIT, IIUI



Co-Supervisor:

Dr. Mohammad Abrar,
Assistant Professor
Bacha Khan University Charsadda

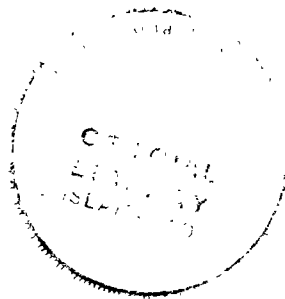


Declaration

I, Faizan Ullah, hereby declare that my Ph.D. thesis titled “*Brain Tumor Segmentation and Grading Using Handcrafted Features and Convolutional Neural Network*” is my work, neither as a whole nor as a part thereof has been copied out from any source except where due reference is made in the text. It is further declared that I have not previously submitted the work presented in the thesis report for partial or full credit for the award of degree at this or any other university.

Faizan Ullah

157-FBAS/PHDCS/F16



Acknowledgments

I am profoundly grateful and humbled as I express my heartfelt appreciation to Allah for His blessings and guidance as a Ph.D. scholar in Computer Science at IIU, Islamabad. It is with immense gratitude that I acknowledge the successful completion of my Ph.D. degree, a milestone that would not have been possible without the support and contributions of numerous individuals.

First, I would like to sincerely thank my esteemed supervisor, Dr. Muhammad Nadeem, Assistant Professor, for his unwavering guidance, invaluable insights, and constant encouragement. His expertise and dedication have played a pivotal role in shaping my research and academic growth. I am equally grateful to my Co-Supervisor, Dr. Mohammad Abrar, for his valuable input and mentorship throughout my Ph.D.

I am indebted to my parents, whose prayers and unwavering support have constantly motivated and inspired me. Their love, belief, and encouragement have been instrumental in shaping my entire academic and professional career.

Furthermore, I would like to express my deep appreciation to all my respected teachers, particularly Prof. Dr. Muhammad Asmat Ullah Khan, Dean Faculty of Computing & Information Technology, Dr. Asim Munir, and Dr. Qaiser Javid, for their guidance, expertise, and valuable feedback. Their dedication to teaching and research has been a constant source of inspiration.

During my Ph.D. journey, I enjoyed the company and guidance of Dr. Abdusalam, Assistant Professor, AWKUM, Mr. Dilawar Shah and Engr. Shujaat Ali, Assistant Professors at BKUC. Their support, mentorship, and intellectual discussions have immensely benefited my research endeavors.

Not to mention the friendship and camaraderie I shared with Mr. Sabir Shah, my brother-like friend and colleague, who has been a constant source of support and motivation throughout my BS, MS, and Ph.D. I cherish the memories we created and the countless hours we spent together, pushing each other to excel.

I also want to extend my heartfelt appreciation to Mr. Masoom Shah, ex-Lecturer at BKUC, for his sincere assistance and guidance during my Ph.D. journey. His support has been instrumental in my research progress.

Finally, I am grateful for the kind support and friendship of all my friends and colleagues at BKUC. Their encouragement, discussions, and collaboration have enriched my academic and personal life.

Although the list of individuals who have contributed to my success is extensive, I would like to express my deepest gratitude to every one of them at the Department of Computer Science at Bacha Khan University, Charsadda. My heartfelt appreciation goes to the Head of Department, Dr. Izaz Ahmad Khan, for his support and encouragement throughout my Ph.D. tenure.

To everyone who has played a part, big or small, in my academic journey, I extend my sincerest thanks. Your support, guidance, and belief in me have been invaluable, and I am forever grateful.

Faizan Ullah

157-FBAS/PHDCS/F16

Dedication

To My:

Parents, wife

Kids: Affan, Hashim,

Brothers & Sisters,

Teachers,

and

Friends

Abstract

Brain tumors are neoplastic formations in the brain that can be classified as either benign or malignant. Their existence can result in diverse neurological symptoms and present substantial health hazards. Prompt and precise identification of brain tumors is essential for timely medical intervention, appropriate treatment strategizing, and enhanced patient outcomes. This study aims to create an improved method for segmenting and grading brain tumors by integrating manually designed features with Convolutional Neural Network (CNN) technology. Brain tumor segmentation entails identifying and demarcating tumor areas in medical imaging, while tumor grading seeks to evaluate the malignancy and seriousness of the tumor. Brain tumors pose a significant global health issue, affecting both individuals and society at large. The American Brain Tumor Association (ABTA) reported in 2021 that approximately 12,000 young adults and 3,400 children received a diagnosis of a primary brain tumor.

The prevalence of brain tumors underscores the immediate requirement for reliable and practical techniques for their identification and characterization. Multiple methodologies have been investigated for the segmentation and grading of brain tumors. Expert manual segmentation is a laborious process susceptible to variations between different observers and may fail to accurately identify subtle tumor boundaries. Conversely, computer algorithms can achieve greater efficiency in automatic segmentation. However, they encounter difficulties in accurately discerning tumor boundaries and distinguishing them from normal brain tissue.

To overcome the constraints of both manual and automatic techniques, this study suggests a sequential strategy that integrates manually designed characteristics with Convolutional Neural Networks (CNNs). The architecture of the Global Convolutional Neural Network (GCNN) consists of two parallel Convolutional Neural Networks (CNNs): the Confidence Surface Pathways CNN (CSPCNN) and the MRI Pathways CNN (MRIPCNN). The CSPCNN is equipped with two pathways, namely the CS Local Pathway and the CS Global Pathway, responsible for extracting local and global features, respectively. The CSPCNN receives manually created features, while the MRIPCNN takes in MRI data from the Benchmark BraTS dataset. The CNNs undergo fine-tuning and training to maximize the performance of segmentation.

The outcomes of the experiments validate the efficiency of the suggested Graph Convolutional Neural Network (GCNN) methodology. This approach records substantial Dice scores, with a score of 0.87 for segmenting the entire tumor, 0.79 for the tumor core, and 0.75 for segments of the tumor that are actively proliferating. The results demonstrate a substantial enhancement in precisely detecting tumor regions when compared to conventional segmentation techniques. The research focuses on tumor grading using a lightweight XGBoost classifier that combines intensity-based, texture-based, and shape-based features extracted from preprocessed MRI data. The classifier's utilization of an ensemble mechanism significantly improves the accuracy of tumor grading. The grading algorithm demonstrated promising outcomes, exhibiting the highest levels of accuracy for grade IV tumors (93.0%), followed by grade II tumors (92.0%) and grade III tumors (90.0%). The precision values exhibited a consistently high accuracy across all tumor grades, ranging from 0.92 to 0.94.

This research thesis introduces an innovative method for segmenting and grading brain tumors by combining manually designed features and Convolutional Neural Networks (CNN). The proposed method showcases its capacity to greatly enhance the precision and effectiveness of brain tumor segmentation and grading, potentially revolutionizing clinical decision-making and patient care. The proposed system utilizes artificial intelligence-based solutions to advance the field of medical imaging and improve brain tumor analysis.

Keywords: *Brain tumor, Health Risks, Handcrafted features, Segmentation, Global-pathway CNN, Local-pathway CNN, Tumor Grading*

List of Acronyms

ABTA	American Brain Tumor Association
ANN	Artificial Neural Network
ASPP	Atrous spatial pyramid pooling
BET	Brain Extraction Tool
BraTS	Brain Tumor Segmentation
CRF	Conditional Random Field
CS	Confidence Surface
CSF	Cerebro Spinal Fluid
CT	Computed Tomography
DSC	Dice Similarity Coefficient
DWI	Diffusion-Weighted Imaging
ED	Edema
ELBP	Extended Local Binary Pattern
FDG	Fluoro Deoxy Glucose
FHNN	Fuzzy Hopfield Neural Network Algorithm
FLAIR	Fluid-Attenuated Inversion Recovery
fMRI	Functional MRI
GA-SVM	a hybrid of genetic algorithm and support vector machine
GBM	Glioblastoma Multiforme
GCN	Graph Convolutional Network
GCNN	Global CNN
GLCM	Gray-Level Co-occurrence Matrix
HGG	High Graded Gliomas
HH	High-High diagonal
HL	High-Low vertical
IoU	Intersection over Union
KNN	K-nearest Neighbor
LBP	Local Binary Patterns
LGG	Low Graded Gliomas
LH	Low-High horizontal
LL	Low-Low approximation
LSFT	Least-squares feature transformation
LVQ	Learning Vector Quantization
ML	Machine Learning
MLP	Multilayer Perceptron
MM-XGB	Multimodal Gradient Boosting
MRI	Magnetic Resonance Imaging

MRS	Magnetic Resonance Spectroscopy
NCC	Normalized Cross-Correlation Flying Ad-hoc Sensor Network
NCR	Necrosis
NET	Non-Enhancing Tumor
PET	Positron Emission Tomography
PNN-RBF	Probabilistic Neural Network-radial Basis Function
RF	Random Forest
RNN	recurrent neural networks
ROC	Receiver Operating Characteristic
ROI	Regions of Interest
SC-ICA	Spectral Clustering Independent Component Analysis
SMO	Sequential Minimal Optimization
SRC	Sparse Representation Classification
SVM	Support Vector Machine
ULDA	Unsupervised Linear Discriminant Analysis
WT	Wavelet Transform
WHO	World Health Organization

Table of Contents

Final Approval.....	i
Declaration.....	ii
Acknowledgments	iii
Dedication	v
Abstract.....	vi
List of Acronyms	viii
List of Tables	xiii
List of Figures.....	xv
Research Contribution.....	xvi
Chapter 1	1
Introduction.....	1
1.1 Brain Tumor Diagnosis	2
1.2 Image Segmentation.....	2
1.3 Brain Imaging Modalities.....	3
1.4 Techniques for Image Segmentation.....	5
1.4.1 Thresholding-based Methods	6
1.4.2 Region-based Methods	6
1.4.3 Active Contour Models	6
1.4.4 Graph-cut-based Methods	6
1.5 Grading of Tumor	7
1.5.1 Grade-I	7
1.5.2 Grade-II	8
1.5.3 Grade-III.....	9
1.5.4 Grade-IV	10
1.6 Challenges and Requirements	12
1.6.1 Non availability of Labeled Data	13
1.6.2 Variability and Heterogeneity of Brain Tumors.....	13
1.6.3 Inter- and Intra-Observer Variability	13
1.6.4 Computational Complexity and Resource Requirements.....	13
1.6.5 Integration with Clinical Workflow	14
1.6.6 Generalization and Transferability	14
1.6.7 Ethical and Regulatory Considerations	14
1.7 Problem Statement and Research Questions	14
1.7.1 Research Questions	16
1.8 Aims and Objectives	16
1.9 Scope of the Study	16

1.10 Research Contribution.....	17
1.11 Structure of the Thesis	18
Chapter 2	21
Literature Review.....	21
2.1 Techniques for Brain Tumor Segmentation.....	23
2.1.1 Conventional Approaches	23
2.1.2 ML based Approaches.....	24
2.1.3 DL based Approaches	27
2.2 Brain Tumor Grading Methods	33
2.2.1 Histopathological Grading	33
2.2.2 Radiological Grading	33
2.2.3 Machine Learning-based Grading Models	36
Chapter 3	43
Research Methodology.....	43
3.1 Data Acquisition and Preprocessing	43
3.1.1 Data Acquisition.....	43
3.1.2 Preprocessing	44
3.2 Handcrafted Features Extraction.....	48
3.2.1 Intensity-based Features	48
3.2.2 Shape-based Features	49
3.2.3 Texture-based Features	50
3.3 Convolutional Neural Network Architecture	51
3.4 Training and Evaluation of the Network.....	53
3.5 Performance Evaluation Metrics	54
3.5.1 Segmentation Evaluation Metrics	54
3.5.2 Grading Evaluation Metrics	55
Chapter 4	56
Brain Tumor Segmentation in MRI with Handcrafted Features	56
4.1 Methodology	57
4.1.1 Hand Crafted Feature Extraction.....	57
4.1.2 Feature Labeling.....	62
4.1.3 Confidence Surface Generation	63
4.1.4 Dataset.....	63
4.1.5 Data Augmentation	64
4.1.6 CNN Architecture	64
4.2 Experiments.....	66
4.3 Chapter Summary.....	71
Chapter 5	72

Multimodal Lightweight Approach for Brain Tumor Grade Prediction.....	72
5.1 Introduction	72
5.2 Methodology	74
5.2.1 Preprocessing	76
5.2.2 Feature Extraction and Selection.....	77
5.2.3 Multimodal Lightweight XGBoost	81
5.2.4 Lightweight Ensemble.....	82
5.3 Results and Discussion.....	83
5.4 Chapter Summary.....	88
Chapter 6	89
Brain Tumor Segmentation Using Federated Learning	89
6.1 Methodology	89
6.1.1 Dataset.....	90
6.1.2 Preprocessing	90
6.1.3 Federated Learning Model's Structure	90
6.1.4 Proposed Model Architecture.....	92
6.1.5 Model Aggregation	94
6.2. Experiments and Results	96
6.2.1 Model Training and Validation	96
6.2.2 Hyperparameter Tuning	97
6.2.3 Comparison with Traditional and Deep Learning Methods	97
6.2.4 The Dice Coefficient, Specificity, and Sensitivity	99
6.2.5 The Influence of Federated Learning on Data Privacy and Security	100
6.2.6 Scalability of the Approach.....	101
Chapter 7	104
Conclusion and Future Work	104
7.1 Conclusion.....	104
7.2 Future Work	105
References	107

List of Tables

Table 1.1: Tumor Grade Comparison Using Differentiation	11
Table 1.2: Tumor Categories and their Properties	12
Table 2.1: Comparative Analysis of Feature Extraction Techniques	25
Table 2.2: Comparison of Machine Learning-based Approaches	27
Table 2.3: Comparison of CNN based Methods for Brain Tumor Segmentation	30
Table 2.4: Comparison of Deep Learning-based Approaches for Brain Tumor	32
Table 2.5: Key Parameters for brain Tumor Grading	35
Table 2.6: An overview of the current machine learning techniques used for	39
Table 2.7: Comparison of Machine Learning-based Grading Models for Brain Tumors	41
Table 3.1: Comparison of Intensity Normalization Techniques	45
Table 3.2: Comparison of Skull Stripping Techniques	46
Table 3.3: Comparison of Image Resampling Methods	46
Table 3.4: Data Augmentation Techniques	47
Table 3.5: Example of Intensity-based Features	49
Table 3.6: Example of Shape-based Features	49
Table 3.7: Example of Texture-based Features	50
Table 3.8: CNN Architecture	51
Table 3.9: Popular CNN Architectures	52
Table 4.1: Architectural detail of CSPCNN Local Pathway	65
Table 4.2: Architectural detail of CSPCNN global Pathway	65
Table 4.3: Architectural detail of Global CNN	65
Table 4.4: Performance Evaluation of Brain Tumor Segmentation Using CNN and GCNN ..	69
Table 4.5: Performance evaluation of the proposed model vs state of the art.	71
Table 5.1: Tumor grades in the BraTS dataset distribution.	76
Table 5.2: Preprocessing procedures for MRI imaging	77
Table 5.3: Overview of Extracted Features	77
Table 5.4: Overview of the Ensemble hyperparameters	83
Table 5.5: Features extracted for various grades of brain tumors	85
Table 5.6: Extracted features' results for each tumor grade	85
Table 5.7: Classification results using MM-XGB for each tumor grade	86
Table 5.8: SVM Classification Results for Each Tumor Grade	87
Table 5.9: RF Classification results for each Tumor Grade	87
Table 6.1: Comparison of Datasets for Brain Tumor Imaging Analysis	90

Table 6.2: The FL architecture consists of server and client components.	91
Table 6.3: Modifications Implemented in the U-Net Framework.....	93
Table 6.4: Essential Variables and Tunable Parameters of the Constructed Model	94
Table 6.5: Overview of the Hyperparameter Tuning Process.....	97
Table 6.6: Evaluating the performance of various learning models for the analysis.....	97
Table 6.7: Evaluation of Performance of Different Models	98
Table 6.8: Summary of the Influence of Client Quantity on Model Performance.....	102
Table 6.9: Effects of model compression and sparsification on communication.....	103

List of Figures

Figure 1.1: BraTS -2018 Single Patient Data	4
Figure 1.2: Chapter wise Structure and Workflow of Study.....	20
Figure 4.1: Feature Extraction process of LBP.....	58
Figure 4.2: DWT sub-band images are in shows the decomposition of brain MR images.....	61
Figure 4.3: Illustrates the feature labeling process	62
Figure 4.4: Illustrates the Confidence Surface generation process	63
Figure 4.5: Proposed CNN Architecture.....	64
Figure 4.6: Pixel Level Neighborhood with Kernel Sizes of 3,5,7, and 9	66
Figure 4.7: Pixel Level Example Labeling	67
Figure 4.8: T1-weighted MRI confidence surface	67
Figure 4.9: T1c-weighted MRI confidence surface	68
Figure 4.10: T2-weighted MRI confidence surface.....	68
Figure 4.11: FLAIR MRI confidence surface.....	69
Figure 4.12: predated MRI model.....	69
Figure 4.13: Training Loss of the Proposed Model	70
Figure 4.14: Training and Validation Loss over 100 Epochs	70
Figure 5.1: An efficient method for classifying brain tumors based on their severity.....	75
Figure 5.2: Various Modalities of a Brain Tumor in BraTS.....	75
Figure 5.3: MRI prior to preprocessing	84
Figure 5.4: MRI after Preprocessing.....	84
Figure 6.1: Server client structure of FL.....	91
Figure 6.2: U-net Architecture.....	92
Figure 6.3: Federated Averaging	95
Figure 6.4: Analyze and compare various neural network models.....	98
Figure 6.5: Model Performance Score.....	99

Research Contribution

The following Research Papers related to this thesis were published in journals during my Ph.D. research.

International Journal Publication:

1. **F. Ullah**, M. Nadeem, M. Abrar., " Evolutionary Model for Brain Cancer-Grading and Classification Technique," *IEEE ACCESS*, 11, pp. 126182 – 126194, 2023.
[IF: 1.833]
2. **F. Ullah**, M. Nadeem, M Abrar., " Revolutionizing Brain Tumor Segmentation in MRI with Dynamic Fusion of Handcrafted Features and Global Pathway-based Deep Learning," *KSII Transactions on Internet and Information Systems*, 18(1), pp. 105-125, 2024.
[IF: 1.67]
3. **F. Ullah**, M. Nadeem, M Abrar *et al.* "Enhancing Brain Tumor Segmentation Accuracy through Scalable Federated Learning with Advanced Data Privacy and Security Measures," *Mathematics*, 11(19), pp. 1-27, 2023.
[IF: 2.4]
4. **F. Ullah**, M. Nadeem, M Abrar., " Brain Tumor Segmentation from MRI Images Using Handcrafted Convolutional Neural Network," *Diagnostic*, 13, pp. 1-15, 2023. [IF: 3.9]

CHAPTER 1

INTRODUCTION

Chapter 1

Introduction

The human brain represents one of the body's most intricate organs. Humans face a variety of ailments throughout their lives, including heart disease, stroke, diabetes, AIDS, and cancer. Sometimes, the conditions worsen, and as a result, many people die. As a result, medical researchers are working hard to combat these diseases promptly. Accurate diagnosis at the proper time is critical in preventing all diseases and conditions [1]. Brain tumors are continuously posing threats to humanity. Brain tumors are irregularly growing tissue that results from uncontrolled cell reproduction. It has no physiological function within the neuro system of the human body. Tumors produce swelling, increase their size, and exert pressure on the brain. It results in the appearance of some abnormal neurological symptoms in the patient. Frequent headaches and migraines could be some of the signs of malignancy. It could also result in eyesight loss [2]. Based on information from the American Brain Tumor Association (ABTA), the prevalence and statistical data regarding brain tumors are outlined as follows. This encompasses a detailed examination of incidence rates, survival statistics, and various classifications of brain tumors, offering insight into the current landscape of brain-related tumor diagnoses and research findings [3].

- Cancer ranks as the second leading cause of death among individuals younger than twenty years old, underscoring the significant health challenge it poses to the pediatric population. This statistic highlights the critical need for ongoing research, effective treatment strategies, and comprehensive support systems to combat cancer in children and improve their survival rates and quality of life.
- In men aged 20 to 39, cancer ranks as the second primary reason for death. Among women in the same age group, 20 to 39, cancer is identified as the sixth most common cause of death.
- Cancer holds the position as the second prevalent cause of death among men aged 20 to 39, demonstrating its significant impact on this age group. In contrast, for women in the same age range, cancer is identified as the sixth

leading cause of death, indicating variations in cancer's prevalence and lethality between genders within this demographic segment.

- In the year 2021, approximately 12,000 young adults were diagnosed with a primary brain tumor, highlighting a considerable incidence of this serious health condition within this age group.
- A study conducted from 2013 to 2017 revealed that brain tumors ranked as the third most common cause of death due to cancer in people over the age of 40, underscoring the significant impact of this condition on mortality rates within this age cohort.

Universally, the second major cause of death in humans is cancer. Cancer is one of the leading causes of death in low-income nations, accounting for over 70% of all deaths, as for 630,000 reported cases identified each year and 350,000 deaths; neck and head malignancies are the sixth most frequent malignancies globally. Brain tumors are a significant contributor to this deadly disease, with 4 to 5 persons per 100,000 each year. This number makes up around 2% of all cancer-related deaths. Every year, 1,50,000 new cancer cases are diagnosed in Pakistan, with 60–80 percent death [4].

1.1 Brain Tumor Diagnosis

Medical practitioners employ a range of procedures to diagnose brain cancers, including X-ray, Positron Emission Tomography (PET), Computed Tomography (CT), and Magnetic Resonance Imaging (MRI) are four advanced imaging technologies widely used in medical diagnostics) [5].

1.2 Image Segmentation

Image segmentation entails partitioning a digital image into separate segments or clusters of pixels, known as image objects. This method simplifies the image's complexity by breaking it down into manageable parts, enabling targeted analysis and interpretation in various image processing and computer vision tasks. This process can reduce the image's dimensionality and facilitate in deeper analysis [6]. Semantic based image segmentation is defined in the literature as a process for predicting a class label in the input image at each pixel [7]. This procedure seeks to describe specific objects or object boundaries inside an image. Image segmentation is crucial in the analysis of

medical images, complementing classification and abnormality detection efforts, and assists physicians in diagnosing diseases [8].

1.3 Brain Imaging Modalities

Brain imaging methods are vital in analyzing brain structure and detecting brain cancers. These techniques provide valuable insights into the brain's structural and functioning characteristics. The commonly utilized brain imaging techniques and their uses in assessing brain structure are listed below.

CT imaging, a widely utilized diagnostic technique, offers critical understanding of the structure and composition of different human tissues, especially the brain. By employing X-rays, CT imaging generates intricate cross-sectional views of the brain, which are instrumental in identifying and detailing brain cancers[9].

Another modality is called Position Emission Tomography (PET). PET imaging is a highly effective imaging technology in medical diagnostics and research. It gives useful information regarding tissues' functional and metabolic activity, such as the brain [10]. PET imaging is particularly useful in the analysis of brain tumors, as it offers insights into tumor metabolism, proliferation, and treatment response. PET imaging entails the injection of a radiotracer, which is a biologically active molecule marked with a positron-emitting radioactive isotope.

Magnetic Resonance Imaging (MRI) represents a non-invasive method pivotal for examining the brain's structure and detecting brain cancers [11]. It creates precise images of the brain using a mix of a powerful magnetic field, radio waves, and advanced computer algorithms. The patient is placed inside a sizable cylindrical magnet during an MRI scan, which generates a potent and consistent magnetic field. The body's hydrogen atoms, which are primarily present in water molecules, align themselves along this magnetic field's direction. These aligned hydrogen atoms collect energy from the radio waves and release it as they realign themselves. The MRI scanner notices this energy release, also known as the MR signal, and processes it to produce high-resolution images.

MRI can better help doctors when other imaging techniques cannot provide enough clues in complicated cases. An MRI scan creates a realistic representation by combining the characteristics of magnetism and radio waves [12]. MRI has become the principal imaging technology in radiology [13]. MRIs provide enough information to detect the tiniest anomalies. The advancements in computational technology are compelling stakeholders to utilize it in diagnostics for the early detection of diseases. This integration seeks to improve the precision and effectiveness of diagnostic processes, underscoring the importance of technological innovations in improving early intervention outcomes. The primary aim of computer-assisted brain tumor diagnosis is to gather essential clinical data regarding the tumor's presence, location, and classification [14].

MRI imaging plays a crucial role in the segmentation of brain tumors, with clinicians employing four distinct MRI weighted techniques to generate a three-dimensional image of the brain. These techniques include a) T1-weighted, b) T1-contrast weighted, c) T2-weighted, and d) FLAIR, as illustrated in Figure 1.1. Furthermore, brain tumors can be categorized into four subtypes [15], i.e., edema, necrosis, enhancing tumor, and non-enhancing tumor.

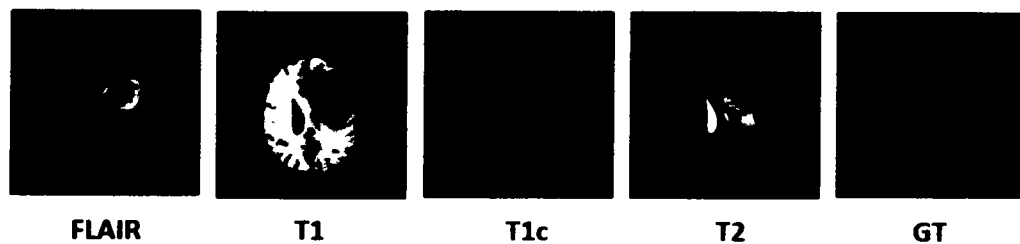


Figure 1.1: BraTS -2018 Single Patient Data

Tumors may manifest as regions of aberrant signal strength compared to the tissues around them, which aids in locating them. T2-weighted images can indicate edema surrounding tumors and are sensitive to changes in tissue water content, giving key details on the degree of tumor infiltration and the involvement of nearby tissues. Tumor visibility is improved in FLAIR images due to the CSF signal's effective attenuation, which contrasts with the surrounding CSF backdrop [16].

MRI is an effective imaging technique for analyzing brain structure and finding brain cancers. For doctors and researchers in the field of neuro-oncology, it is a useful tool due to its capacity to offer detailed anatomical and functional information.

To locate the tumor zone, brain tumor segmentation is completed first, then the healthy and unhealthy zones are determined. Following that, the sub-regions are segmented.

MRI extends beyond mere visualization of brain tumors, offering crucial insights into brain function as well. Functional MRI (fMRI) tracks variations in blood flow and oxygen levels triggered by certain tasks or stimuli, allowing for the detailed mapping of brain activity [17]. This technique is used to identify the areas of the brain involved in critical functions, such as language and motor skills, and helps in surgical planning to avoid damage to these areas during tumor resection.

Furthermore, sophisticated MRI methods like Diffusion-Weighted Imaging (DWI) and Perfusion Weighted Imaging (PWI) provide additional information on the traits of brain tumors. DWI focuses on evaluating the tissue microstructure and detecting cellular barriers through the assessment of water molecules' diffusion patterns. It assists in determining the cellularity of the tumor and identifying portions of solid tumor from those with necrosis or edema. The evaluation of tumor vascularity and angiogenesis is made possible by PWI's assessment of blood flow and vascular perfusion in the brain.

A thorough evaluation of brain tumors is possible because of the combination of different MRI sequences and cutting-edge procedures. It facilitates tumor identification, characterization, and monitoring, aids in treatment planning, and makes it possible to assess therapy effectiveness over time.

1.4 Techniques for Image Segmentation

Approaches to segmenting brain tumors are categorized into various groups based on different conceptual frameworks. The primary types include manual segmentation, traditional machine learning, and deep learning-based segmentation. The process of manually segmenting a brain tumor is costly, time-consuming, subjective, and error prone. As a result, the manual approach to detecting brain tumors is no longer effective. However, quantitative analysis of tumors gives meaningful clues for the treatment, planning, and understanding of tumor properties [18]. The segmentation of brain tumors holds paramount importance in achieving precise diagnoses, formulating effective treatment plans, and monitoring the progression of tumors. Various techniques

have been developed to automate this process and alleviate the subjectivity and time-consuming nature of manual segmentation.

1.4.1 Thresholding-based Methods

Thresholding is a straightforward but popular method for segmenting brain tumors. To distinguish tumor regions from the backdrop in medical imaging, a threshold value must be set. Brain tumors have been classified through intensity-based thresholding techniques, including global thresholding, adaptive thresholding, and Otsu's thresholding [19]. However, these methods may struggle with tumors with heterogeneous intensity distributions or unclear boundaries.

1.4.2 Region-based Methods

By dividing the image into homogenous sections based on similarity in intensity or other feature values, region-based segmentation algorithms seek to locate tumor regions [20]. The region-growing algorithm is a well-known method that builds regions recursively from seed points by including nearby pixels that satisfy specific requirements. The watershed transform is an additional technique that divides the image into catchment basins and treats intensity gradients as topographic relief.

1.4.3 Active Contour Models

Active contour models also referred to as snakes or level sets, are deformable curves or surfaces that can be incrementally modified to match the tumor's boundaries. In these models, the best contour for separating tumor regions from the surrounding tissues is determined using energy minimization methods. For segmenting brain tumors, active contour models with geodesic active contours and Chan-Vese models have been used. They can take into consideration fluctuations in intensity and handle unusual tumor shapes.[21].

1.4.4 Graph-cut-based Methods

The graph theory notion is used by graph-cut algorithms to separate an image into the foreground (tumor) and background regions [22]. A network represents the image, with nodes denoting pixels and edges denoting pairwise affiliations between adjacent pixels.

The graph-cut algorithm identifies the best cut that separates tumors from non-tumor regions while minimizing the energy function. Brain tumor segmentation using graph-cut techniques has proven successful, especially when spatial and intensity priors are used [23].

1.5 Grading of Tumor

As stated by WHO, Gliomas are an aggressive kind of brain related tumor and are categorized into four unique categories based on their aggressive histological features. Glioblastoma Multiforme (GBM), placed in grade IV, is the most severe and has the poorest survivability. Grade-II and grade-III are common types of LGG (Low Graded Gliomas), which are far less severe and infiltrative than grade-IV [2], [3]. Oligoastrocytoma, astrocytoma and oligodendroglioma are common types of LGG. Stages of gliomas, as well as tumor size, location, and shape, are crucial in determining survivability and treatments, which would include surgery, chemotherapeutic, radiation, or a combo of these [4]. As a result, adopting non-invasive strategies to automate tumor grading and segmentation for clinicians in diagnostic and adaptable diagnosis strategies to improve patient care might be advantageous.

1.5.1 Grade-I

Grade-I tumors, referred to as well-differentiated tumors, represent a category of tumors that closely resemble normal cells in their appearance and organization[24]. These tumors exhibit a high degree of cellular differentiation, meaning that the tumor cells retain many of the characteristics and functions of the normal cells from which they originated. In terms of growth rate, Grade-I tumors are generally slow-growing, exhibiting a less aggressive behavior compared to higher-grade tumors. This slower growth rate can be attributed to the tumor cells' relatively well-preserved regulation of cell division and proliferation [25]. The cells in Grade-I tumors are typically uniform in size and shape, demonstrating minimal cellular abnormalities. They exhibit a low mitotic activity, which refers to the rate at which cells divide. The lower mitotic activity reflects the tumor cells' ability to maintain a controlled and orderly pattern of cell division, resembling that of normal cells.

One characteristic that distinguishes Grade-I tumors is their retention of some of the normal tissue architecture and functionality. Despite being neoplastic, Grade-I tumors often maintain a level of organization like the tissue of origin. This preservation of tissue architecture contributes to the tumor cells' ability to conduct their normal functions.

The prognosis for Grade-I tumors is more favorable compared to higher-grade tumors. The slow growth rate and well-differentiated nature of Grade-I tumors often indicate a lower likelihood of aggressive behavior, such as invasion into surrounding tissues or metastasis to distant sites. Consequently, patients with Grade-I tumors tend to have better treatment outcomes and a higher probability of long-term survival.

It's crucial to recognize that the detailed criteria and grading systems for tumors can differ based on the type of tumor and the classification system employed. The information provided here serves as a general understanding of Grade-I tumors and their characteristics.

1.5.2 Grade-II

Grade-II tumors, also referred to as moderately-differentiated tumors, occupy an intermediate position between Grade-I (well-differentiated) and Grade-III (poorly-differentiated) tumors. These tumors display characteristics that demonstrate a moderate level of cellular abnormality [26].

In Grade-II tumors, the cells exhibit a higher degree of cellular atypia compared to Grade-I tumors. Cellular atypia refers to the abnormal appearance and structure of tumor cells, such as variations in cell size and shape. While Grade-II tumors show some loss of tissue organization, they still retain certain features reminiscent of the normal tissue from which they originated [27].

Grade-II cancers tend to develop at a quicker rate than Grade-I tumors. This enhanced growth rate indicates greater cellular activity and proliferation. It should be noted, however, that the development rate of Grade-II tumors is often slower than that of Grade-III tumors, which have a more aggressive and quick growth pattern.

Mitotic activity, or the rate at which cells divide, may be higher in Grade-II cancers than in Grade-I tumors. Mitotic activity is a key sign of cell proliferation and is frequently evaluated throughout the grading process. When compared to well-differentiated tumors, the presence of slightly greater mitotic activity in Grade II tumors implies a higher amount of cell division.

The prognosis for Grade-II tumors hinge on elements including the tumor's type and its location, and patient attributes, highlighting the need for tailored treatment approaches. While Grade II cancers are less aggressive than Grade III tumors, the prognosis can still vary within this group. Additional factors such as the amount of tumor dissemination, responsiveness to treatment, and patient-specific characteristics influence the behavior and fate of Grade II cancers.

It's essential to acknowledge that grading methods and standards might differ based on the tumor category and the categorization system utilized. The material presented here is intended to offer a broad overview of Grade II tumors and their features.

1.5.3 Grade-III

Grade-III tumors, also known as poorly differentiated tumors, represent a category of tumors that exhibit significant cellular abnormalities and a higher level of aggressiveness compared to Grade-I and Grade-II tumors. Understanding the characteristics of Grade-III tumors is crucial for assessing tumor behavior and prognosis [28].

In Grade-III tumors, the cells display marked cellular atypia and architectural disorganization. The cells deviate significantly from their normal counterparts in terms of size, shape, and nuclear characteristics. They often exhibit pleomorphism, which refers to the presence of cells with different sizes and shapes within the tumor tissue [29]. The nuclei of Grade-III tumor cells are highly irregular, with increased chromatin content and prominent nucleoli. These abnormalities reflect the loss of cellular differentiation and the acquisition of malignant features. One distinguishing feature of Grade-III tumors is their increased mitotic activity [30]. Mitotic activity refers to the rate at which cells divide and is an indicator of tumor proliferation. Grade-III tumors demonstrate a higher number of actively dividing cells, leading to an accelerated growth

rate compared to lower-grade tumors. The elevated mitotic activity indicates the tumor's propensity for uncontrolled cell division and progression.

The aggressiveness of Grade-III tumors is further emphasized by their infiltrative growth pattern. These tumors have the capacity to invade surrounding tissues and structures, making complete surgical resection more challenging. The infiltrative nature of Grade-III tumors increases the risk of local recurrence and distant metastasis. The prognosis for Grade-III tumors differs based on various factors, such as the particular type of tumor, location, stage, and individual patient characteristics. Generally, Grade-III tumors have a poorer prognosis compared to lower-grade tumors. The presence of significant cellular irregularities, elevated rates of cell division, and invasive growth behaviors are indicative of a more aggressive disease trajectory and an increased risk of disease advancement.

It is important to note that grading systems and criteria may differ across tumor types and classification systems. The information provided here offers a general understanding of Grade-III tumors and their characteristics. Precise grading and prognostic information should be obtained from expert pathologists and oncologists based on the specific tumor type and context.

1.5.4 Grade-IV

Grade-IV tumors, also known as undifferentiated or anaplastic tumors, represent the highest grade of tumor malignancy [31]. These tumors exhibit significant cellular abnormalities, a high growth rate, and aggressive behavior compared to lower-grade tumors. Understanding the characteristics of Grade-IV tumors is crucial for assessing their prognosis and guiding treatment decisions [32]. Grade-IV tumors are characterized by the absence of differentiation and the presence of highly abnormal cells. The tumor cells appear markedly different from normal cells and lack the typical features associated with specific cell types. The cells exhibit extreme pleomorphism, with irregular sizes, shapes, and nuclei. The nuclei may display prominent nucleoli and abnormal chromatin patterns. These characteristics indicate a loss of cellular specialization and the acquisition of malignant properties.

One of the hallmarks of Grade-IV tumors is their rapid and uncontrolled growth. These tumors demonstrate a high mitotic activity, with a large number of cells actively dividing [25]. The accelerated rate of cell division contributes to the aggressive behavior and invasive nature of Grade-IV tumors. The cells multiply rapidly, leading to tumor expansion and infiltration into surrounding tissues. This infiltrative growth pattern makes complete surgical removal challenging and increases the risk of tumor recurrence.

Grade-IV tumors are often associated with a high potential for metastasis. The malignant cells can detach from the original tumor location and migrate to distant locations through the bloodstream or lymphatic system. The presence of metastases indicates an advanced stage of the disease and significantly impacts the prognosis. The prognosis for Grade-IV tumors is poor due to their aggressive nature and propensity for rapid progression. Grade-IV tumor treatment strategies usually combine surgery, radiation therapy, and chemotherapy. These approaches aim to address the primary tumor and potential metastatic sites effectively. However, the effectiveness of treatment may be limited due to the tumor's aggressive behavior and resistance to therapy.

It should be noted that grading methods and criteria may change between tumor kinds and categorization systems as shown in Table 1.1. Precise grading and prognostic information should be obtained from expert pathologists and oncologists based on the specific tumor type and context.

Table 1.1: Tumor Grade Comparison Using Differentiation

	Grade-I	Grade-II	Grade-III	Grade-IV
Differentiation	Resembles normal cells in appearance and organization	Intermediate characteristics between Grade-I and Grade-III tumors	Significant cellular abnormalities	Cells lack differentiation and exhibit extreme abnormality
Growth Rate	Slow	Slightly faster than Grade-I tumors	Moderate	Rapid and uncontrolled
Mitotic Activity	Low	Slightly increased compared to Grade-I tumors	Increased	High

	Grade-I	Grade-II	Grade-III	Grade-IV
Tissue Organization	Retains some normal tissue architecture and functionality	Some loss of tissue organization	Significant loss of tissue organization	Absence of tissue organization
Invasion	Minimal invasion into surrounding tissues	Limited invasion into surrounding tissues	Increased invasion into surrounding tissues	Aggressive invasion into surrounding tissues
Metastasis	Low likelihood of metastasis	Low likelihood of metastasis	Higher likelihood of metastasis compared to Grade-I and II tumors	High potential for metastasis
Prognosis	Favorable prognosis	Prognosis varies depending on tumor type and other factors	Poorer prognosis compared to Grade-I and II tumors	Poor prognosis due to aggressive behavior
Treatment	Often responsive to treatment	Treatment strategies depend on tumor type and other factors	Requires more aggressive treatment approaches	Limited effectiveness of treatment due to aggressive behavior

As per WHO guidelines, Table 1.2 shows tumor grades with their associated tumor severity and properties.

Table 1.2: Tumor Categories and their Properties

Tumor Grade	Tumor Severity	Tumor Properties
Grade-I	Low Graded	Well distinguished
Grade-II	Intermediate Graded	Moderately distinguished
Grade-III	High Graded	Poorly differentiated
Grade-IV	High Graded	Undifferentiated

1.6 Challenges and Requirements

Developing an advanced approach for segmenting and grading brain tumors utilizing handcrafted features and Convolutional Neural Networks (CNNs) presents a

challenging task fraught with numerous obstacles and limitations. These obstacles and needs must be examined to ensure the suggested methodology's efficacy and application. Some of the significant issues and requirements are as follows.

1.6.1 Non availability of Labeled Data

Securing a large volume of precisely labeled data is essential for the training and assessment of the proposed methodology. However, obtaining labeled medical imaging datasets focused specifically on brain tumors can be challenging due to numerous factors such as privacy concerns, limited access to data, and the need for expert annotations. Efforts must be made to gather a diverse and representative dataset to ensure the model's robustness and generalizability.

1.6.2 Variability and Heterogeneity of Brain Tumors

Brain tumors display considerable diversity in their appearance, size, shape, and location. This variability poses a challenge in designing robust features and developing a methodology that can effectively manage different tumor types. The proposed approach should account for the inherent heterogeneity of brain tumors to ensure accurate segmentation and grading across diverse cases.

1.6.3 Inter- and Intra-Observer Variability

Manual annotation and grading of brain tumors may vary between different radiologists. The subjective nature of interpretation can lead to inconsistencies in segmentation and grading results. The methodology should aim to minimize inter- and intra-observer variability by providing guidelines and standardized procedures for annotation. It should also incorporate quality control measures to ensure consistent and reliable results.

1.6.4 Computational Complexity and Resource Requirements

Approaches based on Convolutional Neural Networks (CNNs) can be computationally intensive, necessitating significant computational resources for both training and inference phases. Adequate computational infrastructure, including powerful hardware and efficient algorithms, is necessary to oversee the computational complexity related

to extensive CNN architectures. The methodology should be designed to optimize computational efficiency while maintaining high accuracy.

1.6.5 Integration with Clinical Workflow

To facilitate practical adoption, the developed methodology should seamlessly integrate into the existing clinical workflow. It should provide timely and interpretable results that can be easily integrated with standard medical imaging software. The user interface and visualization tools should be user-friendly, enabling radiologists and oncologists to effectively utilize the segmentation and grading outputs in their clinical decision-making processes.

1.6.6 Generalization and Transferability

Not only should the suggested approach perform well on the datasets utilized for its development, but it should also show that it can generalize to other datasets. It needs to be adaptable to changes in imaging procedures, apparatus, and patient demographics. The model's capacity to generalize across various clinical situations and adapt to new datasets can be improved using transfer learning approaches, such as pre-training on large-scale datasets.

1.6.7 Ethical and Regulatory Considerations

Respecting patient privacy and adhering to ethical guidelines and data protection regulations are of utmost importance when working with medical imaging data. Obtaining appropriate ethical approvals, informed consent, and ensuring secure data handling practices are essential requirements. The research should prioritize maintaining patient confidentiality and data security throughout all stages of the study.

1.7 Problem Statement and Research Questions

Segmentation and grading of brain tumors play pivotal roles in medical imaging and computer-aided diagnosis, essential for aiding clinicians in making precise diagnoses and formulating treatment plans. These tasks are foundational in understanding the nature and severity of brain tumors, thereby guiding clinical decision-making processes. While handcrafted features have been extensively used to improve

segmentation accuracy by capturing relevant tumor characteristics through domain expertise, data- CNNs have emerged as a promising alternative, capable of learning intricate patterns directly from the data. Despite their success, data-driven models may also extract extraneous features, leading to suboptimal segmentation results. While recent progress in autonomous Convolutional Neural Networks (CNNs) is promising, achieving accurate segmentation remains a challenge owing to the intricate nature of brain tumors. These tumors can vary greatly in shape, size, contrast, and precise location, adding layers of difficulty to the task of precisely delineating tumor boundaries within the brain's intricate structures.

The significant challenge is the selection of appropriate handcrafted features for brain tumor segmentation. Existing research demonstrates that handcrafted features can enhance segmentation accuracy, but the diversity of brain tumors and their unique properties make it challenging to determine the optimal feature set for brain tumor. This challenge is further compounded by conflicting results and dependencies on domain knowledge, necessitating thorough research to identify the most suitable features for improved outcomes.

Despite the accurate and promising results of brain tumor segmentation, the handcraft features are prone to miss the hidden features in the data. On the other hand, CNN extracts feature automatically without human intervention, but it extracts too many irrelevant features. There is evidence that these two approaches are combined. However, these approaches are either work on global or local features. Due to this, some models are classifying core with higher accuracy while others are performing better on the enhancing regions. Such techniques lead to lower accuracy in classifying the whole tumor in MRI scans. Therefore, a hybrid approach is required by combining local, global features to improve brain tumor Segmentation accuracy.

There are four grades of tumor in the clinical practice as advised by WHO for the severity of the tumor. Furthermore, tumor grading presents further challenges, as it involves a classification problem with varying sample availability for detection and grading tasks. Developing separate CNN architectures for each task can lead to overfitting and increased computational resource requirements, making them less practical for real-world applications. To overcome these issues, a novel approach is needed, where a ML algorithm can perform brain tumor grading, avoiding overfitting and minimizing computational complexity.

1.7.1 Research Questions

The question that arises from the detailed discussion of the problem statements are.

1. Which handcrafted features can positively impact brain tumor segmentation?
2. What is the best mechanism for combining automatic features and handcrafted features for improving the detection rate of the brain tumor?
3. How to effectively classify the brain tumor into a different level of deadliness (grading) using CNN?

1.8 Aims and Objectives

With a considerable influence on morbidity and death rates, brain tumors are major global health problem. Brain tumors must be precisely segmented and graded to be diagnosed, treated, and have their prognosis determined. Interest is on the rise in creating reliable and accurate approach for brain tumor analysis due to developments in computational and medical imaging technologies. This study uses a combination of hand-crafted features and CNN to enhance the segmentation and grading of brain tumors. In medical imaging handcrafted features are manually developed, extracted, and combined with past experience and subject knowledge.

The following are the research's goals:

1. To identify robust handcrafted features for brain tumor segmentation.
2. To develop a novel cascaded approach by combining handcrafted features with automatic features using CNN.
3. To enhance brain tumor detection by employing a combination of features that can accurately predict the malignancy of brain-related tumors.

By identifying robust handcrafted features, the research aims to enhance the accuracy and reliability of brain tumor segmentation techniques.

1.9 Scope of the Study

The findings and implications of this research are poised to benefit the discipline of neuro-oncology as well as the field of medical imaging. The proposed method for segmenting and grading brain tumors holds potential for extensive clinical application,

offering benefits to medical professionals such as radiologists and oncologists. The suggested technique can help with treatment planning by increasing the accuracy of tumor identification and categorization, giving doctors a better understanding of the severity and aggressiveness of brain tumors. As a result, personalized patient management is made easier and treatment outcomes are improved. The results of the research can also help develop medical imaging technologies. This study's fusion of handcrafted features and CNNs illustrates the advantages of fusing conventional image analysis methods with deep learning technologies. The advancement of current algorithms and the creation of cutting-edge software tools for automated tumor segmentation and grading might result from this combination, which could function as a springboard for more research and development in medical image analysis. The effectiveness and dependability of clinical processes in medical imaging may be improved as a result.

The findings of this research also set the stage for more research in brain tumor analysis. Researchers in the field can use the identified robust handmade features and the cascaded technique, which combines handcrafted and automated features, as a starting point for further development and improvement. The suggested approach may also serve as an inspiration for the creation of new methods and conceptual frameworks for the study of cancers or illnesses other than brain tumors. The information collected from this study may be used to investigate new directions in medical image processing and develop diagnostic and prognostic tools across a range of healthcare areas. The primary scope of this work is to develop an integrated approach for the segmentation and grading of brain tumors. The study's findings might be used in clinical practice, medical imaging technologies, and next research projects. This study contributes to the progress healthcare overall and improves the quality of life for individuals with brain tumors by refining the diagnostic processes, treatment planning, and patient outcomes in neuro-oncology. Through these enhancements, the study aims to offer more effective and personalized care for those affected by brain tumors, ultimately leading to better health and well-being.

1.10 Research Contribution

1. Extensive review of literature to identify relevant features for brain tumor segmentation (Extensive analysis and experimentation). Extended Local Binary

- pattern feature extraction technique to extract Local features. Generate a confidence Surface.
2. Develop a Global CNN Consist of two parallel CNN. MRI Pathways CNN and Confidence Surface pathway CNN to achieve segmentation
 3. Collect and annotate private and Benchmark dataset according to WHO grades. Use Skull stripping and ensemble XGBoost for grade prediction.

1.11 Structure of the Thesis

The composition of the thesis is structured as follows:

Chapter 1 Introduction to brain tumor, Diagnosis, Image Segmentation, Imaging Modalities, Grading of tumor, Challenges, Objectives, Problem Statement and research Question of the research.

Chapter 2 Present and summarizes literature review, findings of the various state of arts techniques on brain tumor segmentation and grading. These techniques are assessed on various parameters and other factors that are further used to detect the tumor.

Chapter 3 outlines the methods employed to fulfill the research objectives. The methodology consists of several inter-dependent sub-phases that show the working procedure in a figure of the research framework. Handcrafted features, CNN architecture, grading of tumor, and performance metrics for the proposed schemes are added at the end of this chapter.

Chapter 4 presents the extraction of handcrafted features. A Global CNN architecture consists of two parallel CNN. MRI pathway CNN and Confidence Surface pathway CNN. Where each CNN is further consisting of two pathways global and local to extract more relevant and details features from MRI.

Chapter 5 Presents the multimodal lightweight approach for Brain Tumor Grade Prediction. Proposed scheme based on the boosting techniques which efficiently predict the tumor grade.

Chapter 6 delves into Federated Learning as applied to brain tumor segmentation within medical imaging, emphasizing the protection and confidentiality of patient information. The suggested framework promotes collaborative learning through the training of the segmentation model with decentralized data from various healthcare facilities,

prioritizing the confidentiality of raw data. It employs a server-client architecture, where the server orchestrates the training protocol, and clients perform updates to the model locally using their specific datasets. This approach allows for the enhancement of the model's accuracy and generalizability without compromising the privacy of individual data sources.

Chapter 7 presents the conclusion and outlines future work for this research. Future work includes exploring advanced techniques, conducting extensive clinical validation, and addressing challenges like tumor heterogeneity. These efforts aim to further enhance brain tumor analysis and benefit medical imaging and neuro-oncology.

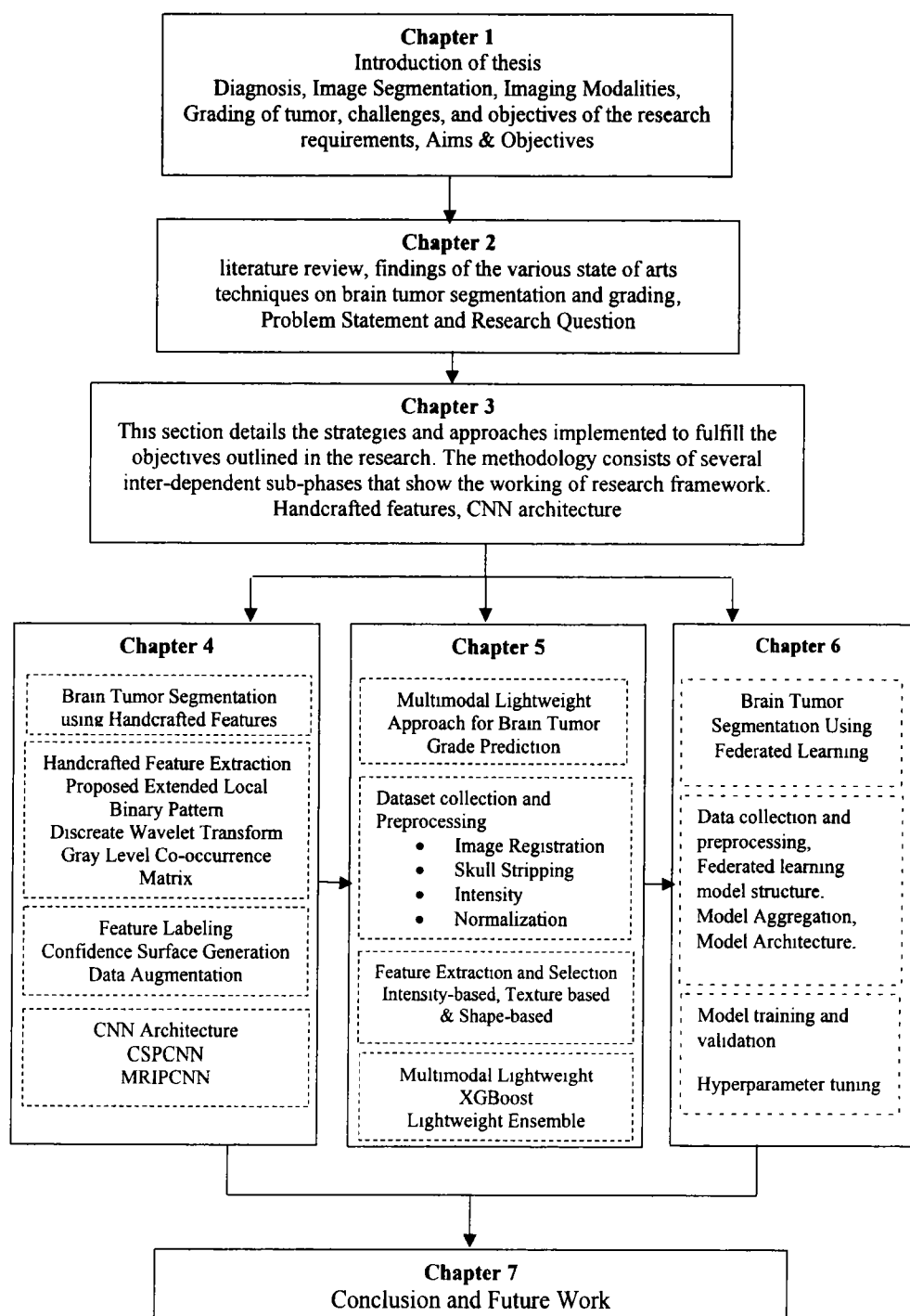


Figure 1.2: Chapter wise Structure and Workflow of Study

CHAPTER 2

LITERATURE REVIEW

Chapter 2

Literature Review

Brain tumors represent atypical formations that develop within the brain or its enclosing tissues. They can be categorized as primary tumors that develop in the brain or secondary tumors that develop because of disease spreading from other body areas. Brain tumors may originate from different kinds of brain cells, including glial cells, neurons, and the meninges. These growths can be categorized as either benign, meaning they are not cancerous, or malignant, indicating they are cancerous.

The origin and activity of the cells can be used to classify varied forms of brain tumors. The most common types of gliomas, encompassing astrocytomas, oligodendrogliomas, and ependymomas, arise from glial cells. Pituitary adenomas grow inside the pituitary gland, whereas meningiomas start off in the meninges. Children are the main demographic for medulloblastomas, which develop in the cerebellum. Additionally, Metastatic brain tumors arise when cancer cells from other regions of the body spread to the brain.

Around the world, brain tumors are a serious health burden. Global cancer data show that they account for a sizable portion of cancer cases and are linked to sizable morbidity and death. Beyond just causing physical symptoms, they may also have an influence on a person's motor skills, cognitive abilities, and overall quality of life if they have a brain tumor.

Planning successful therapy for brain tumors depends on a prompt and accurate diagnosis. Nonetheless, the intricate structure of the brain and the variability of tumors introduce significant challenges in diagnosing brain tumors. Magnetic Resonance Imaging (MRI) stands as the foremost imaging technique for the detection and detailed assessment of brain tumors. However, manual MRI scan interpretation may be time-intensive, subjective, and dependent on the radiologist's skill.

MRI serves as the key diagnostic tool for both identifying and characterizing brain tumors. Among them, MRI stands out as it offers comprehensive anatomical images and is commonly employed for initial detection and characterization purposes. CT

scans offer rapid imaging and can help assess tumor vascularity and bony involvement. PET provides functional information about metabolic activity in tumors, while magnetic resonance spectroscopy (MRS) allows the assessment of biochemical changes associated with brain tumors.

Segmentation involves outlining tumor areas within medical images. Precise segmentation is vital for devising treatment plans, tracking tumor growth, and assessing the effectiveness of treatments. Conventional segmentation techniques have relied on manual or semi-automatic techniques, where experts manually outline tumor regions. However, these methods are time-intensive, prone to variability among observers and not scalable to large datasets.

Grading involves assigning a tumor to a specific category based on its aggressiveness and potential for growth. Tumor grade is an essential prognostic factor that influences treatment decisions and patient outcomes. The categorization scheme by the World Health Organization (WHO) is widely adopted for grading brain tumors. It sorts tumors into various grades according to histological characteristics, the level of cell division activity, irregularities in cell appearance, and the occurrence of cell death or blood vessel formation.

Handcrafted features are quantitative measurements designed to capture specific characteristics of brain tumors. These characteristics are meticulously crafted by hand and can be derived from medical images, offering essential insights for the analysis of tumors. Examples of handcrafted features include shape descriptors, texture features, intensity statistics, and wavelet-based features. These features can be utilized as inputs to machine learning algorithms for segmentation, grading, and other tasks.

CNNs have become effective tools for analyzing medical images, including grading and segmenting brain tumors. From unprocessed visual data, CNNs may automatically develop hierarchical representations, facilitating more precise and effective analysis. They have demonstrated potential across various medical imaging applications, often surpassing the performance of traditional approaches.

2.1 Techniques for Brain Tumor Segmentation

For the purposes of diagnosis, setting a course of therapy, and patient monitoring, accurate segmentation of brain tumors is essential. Many other approaches have been suggested throughout the years to deal with this difficult problem. This subsection provides a detailed examination of brain tumor segmentation techniques, focusing on recent advancements as well as their benefits and drawbacks.

2.1.1 Conventional Approaches

Conventional approaches for brain tumor segmentation have been widely explored and are often based on manual delineation by expert radiologists. These methods involve subjective and time-consuming processes that rely on the expertise of the operator.

Thresholding techniques, such as Otsu's method [19], are commonly employed in conventional approaches. Otsu's method identifies an optimal threshold for distinguishing tumor areas from the background by analyzing the intensity value histogram. By selecting a threshold that maximizes the variance between classes, Otsu's method can effectively segment tumors. Nevertheless, these techniques are susceptible to fluctuations in image intensity and noise, which can result in imprecise segmentation outcomes.

Region growing algorithms, such as the watershed algorithm [33], are another type of conventional approach used for brain tumor segmentation. These algorithms aim to expand regions from seed points based on similarity criteria, such as intensity or texture. By iteratively adding neighboring pixels that meet certain criteria, the algorithm grows the tumor region. However, these methods are highly dependent on the selection of seed points and can be influenced by image artifacts and noise, leading to under- or over-segmentation. Morphological operations, including erosion and dilation, are often applied to refine tumor boundaries in conventional approaches. Erosion shrinks the segmented regions, while dilation expands them. By iteratively applying these operations, the boundaries of tumor regions can be enhanced or smoothed. However, these operations may also result in the loss of small tumor structures or the inclusion of non-tumor regions, impacting the accuracy of the segmentation.

2.1.2 ML based Approaches

Machine learning-based approaches, with their capacity to autonomously extract discriminative features from data, possess significant potential in brain tumor segmentation. The evolution of deep learning algorithms, coupled with the presence of extensive, labeled datasets has recently driven significant progress in these methodologies.

The Support Vector Machine (SVM) is a commonly employed machine learning technique for brain tumor segmentation. SVMs navigate through a high-dimensional feature space to discover the optimal hyperplane that distinguishes between various classes. The efficiency of SVMs in brain tumor segmentation has been investigated in several research. For instance, Menze *et al.* [34] applied SVMs to segment brain tumors using handcrafted features derived from multimodal MRI images. Although SVMs have shown promising results, their performance heavily relies on the quality of handcrafted features, which may not capture all the intricacies of tumor boundaries and structures.

Deep learning models, notably CNNs, have transformed medical image segmentation in recent years, including segmentation of brain tumors. Instead, it requires explicit feature engineering, CNNs may automatically develop hierarchical representations from the unprocessed input data.

Ronneberger *et al.* [35] claim U-Net is a noteworthy CNN design for segmenting brain tumors. The encoder-decoder structure of the U-Net design includes skip links, which allow the network to maintain spatial information during the upsampling process. Due to its capacity to record minute data and address problems with class imbalance, U-Net is commonly employed for segmenting brain tumors.

Furthermore, 3D CNNs have gained attention in brain tumor segmentation as they can capture 3D contextual information. These networks operate directly on volumetric data, considering the spatial relationships between slices. Kamnitsas *et al.* Suggested the implementation of a 3D fully convolutional network (FCN) integrated with a fully connected conditional random field (CRF) to enhance the accuracy of brain lesion

segmentation. This architecture demonstrated superior performance as compared to 2D approaches, particularly in capturing minute details and handling tumor heterogeneity.

The researchers have employed a range of feature extraction strategies. The research community within the domains of computer vision and image processing has considered two more general kinds of feature extraction, namely global and local.

The first statistics order included in the global feature sets consist of intensity, as well as second-order statistics like Gabor features, Wavelet Transform (WT), Gray-Level Co-occurrence Matrix (GLCM), and structural components [37].

For tumor recognition and classification [38], the authors utilized discrete wavelet transformation-based and GLCM based approaches. Low-level features conveniently depict the image; yet, because most gliomas have identical texture, border, form, and volume, low-level features, and their representational ability are restricted. [39] used DWT to get the features and detailed coefficient level-3 decomposition is used. In addition, Color Moments (CM) are utilized to minimize the coefficient. Afterwards, the output is forwarded into an Artificial Neural Network (ANN) to distinguish between normal and pathological brain MR images.

The local feature is classified as the second type of feature. Local feature extraction is essential for brain tumor detection. Fisher vector (FV), scale-invariant feature transformation (SIFT), and bag-of-words (BoW) are all instances of local features. The research community has utilized BoW for the purposes of retrieving and categorizing medical imaging. For instance, in mammography, the categorization of breast tissue density [40], Retrieval and categorization of X-ray images at the pathology and organ levels [41], as well as content-based retrieval of brain tumors. Cheng *et al.* [42] utilize local based statistical features SIFT, FV, and BoW to extract tumor area from brain. The summarized comparison is presented in Table 2.1. Global features are utilized in GLCM [38], Gabor [37] and DWT [39], Local features FV [42] and LBP [40].

Table 2.1: Comparative Analysis of Feature Extraction Techniques

Ref	Year	Technique used	Features	Classifier	Limitation
[44][38]	2012	GLCM, DWT	Global Features	Probabilistic Neural Network (PNN)	A limited no. of the feature set is fed to classifiers. Using only two types of features results in low accuracy.

Ref	Year	Technique used	Features	Classifier	Limitation
[48][42]	2016	FV, SIFT, BoW,	Local Features	Content based image retrieval	High dimension features are used which makes the proposed system computationally expensive
[46]	2018	LBP	Local Features	CNN	Classification of breast tissue density in mammogram
[43]	2020	GLCM, WT, Gabor feature,	Global Features	KNN, LSTM	May ignore more key features as such techniques do not use pixel-level information
[45]	2020	3 level DWT, Color Shape, mean, standard deviation	Global Features	CNN	Local-level information is ignored which impacts results negatively.

Attention-based models have also emerged as a promising direction in brain tumor segmentation. These models employ attention mechanisms, enabling the network to concentrate on relevant areas while filtering out unimportant or noisy attributes. Chen *et al.* [43] introduced deep contour-aware networks (DCAN) that integrate contour information into the segmentation process, achieving accurate gland segmentation. Attention mechanisms have shown potential in enhancing segmentation accuracy by emphasizing important tumor regions and reducing false positives. Recent literature in machine learning-based brain tumor segmentation also explores hybrid approaches that combine handcrafted features with deep learning models. These approaches aim to leverage the complementary strengths of both techniques, enhancing the its capabilities to capture both local and global tumor features [44]. SVM, Random Forest (RF), k-Mean, and fuzzy C-Mean are examples of traditional ML approaches used for brain tumor segmentation. A few other classifiers, including support vector machine [45]. PSO (Particle Swarm Optimization), Sequential Minimal Optimization (SMO), Learning Vector Quantization (LVQ), Multilayer Perceptron (MLP), K-Nearest Neighbor (KNN), a hybrid approach combining Genetic Algorithm and Support Vector Machine (GA-SVM), Spectral Clustering Independent Component Analysis (SC-ICA), Least Squares Regression, Probabilistic Neural Network-Radial Basis Function (PNN-RBF), and Artificial Neural Network (ANN) [46], normalized cross-correlation (NCC) While the bulk of these technologies are efficient, deep learning algorithms produce the greatest outcomes [47]. Table 2.2 present ML based techniques for brain tumor segmentation.

Table 2.2: Comparison of Machine Learning-based Approaches for Brain Tumor Segmentation

Approach	Key Features	Advantages	Disadvantages
SVM	Robust Classification	Effective tumor and non-tumor region distinction, Ability to capture complex patterns	- Heavy reliance on manual feature engineering - Sensitivity to feature selection
KNN	Non-parametric Method	- No assumptions about data distribution	Computationally expensive during inference
Random Forest	Decision trees, feature selection	Manages high-dimensional data	Less suitable for capturing complex spatial relationships
Convolutional Neural	CNN automatically learns relevant features	Efficient, end-to-end learning	High computational cost
Multi-scale Feature Fusion	Multi-scale features, fusion techniques	Captures both local and global information	May require careful selection and combination of features
3D CNN	Volumetric data, captures 3D contextual information	Considers spatial relationships between slices	Computationally expensive, requires large memory

2.1.3 DL based Approaches

In recent years, segmentation of brain tumor regions has garnered considerable interest. Numerous studies have developed diverse techniques for segmenting and classifying tumor regions on MRI imaging. This increasing interest highlights the significance of developing automated tools for the segmentation of brain tumors [34].

Deep learning methods, particularly Convolutional Neural Networks (CNNs), have been applied to a wide array of computer vision challenges, achieving state-of-the-art results. Image classification [48], object recognition [49] and biomedical image segmentation [50] are just a few examples. CNN has the potential to understand in a hierarchical order progressively complicated features directly from data. This distinct property has not only made CNN the first option that many biomedical image researchers attempted on brain tumor segmentation brain task to investigate its segmentation accuracy but also stated, that research that employed CNN based model primarily concentrates on designing networks rather than following the traditional ML pipeline (i.e., image preprocessing, features selection, feature extraction,

dimensionality reduction and finally training classifier). In this regard, different researchers proposed distinct CNN architectures and processed the MRI modalities in distinct fashions (i.e. either 2D patches based or 3D patches based) and obtained competitive segmentation results [51].

Khan *et al* proposed cascaded CNN [52] based on two paths to segments sub-region of brain tumor. Three types of handcrafted features are extracted and SVM is utilized to perform classification. The author achieves a dice similarity score (DSC) of 0.76 on core, 0.81 on a complete, and 0.73 on enhancing tumor, respectively. As discussed above, the authors have used two-path CNN with the same input and kernel size for both global and local pathways. A small kernel dimension is used in global pathways that affect the segmentation results.

Kleesiek *et al.* [53] presented a 3D-CNN framework. A CNN is fed with 3D patches or voxel cubes derived from different brain MRI slices. The model then predicts the label of the tissue located at the center of each cube. They reported an average score of 0.87 for the entire tumor region, whereas the score was for the active tumor region at 0.73 for the BraTS dataset. Even though the suggested network produced favorable performance among three tumors, the network computational overhead was higher due to the CNN (i.e., 3D-CNN) based on 3D patches compared to 2D patches-based approaches. Only one type of feature is considered which provides insufficient information. Only local features are extracted, and global features are ignored, which is most important for segmentation.

An architecture for a 2D-CNN based on 2D patches was created by Zikic *et al.* [54]. This model is capable of segmenting tumors. It lessens the system's computational load. According to the study, the core tumor region's dice score was 0.736 and the total tumor region's dice score was 0.83. The score was 0.69 for the BraTS dataset's active tumor area. To distinguish brain tumor fragments, a shallow CNN with a tiny patch size is introduced.

The authors have utilized a small patch size, which is not good for extracting global features. That the proposed system uses a non-overlapping Max pooling layer. There is a high chance it will miss key features. By identifying different sized patches at the same time, Havaei *et al.* [55] proposed CNN architecture that consists of two pathways. It works in sequence to analyze local and global features of brain MRI data. In this work

each pathway takes patches from separate MRI modalities, with the local pathway using 33×33 pixel patches and the global pathway using 65×65 pixel patches. To determine the label of the central pixel, both paths are centered at the same spot. With an overall accuracy of 0.88 for the whole tumor region, 0.79 for the core tumor region, and 0.73 for the active tumor region, the results on the BraTS dataset were good. The authors have implemented a two-pathway CNN, although with fewer layers and a larger kernel size. High computational cost is caused by a large kernel size.

The brain tumor was divided into three categories by Wang *et al.* [39]. The authors suggested a method for complete tumor, core tumor, and full tumor that uses two different CNNs. The first network is responsible for segmenting the entire tumor. The output's bounding box from the first network is subsequently fed as input to the second network, which is designed to focus on segmenting the main tumor area. The second network operates on a subset of the first network's output to achieve a more refined segmentation of the core and complete tumor. The process involves segmenting the enhancing tumor through utilization of the bounding box derived from the core tumor segmentation outcomes.

Due to the involvement of a high set of variables in three CNNs, this approach works well but is computationally costly. Local features, on the other hand, were only concentrated on its strategy via smaller size convolutional kernels. Furthermore, during the testing phase, researchers employed data augmentation, which doubled the processing time of their suggested technique.

Savadikar *et al.* [56] proposed the segmentation problem for the BraTS challenges. The study employed Probabilistic UNet to see how sampling alternative segmentation maps and 2D segmentation models affected the results. In the UNet architecture, self-attention is utilized in both the prior and posterior systems to ensure the coherence of the proposed models. It investigates how raising the attention block count affects segmentation quality. The segmentation's reported Dice scores are as follows: 0.81898 for the entire tumor, 0.71681 for the tumor core, and 0.68893 for the portion of the tumor that is enhancing.

Kayalibay *et al.* [57] employed a three-dimensional kernel and a CNN-based algorithm. According to the authors' analysis of the BraTS 2013 and 2015 datasets, the overall tumor region had a dice score of 0.87, the core tumor region has a dice score of 0.74,

TH-27346

and the active tumor region has a dice value of 0.71. The dice score was 0.85 for the whole tumor region, 0.72 for the core tumor region, and 0.61 for the active tumor region.

Iqbal *et al.* [58]. used a deep CNN to show how to segregate brain tumors in MRI images. The proposed methodology was based on the BraTS segmentation challenge dataset, comprising images acquired through four distinct modalities. As a result, the researchers provide an improved version of an existing network to address the segmentation problems. In the network architecture, multiple neural network layers are linked in sequence, with convolutional feature maps supplied at the peer level. Experimental outcomes using the BraTS 2015 benchmark dataset underscore the efficacy and advancement of the suggested strategy relative to previous methods in this research domain. Table 2.3 displays the comparison in its simplest form. 3D-CNN [53], Slice wise 2D [54], 3D-patches [57], Global and local 2D [55], Multi2D [58], Two different CNNs [39] and 2D-CNNs [52].

Table 2.3: Comparison of CNN based Methods for Brain Tumor Segmentation

Ref.	Method	Dataset	Performance Measure (Dice Score)		
			Whole tumor	Core tumor	Active tumor
[53][59]	3D-CNN using 3D convolutional filters	BraTS	0.87	0.77	0.73
[60]	Slice wise 2D-patches are extracted by 2D-CNN	BraTS	0.83	0.73	0.69
[63]	3D-patches are extracted by using 3D-CNN	BraTS	0.86	0.74	0.71
[61]	Global and local 2Dpatches having cascaded two pathways 2 D-CNNs	BraTS	0.86	0.79	0.73
[58][64]	Extract multi 2D patches by using pixel level. Different CNN layers.	BraTS	0.67	Not reported	Not reported
[45]	Two different CNNs for segmentation and detection	BraTS	0.89	0.83	0.78
[52][58]	2D-CNNs	BraTS	0.76	0.81	0.73

Leveraging its ability to autonomously produce hierarchical representations from unprocessed image data, deep learning has become a prevalent method for brain tumor segmentation. Within this area, Convolutional Neural Networks (CNNs) have been instrumental, demonstrating exceptional efficacy across numerous applications in computer vision and the analysis of medical imagery. Deep learning-based methods have produced cutting-edge outcomes and have showed substantial potential in properly segmenting brain tumors.

U-Net, developed by Ronneberger *et al.* [35] is a deep learning architecture that is frequently used for segmenting brain tumors. It uses an encoder-decoder structure with skip links to gather contextual data on a local and global level. While the decoder component reconstructs the segmentation map by upsampling and concatenating data from prior layers, the encoder component collects high-level features.

Several adjustments and extensions have been made to improve CNNs' segmentation of brain tumors even further. Dilated convolutions, which Yu *et al.* [59] proposed, allow the network to successfully manage tumors of various sizes and record multi-scale information. Atrous spatial pyramid pooling (ASPP), which incorporates parallel dilated convolutions at various sizes to effectively capture contextual information, was suggested by Chen *et al.* [60].

In addition to CNNs, researchers have explored the application of other deep learning models like recurrent neural networks (RNNs) and graph convolutional networks (GCNs) for brain tumor segmentation. RNNs are specifically adept at capturing spatio-temporal information by leveraging temporal dependencies in sequential data, such as time series imaging [55]. On the other hand, GCNs utilize graph structures to model interactions between image regions, leading to improved segmentation accuracy [61].

DL based approaches offer several advantages in brain tumor segmentation. Firstly, deep learning models have the capacity to autonomously identify relevant features directly from the image's raw data, eliminating the need for manual feature extraction. This ability enables them to detect complex patterns and nuanced details that might be overlooked by conventional approaches [62]. Secondly, deep learning models exhibit high flexibility and adaptability, allowing them to generalize well across different

datasets and tumor types [63]. Moreover, these models effectively manage the innate variability and intricacy of brain tumor imagery.

However, there are certain pitfalls with deep learning-based approaches. A significant hurdle is the necessity for vast quantities of labeled training data. Deep learning models typically require substantial annotated images to achieve optimal performance [64]. Acquiring these datasets can be a lengthy and resource-intensive endeavor, especially for rare tumor types. Furthermore, deep learning models require considerable computational power, necessitating extensive resources for both training and inference phases [65]. Moreover, the limited interpretability of deep learning models poses a challenge to their integration into clinical practice, where transparent and explainable decision-making is critical for medical applications [66].

Despite these difficulties, deep learning-based methods are nonetheless making substantial progress in the segmentation of brain tumors. To further improve the performance and application of deep learning models in clinical practice, current research focuses on creating innovative architectures, enhancing training methodologies, and tackling the interpretability and generalization difficulties.

Overall, by utilizing automated feature learning, deep learning-based techniques, CNNs, have transformed brain tumor segmentation. In the realm of neuro-oncology, these techniques provide precise and effective segmentation solutions, opening the door to better diagnosis, treatment planning, and patient care as show in Table 2.4.

Table 2.4: Comparison of Deep Learning-based Approaches for Brain Tumor Segmentation

Technique	Key Features	Advantages	Disadvantages
U-Net	Encoder-decoder structure	Captures local and global information	Requires large, annotated datasets
Dilated CNN	Multi-scale information	Manages tumors of varied sizes	Computational complexity
ASPP	Parallel dilated convolutions	Efficiently captures contextual information	Interpretability issues
RNN	Temporal dependencies	Captures spatio-temporal information	Longer training times

Technique	Key Features	Advantages	Disadvantages
GCN	Graph-based modeling	Model's interactions between regions	Complex graph construction

2.2 Brain Tumor Grading Methods

Brain tumor grading that is accurate and dependable is essential for determining therapy options and patient outcomes. Various approaches have been presented to determine the grade of brain tumors, based on their histological characteristics. This section gives a summary of the current ways for grading brain tumors, including automated computational systems and conventional histological grading systems.

2.2.1 Histopathological Grading

Traditional histological grading systems, such as the WHO grading system, have long been utilized for brain tumor grading [67]. These grading systems classify brain tumors into distinct categories based on histological attributes such as cellular irregularities, the rate of cell division, tissue death, growth of new microvessels, and patterns of tumor spread into surrounding tissues. The WHO grading system classifies tumors into low-grade (I and II) and high-grade (III and IV) categories, with higher grades indicating more aggressive and malignant tumors. These grading systems provide valuable prognostic information and guide treatment decisions.

While traditional histological grading systems have been widely adopted, they are subject to certain limitations. One of the principal limitations is the reliance on subjective visual assessment by pathologists, which can introduce inter-observer variability. Different pathologists may interpret histological features differently, leading to inconsistencies in tumor grading. This subjectivity can affect treatment planning and patient outcomes. To tackle these challenges, researchers have been exploring automated and objective approaches for brain tumor grading.

2.2.2 Radiological Grading

Radiological grading parameters play a crucial role in assessing brain tumor grade and guiding treatment decisions. These parameters are derived from various radiological imaging modalities, such as MRI, CT, and PET. They provide valuable insights into

the tumor's characteristics, including size, shape, enhancement patterns, edema, necrosis, and vascularization. This section provides a comprehensive literature review of the radiological grading parameters used in brain tumor grading. One of the commonly used radiological grading parameters is tumor size. Larger tumor size is often associated with higher-grade tumors and increased aggressiveness. Numerous studies have reported a positive relationship between tumor size and tumor grade. For example, He *et al.* [68] discover that larger tumor size was significantly associated with high-grade gliomas. Demonstrated that tumor size was a strong predictor of tumor grade in gliomas.

Enhancement patterns observed on contrast-enhanced MRI scans are also important radiological grading parameters. These patterns provide information about the tumor's vascularization and angiogenic activity. Heterogeneous enhancement and irregular borders in imaging studies are commonly linked with tumors of a higher grade. Conversely, homogeneous enhancement is more common in low-grade tumors. Wu *et al.* [69] carried out research on glioblastomas, discovering that ring enhancement, indicative of central necrosis, strongly suggested the presence of high-grade tumors.

The presence of peritumoral edema is another significant radiological parameter in brain tumor grading. Edema is typically observed as hyperintense regions surrounding the tumor on T2-weighted or FLAIR images. Higher-grade tumors tend to exhibit extensive peritumoral edema due to increased invasiveness and breach in the blood-brain barrier. Ellingson *et al.* [70] explored the connection between edema volume and tumor grade in gliomas and demonstrated a positive correlation between edema volume and higher tumor grades.

Necrosis, often seen as hypointense or non-enhancing regions within the tumor, is a radiological parameter associated with high-grade tumors. It is indicative of tumor cell death and represents an aggressive phenotype. Necrosis is commonly assessed using T1-weighted or T2-weighted MRI scans. Lam *et al.* [71] conducted a study on gliomas and reported that the presence and extent of necrosis were significantly associated with higher-grade tumors.

Other radiological parameters, such as the presence of satellite lesions, vascularization patterns, and diffusion characteristics assessed by diffusion-weighted imaging (DWI),

have been explored for their association with tumor grade as well. These parameters provide additional insights into tumor behavior and can assist in distinguishing between low-grade and high-grade tumors.

Recently, there has been an increasing focus on employing sophisticated imaging methods, such as perfusion imaging, spectroscopy, and radiomics, for radiological grading of brain tumors. These techniques provide quantitative measurements of blood flow, metabolite concentrations, and radiomic features, respectively, which can enhance the accuracy of tumor grading. For example, Jain *et al.* [72]. employed dynamic susceptibility contrast perfusion imaging as a method to estimate the grade of gliomas. Radiological grading parameters play a crucial role in brain tumor grading. Tumor size, enhancement patterns, peritumoral edema, necrosis, and other imaging characteristics provide valuable information for assessing tumor grade and guiding treatment decisions. The integration of advanced imaging techniques further enhances the accuracy and precision of radiological grading. However, it is crucial to recognize that histological results and clinical information should be included when interpreting radiological grading criteria. This comprehensive approach ensures accurate tumor grading and facilitates well-informed treatment decisions for patients as show in Table 2.5.

Table 2.5: Key Parameters for brain Tumor Grading

Parameters	Key Features	Advantages	Disadvantages
Tumor Size	<ul style="list-style-type: none"> - Larger size associated with higher-grade tumors. - Positive correlation with tumor grade 	<ul style="list-style-type: none"> - Strong predictor of tumor grade 	<ul style="list-style-type: none"> - May vary depending on tumor location. - Size measurement may be subjective - Inter-observer variability
Enhancement Patterns	<ul style="list-style-type: none"> - Heterogeneous or irregular enhancement in high-grade tumors - Homogeneous enhancement in low-grade tumors 	<ul style="list-style-type: none"> - Provides insights into tumor vascularization - Helps differentiate between grades 	
Peritumoral Edema	<ul style="list-style-type: none"> - Presence of hyperintense regions surrounding the tumor - Positive correlation with higher tumor grades 	<ul style="list-style-type: none"> - Indicates tumor invasiveness 	<ul style="list-style-type: none"> - Measurement variability - Edema may be present in low-grade tumors

Parameters	Key Features	Advantages	Disadvantages
Necrosis	<ul style="list-style-type: none"> - Hypointense or non-enhancing regions within the tumor - Associated with higher-grade tumors 	<ul style="list-style-type: none"> - Indicates aggressive tumor phenotype 	<ul style="list-style-type: none"> - Necrosis may be absent in low-grade Tumors
Other Parameters	<ul style="list-style-type: none"> - Satellite lesions, vascularization patterns, and DWI Characteristics 	<ul style="list-style-type: none"> - Provide additional insights into tumor behavior - Aid in differentiating tumor grades 	<ul style="list-style-type: none"> - Variability in interpretation - Dependent on imaging technique
Advanced Imaging Techniques	<ul style="list-style-type: none"> - Perfusion imaging, spectroscopy, and radiomics - provide additional quantitative measurements of blood flow, metabolite concentrations, and radiomic features 	<ul style="list-style-type: none"> - Quantitative measurements enhance accuracy and precision of grading - Improves grade prediction 	<ul style="list-style-type: none"> - Resource-intensive - Technique-specific considerations

2.2.3 Machine Learning-based Grading Models

Machine learning-based grading models have gained considerable focus in recent times for their potential to provide automated and objective tumor grading in brain tumor research [73]. These models harness the capabilities of machine learning algorithms to interpret intricate imaging data and identify significant features for precise tumor grading. This section offers an overview of the machine learning-based grading models used in brain tumor research, highlighting their key features, advantages, and recent developments. One commonly used machine learning algorithm in brain tumor grading is the SVM [74]. SVM is a type of supervised learning algorithm that has proven to be effective in tackling a range of medical image analysis tasks, such as the classification of brain tumors based on their severity. SVM grading models employ a collection of manually designed features extracted from imaging data, including intensity, texture, and shape features, for the purpose of training a classifier. These models have shown encouraging outcomes in accurately assessing the grade of brain tumors by analyzing their histological characteristics. Bauer *et al.* [75] developed an SVM-based grading model for gliomas using multimodal MRI data and achieved high accuracy in distinguishing low-grade from high-grade tumors.

Another popular machine learning algorithm for brain tumor grading is the RF algorithm [76]. RF is an ensemble learning approach that utilizes multiple decision trees to make predictions. RF-based grading models utilize a similar set of handcrafted features as SVM-based models but leverage the ensemble approach for the improvement of overall correctness and robustness of the system. Sohn *et al.* [77].proposed an RF-based grading model for gliomas using radiomics features extracted from multimodal MRI data. Their model achieved excellent performance in differentiating between low-grade and high-grade gliomas.

Deep learning-based models, notably CNNs, have demonstrated significant promise for grading brain tumors in addition to SVM and RF [78]. Without the need of manually created features, CNNs may automatically develop hierarchical representations from unprocessed imaging data. These models can more accurately grade images because they can identify complex patterns and spatial correlations in the images. Using multimodal MRI data, created a CNN-based grading model for gliomas. Their model successfully distinguished between various grades of gliomas with state-of-the-art performance.

In the past, pathologists have manually classified brain tumor grading by examining the histological features found in the tumor [79]. Categorizing brain tumors is essential for determining the best treatment approach; however, manual techniques can exhibit variability. Enhancing precision and uniformity is imperative for achieving superior patient results.

Recently, machine learning (ML) methods have become a practical technique for assessing the severity of brain tumors by analyzing medical images as input data. ML algorithms can accurately and automatically classify tumor grades by recognizing patterns and features in medical imaging [80]. Several studies have examined the use of machine learning (ML) techniques to classify brain tumor grades and have determined that ML techniques can successfully distinguish between different grades. Brain tumors, a heterogeneous group of neoplasms, can arise in various regions of the brain. Tumors can be categorized according to their histological features, where Grade-I tumors are the least aggressive and Grade-IV tumors are the most aggressive. Precise classification of brain tumors is crucial as it assists in selecting the most appropriate treatment strategy and accurately forecasting patient outcomes. The study has focused

on developing machine learning models to enhance the accuracy of classifying brain tumors. Certain models utilize extracted features from MRI scans, such as texture, shape, and intensity, to categorize the various grades of brain tumors. Convolutional Neural Networks (CNNs), which are subsequently employed for classification, are trained using these features. For example, Akkus *et al.* [81] employed a CNN to precisely categorize gliomas into low-grade and high-grade categories, achieving a success rate of 93.3%. Havaei *et al.* [55] employed CNN for the purpose of categorizing brain tumors into four distinct grades, resulting in an impressive overall accuracy rate of 89.4%. Principal component analysis (PCA) and autoencoders have been utilized for the classification of brain tumor grading. For example, in Li *et al.* [82] The gliomas' MRI images were subjected to PCA analysis to extract characteristics, yielding an accuracy of 91.67% for low-grade gliomas and 95.83% for high-grade gliomas. Ain *et al.* [83] utilized a co-training algorithm to categorize gliomas as either low-grade or high-grade, achieving a notable accuracy rate of 91.6%. Ahuja *et al.* [84] Applied transfer learning to categorize gliomas as either low-grade or high-grade, achieving a remarkable accuracy of 94.75%. Park *et al.* [85] employed artisanal characteristics to forecast the grades of meningiomas using MRI scans. They obtained characteristics pertaining to brightness, pattern, and form and employed a Random Forest classifier to forecast the grade of meningioma. Their approach attained a precision of 0.93 in forecasting meningioma grades. Several studies have examined the utilization of manually created characteristics obtained from alternative imaging techniques, in conjunction with MRI, for the purpose of classifying brain tumors. Sollini *et al.* [86] to forecast the grades of gliomas, hand-crafted features extracted from CT scans were utilized. The researchers extracted features related to shape, texture, and intensity and employed a Support Vector Machine (SVM) classifier to forecast the grade of glioma. They achieved a high accuracy of 0.89 in predicting the grade of glioma. Kamnitsas *et al.* [87] applied a 3D CNN to automatically grade and segment tumors on MRI scans, achieving an accuracy of 92.7%. The proposed model successfully utilized a vast dataset of MRI scans to precisely forecast tumor grades and segment different types of tumors. Gull *et al.* [88] utilize a DL approach to classify cancers into low- and high-grade categories. The classification task achieved a highly promising accuracy of 95.5% by using a dataset of MRI images sourced from the cancer imaging library. Wasule *et al.* [89] the brain tumors were categorized into four classes, namely I, II, III, and IV, based on specific attributes extracted from the MRI scans using the SVM and KNN

algorithms. The suggested technique utilizes the MRI images obtained from the BraTS 2015 dataset. The SVM method outperformed other methods in terms of accuracy, precision (Pr), recall (Rec), and F1-score. Chen *et al.* [90] evaluated the efficacy of SVM, KNN, and Random Forest (RF) algorithms in classifying brain tumor grades based on diffusion-weighted imaging (DWI) data. The SVM algorithm exhibited the highest accuracy and F1 score, whereas the RF algorithm demonstrated the highest Precision (Pr) and Recall (Rec). Pan *et al.* [91] evaluated the efficacy of SVM, KNN, and CNN algorithms in classifying brain tumor grades based on MRI data. A dataset comprising 295 brain tumor images was utilized, accompanied by accurate labels indicating the grade of the tumor. The researchers discovered that the CNN algorithm exhibited superior performance compared to the other algorithms in terms of accuracy, precision, recall, and F1 score. Zhang *et al.* [92] Analyzed the efficacy of various machine learning (ML) techniques in classifying and assessing 368 brain tumor images based on accurate tumor grade labels. The evaluated algorithms included Support Vector Machines (SVM), K-Nearest Neighbors (KNN), Decision Trees (DT), Random Forests (RF), and Convolutional Neural Networks (CNN). It was found that the SVM method ranked second to the CNN algorithm in terms of accuracy, precision, recall, and F1 score.

In summary, these studies indicate that ML algorithms, such as SVM, KNN, DT, RF, and CNN, can be successful in classifying brain tumor grades. The optimal algorithm selection can be influenced by factors such as the nature of the imaging data, the dataset's magnitude, and the specific performance metrics employed for algorithm evaluation. This study involved comparing these algorithms using an expanded dataset of brain tumor images. The efficacy of the algorithms was evaluated through several performance metrics in order to determine the most effective algorithm to classify brain tumor grading. Table 2.6 summarize the existing techniques SVM, KNN [89], SVM [81], RF, SVM, KNN [90], SVM, RF [91], CNN [83], SVM [85], KNN, DT, CNN [92], ML [93] and CNN [88].

Table 2.6: Summary of Existing Machine Learning Techniques Used for Classifying Brain Tumors

References	Algorithms Compared	Dataset Size	Imaging Data	Performance Metrics			
				Acc	Rec	Prc.	F1-score
Wasule <i>et al.</i> [95]	SVM, KNN,	60	MRI	93.0	--	--	--

References	Algorithms Compared	Dataset Size	Imaging Data	Performance Metrics			
				Acc	Rec	Prc.	F1-score
Akkus <i>et al.</i> [87]	SVM	--	MRI	0.86	0.78	0.89	--
Chen <i>et al.</i> [96]	RF, SVM, KNN, LDA.	--	DWI	90.0	--	89.0	--
Li <i>et al.</i> [82][88]	SVM, RF, LR	--	MRI	89.5	90.2	85.7	--
Havaei <i>et al.</i> [61]	3D CNN	285	MRI	83.5	--	81.0	--
Pan <i>et al.</i> [97]	SVM, KNN, CNN	295	MRI	--	--	--	--
Ain <i>et al.</i> [89]	CNN	150	MRI	93.7	94.8	92.5	93.6
Park <i>et al.</i> [91]	SVM	75	MRI	83.3	--	86.2	--
Kouli <i>et al.</i> [93][99]	ML	200	MRI	--	--	--	--
Gull <i>et al.</i> [94]	CNN	153	MRI	--	--	--	95.5

Recent advancements in machine learning-based grading models have focused on incorporating advanced techniques such as transfer learning and deep ensemble learning. Transfer learning allows models to leverage pre-trained networks on large-scale datasets. It enabled them to learn from a huge data and improve generalization. Rehman *et al.* [94] presented a transfer learning-based grading model for gliomas using a pre-trained CNN model. Their model achieved superior performance in grading gliomas compared to traditional machine learning models. Ensemble learning approaches, such as deep ensemble learning, combine multiple models to make predictions and improve grading accuracy. Fasihi *et al.* [95] Created a sophisticated grading model for gliomas using deep ensemble learning, which involved training and combining multiple CNN models. Their model surpassed individual models and achieved exceptional accuracy in glioma grading. The efficacy of machine learning-based grading models is significantly influenced by the quality and diversity of the training datasets. The presence of extensive, annotated datasets is essential for effectively training precise and resilient models. Moreover, the comprehensibility of machine learning models in brain tumor grading continues to be a hurdle, given the opaque nature of deep learning models that hampers the comprehension of the underlying rationale behind the grading determinations. The integration of various imaging modalities, such as MRI, CT, and PET, has been demonstrated to improve the precision of grading models. By integrating complementary information from various modalities, the models are able to encompass a more comprehensive perspective of

tumor characteristics. Hang *et al.* [96] created a multi-modal fusion model for the classification of glioma that integrated features derived from MRI and PET images. The fusion model outperformed single-modal models and achieved improved accuracy in glioma grading. Radiomics entails the extraction of numerous quantitative attributes from medical imagery, which are then utilized as inputs for machine learning models. These features capture subtle variations in tumor characteristics and can provide valuable information for grading. A radiomics-based grading model for gliomas was proposed by Zhang *et al.* [97] employing a blend of radiomic features generated manually and deep features extracted from a pre-trained CNN. The model achieved a high level of accuracy in differentiating between low-grade and high-grade gliomas. Ensemble learning techniques have been employed to enhance the versatility and resilience of grading models. Deep ensemble learning uses a variety of models to produce predictions by combining many deep learning models.

One of the obstacles faced by grading models based on machine learning is the lack of interpretability. Understanding the decision-making process of these models is crucial for gaining insights into the grading criteria. Recent research has focused on developing methods to explain and interpret the predictions of these models. Hayashi *et al.* [98] proposed an interpretable grading model for gliomas using a combination of deep learning and symbolic rule extraction. The model provided both accurate predictions and interpretable rules for tumor grading.

Table 2.7: Comparison of Machine Learning-based Grading Models for Brain Tumors

Grading Model	Advantages	Disadvantages	Ref.
Transfer Learning	Leverages pre-trained models for improved performance	Requires large-scale pre-training datasets	[100]
Multi-modal Fusion	Integrates complementary information from multiple modalities	Requires image registration and alignment across modalities	[102]
Radiomics	Captures subtle variations in tumor characteristics	Requires extraction of many radiomic features	[103]
Deep Ensemble Learning	Enhances model robustness and generalization	Increases computational complexity	[105]
Explainability and Interpretability	Provides interpretability of model predictions	May sacrifice some predictive performance	[104]

The recent progress in ML-based grading models has demonstrated considerable promise in improving the accuracy and reliability of brain tumor classification. Nevertheless, it is crucial to verify the accuracy and reliability of the models by testing them on varied and inclusive datasets. Additionally, it is essential to incorporate clinical and histopathological information into the models to achieve a thorough assessment of grading. Continued research and development in this field will improve the efficacy of machine learning-based grading models for clinical decision-making in the management of brain tumors as shown in Table 2.7 such as Transfer Learning [94], Multi-modal Fusion [96], Radiomics [97], Deep Ensemble Learning [99], Explainability and Interpretability [98].

CHAPTER 3

RESEARCH METHODOLOGY

Chapter 3

Research Methodology

This section concentrates on the research approach used to accomplish the stated goals. There are multiple connected sub-phases in the technique.

3.1 Data Acquisition and Preprocessing

This chapter presents the segmentation and grading process for brain tumors, which makes use of hand-crafted features and CNN. This section focuses on data collection and preprocessing, which are essential procedures in making sure that the input data are of high quality and appropriate for further analysis.

3.1.1 Data Acquisition

The methodology's first phase is the gathering of medical imaging data. Due to its superior soft tissue contrast and non-invasiveness, MRI is the modality that is most frequently employed for the investigation of brain tumors. High-resolution volumetric images of the brain are obtained by scanning patients with MRI equipment during the data collection procedure. Multiple sequences, including T1-weighted, T2-weighted, and contrast-enhanced T1-weighted images, are frequently included in this. The MRI sequences selected for a study are determined by the specific research requirements and the sort of data required for tumor segmentation and grading.

During data acquisition, it is essential to adhere to ethical guidelines and obtain appropriate informed consent from patients. Additionally, ensuring data quality is crucial. This involves following standard imaging protocols, including consistent positioning and image acquisition parameters across different patients and imaging sessions. Quality control measures should be implemented to identify and address any artifacts or imaging inconsistencies that may affect the subsequent analysis. In this research work two versions of benchmark BraTS dataset are used. BraTS 2018 [100], and BraTS 2020 [101]. The BRATS 2020 challenge dataset consists of multi-modal MRI images, which means it includes different types of MRI sequences, typically including T1-weighted (T1): Provides anatomical information about brain tissues. T1-weighted with contrast (T1c): Enhances contrast for better visualization of tumors and

other abnormalities. T2-weighted (T2): Helps to identify edema and tumor extent. T2 Fluid Attenuated Inversion Recovery (FLAIR): Sensitive to edema and useful for detecting tumor boundaries. These different MRI sequences offer complementary information that aids in accurate brain tumor segmentation and analysis.

3.1.2 Preprocessing

After the MRI data is collected, many preprocessing methods are employed to enhance the images' quality and speed up subsequent analysis. Common preprocessing procedures include the following.

3.1.2.1 Image Registration

Image registration is accomplished to align the acquired images spatially, correcting for any patient motion or misalignment between sequences. This step ensures that corresponding regions in different sequences are aligned correctly and facilitates accurate tumor segmentation and grading. Common registration techniques include rigid registration, affine registration, and deformable registration.

Rigid Registration is used to adjust translation, rotation, and scaling parameters to align images. Suitable for correcting small misalignments. The affine registration includes shearing and non-uniform scaling. It is suitable for correcting moderate misalignments. Further, deformable registration accommodates non-linear variations between images and local deformations. It is able to capture intricate anatomical variances and fix significant misalignments. Could make computations more complicated.

For tumor grading, we used Rigid Registration by utilizing the Elastix library in Python due to its versatility.

3.1.2.2 Intensity Normalization

Intensity normalization is applied to normalize the intensity values across different images and sequences, reducing the impact of intensity variations caused by imaging parameters or patient characteristics. Normalization techniques aim to achieve consistent intensity scales and improve the comparability of different images. Methods such as histogram matching, Z-score normalization, or linear scaling can be used for intensity normalization presented in Table 3.1.

Table 3.1: Comparison of Intensity Normalization Techniques

Technique	Description
Histogram Matching	Adjusts the intensity values of an image to match the histogram of a reference image, aligning the intensity distribution across different sequences.
Z-score Normalization	The procedure entails calculating the intensity values' average and standard deviation before normalizing them to have a mean of 0 and a standard deviation of 1. This guarantees consistent intensity scales over the entire image.
Linear Scaling	Rescales the intensity values of an image to a predefined range, such as [0, 1] or [0, 255], preserving the relative intensity relationships while adjusting the dynamic range.

3.1.2.3 Noise Reduction and Filtering

Noise reduction techniques are employed to suppress noise and improve image quality. MRI images are susceptible to noise, which can affect the accuracy of tumor segmentation. Popular techniques for reducing noise encompass Gaussian filtering, median filtering, and wavelet denoising. Gaussian filtering applies a Gaussian filter to the image, smoothing out high-frequency noise while preserving important structures. The median filtering uses the median value of each pixel's immediate neighborhood to replace each one's value and decrease noise spikes while keeping edges and structures. In addition, wavelet denoising applies a wavelet transform to the image and thresholds the wavelet coefficients to remove noise. Finally, wavelet denoising is effective in preserving image details while reducing noise levels.

3.1.2.4 Skull Stripping

Skull stripping, also known as brain extraction, is performed to remove non-brain tissues from the images, including the scalp, skull, and other extracranial structures. This step is essential for isolating the brain region and improving the accuracy of subsequent analysis. Various skull stripping algorithms exist, including thresholding-based methods, region-growing techniques, or atlas-based approaches shown in Table 3.2.

Table 3.2: Comparison of Skull Stripping Techniques

Technique	Description
Thresholding-Based Methods	Utilizes intensity thresholding to segment the brain from the surrounding tissues. Simple and efficient but may fail in cases with intensity variations or when the brain region is not clearly defined.
Region-Growing Techniques	Seeds a region within the brain and grows it by iteratively adding neighboring voxels with similar characteristics. Suitable for handling intensity variations but may be sensitive to seed selection and noise.
Atlas-Based Approaches	Utilizes pre-segmented brain atlases as references for guiding the segmentation process. Offers accurate results but requires atlases aligned with the target images and may be influenced by inter-subject anatomical variations.

For skull extraction, an open source tool, BET was utilized in the experiments.

3.1.2.5 Image Resampling

Image resampling is employed to achieve a uniform voxel size or spatial resolution across different images. Resampling ensures consistency in the image dimensions and voxel spacing, facilitating the application of subsequent analysis techniques that may require uniform spatial sampling. Common resampling approaches include nearest-neighbor interpolation, linear interpolation, or spline interpolation presented in Table 3.3.

Table 3.3: Comparison of Image Resampling Methods

Method	Description
Nearest Neighbor	Gives the corresponding voxel in the resampled image the intensity value of the nearest voxel in the original image, producing a piecewise constant representation.
Linear Interpolation	Creates a smooth representation by computing each voxel's intensity value in the resampled image as a weighted average of the intensities of its nearby voxels.
B-spline Interpolation	Approximates the intensity values in the resampled image using a B-spline interpolation algorithm, resulting in a smooth and continuous representation.

For MRI image resampling, 1mm × 1mm × 1mm voxel size was used.

3.1.2.6 Augmentation of MRI

Methods for augmenting data are utilized to expand and enrich the training dataset. The segmentation and grading models' ability to generalize is improved through augmentation. Various augmentation techniques can be applied, including geometric transformations such as rotation, translation, scaling, or flipping. Additionally, intensity variations, such as contrast adjustment or additive noise, can be introduced to simulate different imaging conditions shown in Table 3.4.

Table 3.4: Data Augmentation Techniques

Technique	Description
Geometric Transformations	The MRI is transformed, such as by rotating, translating, scaling, and flipping. The differences in patient placement or imaging orientations are mimicked by these transformations.
Intensity Variation	Introduces variations in image intensities, such as contrast adjustment, additive noise, or gamma correction. These variations simulate differences in imaging parameters, scanner characteristics, or pathologies.

To inflate the existing dataset, geometric transformation was applied to the images.

3.1.2.7 Annotation and Ground Truth Generation

For supervised learning approaches, expert radiologists or medical professionals generate ground truth annotations. The annotations involve manually delineating the tumor regions and assigning appropriate tumor grades based on established criteria. The annotations serve as the reference standard for training and evaluating the segmentation and grading models. The process of annotation is time-extensive and requires expertise in tumor identification and grading.

During the annotation process, it is crucial to ensure inter-observer agreement by involving multiple experts and conducting quality control checks. Discrepancies or disagreements among experts can be resolved through consensus or by involving a senior expert to make the final decision.

The input data is prepared for the succeeding stages of the approach, which include feature extraction, model training, and evaluation, by adhering to the data gathering and preparation methods described above. The accuracy and dependability of the brain tumor segmentation and grading system depend on how well and appropriately the data preprocessing stages were executed.

3.2 Handcrafted Features Extraction

The second stage of the methodology involves extracting handcrafted features from the preprocessed brain tumor images. Handcrafted features are manually designed and engineered to capture specific characteristics and patterns that are relevant for brain tumor segmentation and grading. These features serve as input to the subsequent classification or regression models. Handcrafted features are derived from domain-specific knowledge in medical imaging. This proficiency enables the identification and isolation of characteristics that are specifically pertinent to the structure and attributes of brain tumors. By leveraging domain expertise, handcrafted features can capture specific aspects of tumor appearance that are known to be significant in diagnosis and grading. Unlike features automatically extracted by deep learning models, handcrafted features provide greater interpretability. This is crucial in medical applications where understanding the basis for a model's decision-making process can be as crucial as the decision itself. Handcrafted features allow for a clear understanding of what characteristics the model is considering, which aids in gaining the trust of medical practitioners. Although CNNs are powerful in feature extraction, they sometimes lack the ability to capture subtle yet clinically relevant features. Handcrafted features can complement these models by providing targeted information that might be overlooked by purely data-driven approaches.

3.2.1 Intensity-based Features

The statistical characteristics of the pixel intensities within the tumor region are described by intensity-based features. These features provide information about the intensity distribution, texture, and spatial variations within the tumor shown in Table 3.5. Common intensity-based features include:

1. **Mean Intensity:** This represents the average intensity value within the tumor region.
2. **Standard Deviation:** Measures the variation or spread of intensity values within the tumor region.
3. **Histogram Features:** Histogram-based features capture the intensity distribution within the tumor. Examples include the number of peaks, entropy, skewness, and kurtosis.

For intensity-based features, statistical measures employed such as mean, standard deviation, skewness, and kurtosis.

Table 3.5: Example of Intensity-based Features

Feature Name	Description
Mean Intensity	Average intensity value within the tumor region.
Standard Deviation	Measure of variation in intensity values within the tumor region.
Number of Peaks	Number of peaks in the intensity histogram of the tumor region.
Entropy	Measure of randomness or information content in the intensity histogram.
Contrast	Quantifies the difference in intensity between neighboring pixels in the tumor region.
Correlation	Measures the linear dependence between the intensities of neighboring pixels in the tumor region.

3.2.2 Shape-based Features

The geometric characteristics of the tumor region are described by shape-based attributes. These characteristics depict the size, symmetry, and contour characteristics of the tumor presented in Table 3.6. Common shape-based features include:

1. Area: Shows how many pixels or voxels are there in the overall tumor region.
2. Perimeter: determines the contour or length of the tumor.
3. Compactness: The ratio of the tumor's area to its perimeter square measures the tumor's roundness or compactness.
4. Eccentricity: Describes the elongation or eccentricity of the tumor, ranging from 0 (circular) to 1 (highly elongated).
5. Solidity: The ratio of the tumor region's surface area to that of its convex hull, which reveals the solidity or concavity, respectively.

For shape based features, all of the above features were used.

Table 3.6: Example of Shape-based Features

Feature Name	Description
Area	The total amount of pixels or voxels located in the tumor area.

Feature Name	Description
Perimeter	Length of the tumor boundary or contour.
Compactness	ratio of the area to the perimeter's square, indicating how compact or oblong the tumor is shaped.
Eccentricity	Degree of elongation or eccentricity of the tumor, ranging from 0 (circular) to 1 (highly elongated).
Solidity	The ratio of the tumor's area to its convex hull's area reflects the tumor's solidity or degree of concavity.

3.2.3 Texture-based Features

The spatial distribution and patterns of pixel intensities within the tumor region are captured by texture-based features. These characteristics reveal details regarding the smoothness, coarseness, and textural variations inside the tumor. Typical texture-based characteristics are shown in Table 3.7.

1. Co-occurrence at the Gray Level Matrix: Based on the brightness of the pixels, GLCM-based features quantify the spatial relationship between pairs of pixels. Contrast, energy, homogeneity, and entropy are a few examples.
2. Local Binary Patterns (LBP): By comparing each pixel with its surrounding pixels, LBP features characterize the local texture patterns within the tumor region. Variations in texture like uniformity, smoothness, or coarseness are captured by these qualities.
3. Gabor Filter Reactions: Using varying scales and orientations, Gabor filters are used to extract texture characteristics. These characteristics record textural patterns related to brain malignancies.

For tumor segmentation, we used GLCM and extended LBP.

Table 3.7: Example of Texture-based Features

Feature Name	Description
Contrast	Measures the local intensity variations or differences within the tumor region.
Energy	Represents the sum of squared GLCM elements, indicating the uniformity or homogeneity of the texture.

Feature Name	Description
Homogeneity	Measures the closeness or similarity of intensity values within the tumor region.
Entropy	Describes the randomness or information content in the texture distribution.
LBP Histogram	Histogram-based representation of the local binary patterns within the tumor region.
Gabor Features	Responses of Gabor filters at different scales and orientations, capturing specific texture patterns relevant to brain tumors.

The handcrafted features extracted from the preprocessed brain tumor images serve as inputs to the subsequent segmentation and grading models. These features capture important characteristics of the tumors, including intensity, shape, and texture properties, enabling the models to learn and make accurate predictions.

3.3 Convolutional Neural Network Architecture

CNNs have demonstrated exceptional performance in numerous computer vision applications. CNNs are widely used for segmenting and classifying brain tumors because of their capacity to learn hierarchical representations from input data. The following segment outlines the structure of the Convolutional Neural Network (CNN) model employed within the proposed approach.

3.3.1 Basic CNN Architecture

Multiple layers, including convolutional layers, pooling layers, and fully linked layers, make up the fundamental structure of a CNN. By applying filters to the input images that convolve, the convolutional layers are essential in the learning of local features. The feature maps' spatial dimensionality is decreased by the pooling layers' downsampling of the feature maps. The classification or regression tasks are then conducted by the fully connected layers using the features that have been learned, presented in Table 3.8.

Table 3.8: CNN Architecture

Layer Type	Output Size	Kernel Size	Activation
Convolutional	32×32×32	3×3×3	ReLU

Layer Type	Output Size	Kernel Size	Activation
Convolutional	32×32×32	3×3×3	ReLU
Max Pooling	16×16×16	2×2×2	-
Convolutional	16×16×16	3×3×3	ReLU
Convolutional	16×16×16	3×3×3	ReLU
Max Pooling	8×8×8	2×2×2	-
Fully Connected	512	-	ReLU
Fully Connected	256	-	ReLU
Output	C (Classes)	-	Softmax

An illustration of a CNN architecture for segmenting and grading brain tumors is shown in Table 3.8. The brain tumor images that have undergone preprocessing are depicted as a three-dimensional volume with dimensions of 32×32×32. In the convolutional layers, the Rectified Linear Unit (ReLU) activation function is applied, featuring a kernel dimension of 3×3×3. For the max pooling layers, a pooling dimension of 2×2×2 is adopted. The architecture includes fully connected layers with 512 and 256 units, respectively, also incorporating the ReLU activation function. The output layer employs a softmax activation function to obtain classification or regression predictions for multiple classes.

3.3.2 Advanced CNN Architectures

To enhance the effectiveness of brain tumor segmentation and grading, numerous advanced architectures have been proposed in addition to the fundamental CNN architecture. These architectures include U-Net, V-Net, and ResNet, among others. These models often incorporate skip connections, residual connections, or attention mechanisms to enhance the learning and representation capabilities of CNN shown in Table 3.9.

Table 3.9: Popular CNN Architectures

Model	Description
U-Net	Uses skip links and a U-shaped design to collect contextual data on both a local and global scale.

Model	Description
V-Net	Extends U-Net with volumetric convolutions and residual connections to improve the segmentation performance.
ResNet	Introduces residual connections, which provide the network the ability to learn residual mappings and stop gradients from vanishing.

The U-Net, V-Net, and ResNet architectures are examples of advanced CNN architectures commonly employed in brain tumor segmentation and grading tasks. Such designs have demonstrated encouraging results in enhancing the accuracy and robustness of the models.

3.4 Training and Evaluation of the Network

This segment offers an in-depth discussion on the methodologies employed for training and testing CNNs used in the classification and segmentation of brain tumors. This covers the procedures for data collection, preprocessing, network design, training, and assessment measures.

3.4.1 Training Procedure

Using the prepared dataset and the specified architecture, the CNN model is trained. The following steps were performed.

1. Division of Dataset into Training and Validation Groups: The dataset is divided into training and validation groups to guarantee that each group includes a representative distribution of different types of tumors and their respective grades.
2. Loss Function: A suitable loss function, such as cross-entropy loss for classification or Dice loss for segmentation, is defined based on the job.
3. Optimization technique: Throughout the training process, the network's parameters are adjusted utilizing optimization methods such as Stochastic Gradient Descent (SGD) or Adam.
4. Mini-batch Training: After each mini-batch, the network parameters are modified, and new mini-batches of training data are created. As a result, convergence occurs more quickly, and computational resources are used effectively.

5. **Backpropagation and Parameter Update:** Backpropagation is employed to determine the gradients of the loss function relative to the parameters of the network. The optimizer then makes parameter adjustments in a manner that minimizes loss.
6. **Learning Rate Schedule:** A learning rate schedule is often employed to control the step size of parameter updates. It may decrease over time to ensure finer convergence.
7. **Regularization Techniques:** To avoid overfitting and enhance generalization, regularization techniques like dropout or weight decay can be used.

The training session persists for a specified number of epochs until a convergence criterion is met. Throughout this period, the performance of the model on the validation set is closely monitored to prevent overfitting and to identify the most effective model configuration.

3.5 Performance Evaluation Metrics

To investigate the accuracy and usefulness of the brain tumor segmentation and grading system, its performance must be reviewed. A variety of evaluation metrics are available for measuring the performance of the system. This section discusses standard evaluation criteria for segmentation and grading tasks.

3.5.1 Segmentation Evaluation Metrics

For both the segmentation and grading tasks related to brain tumors, multiple metrics are employed to evaluate the effectiveness of the trained CNN model. These metrics offer numerical evaluations of the model's performance and correctness. Common evaluation metrics are as follows:

- **Dice Similarity Coefficient (DSC):** The DSC calculates the overlap between segmentation mask predictions and ground truth masks, with larger values indicating more accurate segmentation. Values between 0 and 1 imply superior segmentation accuracy.
- **Sensitivity and Specificity:** Sensitivity indicates how well the model can recognize tumor regions, while Specificity measures how well the model can detect non-tumor regions.

- **Classification Accuracy:** This metric assesses how well the model has graded the tumors by counting the proportion of correctly classified tumor grades.
- **Receiver Operating Characteristic:** The ROC curve illustrates the model's performance by plotting the true positive rate against the false positive rate at various threshold levels.

3.5.2 Grading Evaluation Metrics

For evaluating the grading performance, the following metrics can be used:

1. **Classification Accuracy:** Classification accuracy represents the proportion of tumor grades correctly identified from the total tumor cases, serving as a comprehensive assessment of the grading performance.
2. **Cohen's Kappa Coefficient:** Cohen's Kappa coefficient assesses the agreement between anticipated and actual tumor grades, taking into consideration the likelihood of coincidental agreement. It has a scale of -1 to 1, with 1 representing complete agreement.
3. **Receiver Operating Characteristic (ROC) Curve:** The ROC curve evaluates the performance of a grading system across different classification thresholds by plotting the true positive rate (sensitivity) against the false positive rate (1 - specificity). The area under the ROC curve (AUC) provides a quantitative measure of the system's overall grading effectiveness.
4. **Confusion Matrix:** The confusion matrix encapsulates the predicted versus the actual tumor grades, as well as the number of correctly and incorrectly categorized tumors for each grade. It elucidates the precise faults committed by the grading system.

CHAPTER 4

BRAIN TUMOR SEGMENTATION IN MRI WITH HANDCRAFTED FEATURES

Chapter 4

Brain Tumor Segmentation in MRI with Handcrafted Features

Gliomas represent the most common form of malignant brain tumors, exhibiting the highest rates of mortality and occurrence. Manual segmentation of brain tumors, on the other hand, is labor-intensive, susceptible to mistakes and heavily reliant on the radiologist's expertise and experience. The results of manual brain tumor segmentation provided by different radiologists for the same patient may differ. Consequently, more robust and reliable techniques are needed. Biomedical image researchers developed several semi-automatic and fully automatic brain tumor segmentation methods based on either a typical ML pipeline and accurate (handcrafted feature based, etc.) or a data driven strategy (e.g., CNN). Existing methods rely on either handcrafted features (such as symmetry analysis, alignment-based features analysis, or textural properties) or CNN. Manual features seek to model domain knowledge, whereas CNN techniques primarily attempt to create features in an unsupervised manner. Combining various approaches in a cascaded manner has the potential to outperform either feature-based or data-driven (e.g., CNN) techniques alone. The output of custom feature-based ML approaches is intelligently combined and used as previous knowledge as part of a revolutionary cascaded strategy that is described. It makes use of the BraTS dataset. T1, T1c, T2, and FLAIR are the four MRI modalities that are available for each patient. Additionally, there is manual ground truth data provided for the patients. One of the most utilized performance measures is Dice Similarity (DS). It evaluates the level of similarity between the segmentation performed manually using known ground truth and the segmentation conducted computationally. A Global Convolutional Neural Network (GCNN) has been created for segmenting brain tumors, which utilizes a combination of handcrafted features and deep learning techniques. The proposed GCNN architecture, which contains of two parallel CNNs, CS Pathways CNN (CSPCNN) and MRI Pathways CNN (MRIPCNN), achieved high accuracy in segmenting brain tumors in the BraTS dataset. This work holds significant potential for improving the precision

of brain tumor segmentation, thereby assisting clinicians in enhancing diagnosis and treatment planning.

4.1 Methodology

The study process for our suggested extended handcrafted feature-based ML strategy for brain tumor segmentation using various MRI pathways is highlighted in this part. To measure the success of our suggested strategy, we used the Dice Similarity Score (DSS) as an assessment tool. This methodology consists of handcrafted feature extraction, feature labeling, confidence surface generation, and acquisition of the dataset. A new cascaded approach for fully automated brain tumor segmentation is developed that first customizes HGG and LGG in MRI images. Then, the results of HGG and LGG are fed as input to Deep Neural Networks in the form of previous information. Due to significant variations in the presence, absence, density, contrast and location of the tumor, the embedding of prior knowledge is challenging in brain tumor segmentation as compared to other similar medical tasks.

4.1.1 Hand Crafted Feature Extraction

Different handcrafted features were calculated like Extended Local Binary Pattern (ELBP), DWT, and GLCM. In this study, we employed a set of sophisticated handcrafted features, each selected for their proven efficacy in capturing distinct aspects of image texture and form that are indicative of tumor presence. ELBP serve as an effective texture descriptor, capturing local texture details through a comparison of each pixel to its surrounding neighbors and encoding the outcomes as binary numbers. We used ELBP due to its robustness to changes in illumination, which is particularly important in MRI images where intensity inhomogeneity can be a challenge. By using an extended version of LBP, we were able to capture fine-grained texture details that are often present in tumor regions, providing a subtle indication of pathological changes. DWT is utilized for its ability to decompose images into a hierarchical set of wavelet coefficients, capturing both frequency and spatial information. This is particularly useful for identifying irregular patterns and edges, which are common characteristics of brain tumors. The multi-resolution analysis provided by DWT allows us to distinguish between various textures and shapes within the MRI images, which are essential for accurate tumor segmentation. GLCM is a statistical approach that

quantifies how often pairs of pixel intensity values occur adjacent to each other in an image, providing a measure of the spatial distribution of gray levels. By calculating the GLCM for different orientations and distances, we can derive a comprehensive set of texture features, such as contrast, correlation, energy, and homogeneity. These features are instrumental in differentiating between the heterogeneous textures of tumor tissues and the more uniform appearance of healthy brain regions.

Each of these handcrafted features brings a unique set of information to the table, and their combination is powerful for the task at hand. For instance, while ELBP excels in capturing edge-like structures that may signify the periphery of a tumor, GLCM offers insights into the texture regularity which might indicate tumor homogeneity or heterogeneity. DWT complements these by providing a macro and micro perspective on the image through its multi-scale analysis.

Together, these handcrafted features form a comprehensive feature set that feeds into the subsequent machine learning models, laying the groundwork for precise and reliable brain tumor segmentation. The choice of these features was motivated by their successful application in previous research, their compatibility with the MRI data, and their ability to capture a wide range of tumor characteristics, thus ensuring robustness in the face of diverse tumor presentations.

4.1.1.1 Extended Local Binary Pattern

Local Binary Pattern (LBP) is a robust non-parametric method for feature extraction. This technique extracts comparatively accurate features with high accuracy and reasonable processing time. It applies a 3×3 mask to extract the grayscale value of the middle pixel. Figure 4.1 depicts the prime idea of this work.

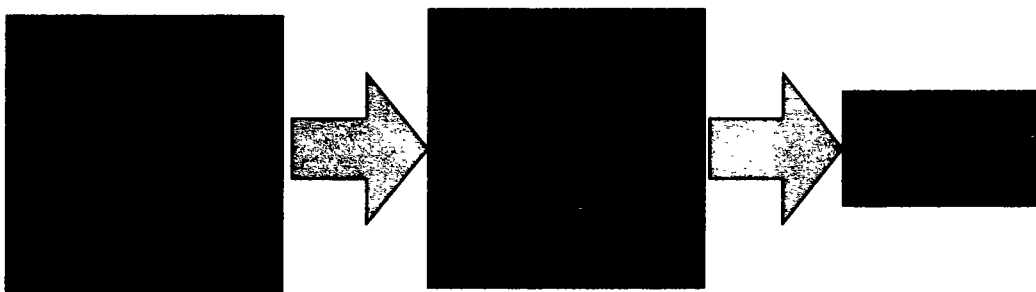


Figure 4.1: Feature Extraction process of LBP

In this process, it calculates the middle pixel with the neighbor pixels to convert the numeric value to binary. If the value of the neighboring pixel is greater than the center

value, assign them a value of 1; otherwise, assign them a value of 0. Finally, the decimal value is calculated from extracted 1's and 0's to obtain the LBP operator of the middle value. This procedure is repeated for every image by shifting the mask in each individual image. This process is computationally inexpensive and produces more accurate results. However, the LBP cannot completely display the structure of the image. Similarly, it cannot contain all the spatial information. The LBP uses scaling, recurrence, and introduction as coding for every pixel. In this way, it compromises precision. To address these issues, we use the Extended Local Binary Pattern (ELBP), as shown in algorithm 4.1. ELBP is an enhanced algorithm that uses scaling, recurrence, and introduction as a coding scheme in a parallel manner. Thus, it improves the performance of LBP by using parallelism and increases the precision by concurrently using these coding schemes. The resultant algorithm enhances the arrangement exactness of the proposed brain tumor location framework.

Algorithm 4.1: Extended Local Binary Pattern

INPUT

```

Function ELBP(image):           // Extended Local Binary Pattern Function
rows, cols = size(image)         // Input Image
ELBP(image) = initialize a 2D array of size (rows, cols) with zeros
For each row in range(2, rows - 2):
  For each col in range(2, cols - 2):
    center_pixel = image[row, col]
    binary_code_5x5 = "
1. Calculate 5x5 LBP binary code
  For i in range(-2, 3):
    For j in range(-2, 3):
      IF i == 0 and j == 0:
        continue
      neighbor_pixel = image[row + i, col + j]
      binary_code_5x5 += '1' if neighbor_pixel >= center_pixel else '0'
2. Count the number of 1s in 5x5 binary code
  count_ones = count_ones_in_binary(binary_code_5x5)
  IF count_ones < 7:
3. Switch to 3x3 neighborhood if less than 7 1s in 5x5 binary code
  binary_code_3x3 = "
  For i in range(-1, 2):
    For j in range(-1, 2):
      IF i == 0 and j == 0:
        continue
      neighbor_pixel = image[row + i, col + j]
      binary_code_3x3 += '1'
      IF neighbor_pixel >= center_pixel else '0'
  Elbp_code = binary_code_3x3
Else

```

```

        Elbp_code = binary_code_5x5
        Elbp_image[row, col] = binary_to_decimal(elbp_code)
    return Elbp_image
4. Function count_ones_in_binary(binary_code):
    count = 0
    For bit in binary_code:
        IF bit == '1':
            count += 1
    return count
5. Function binary_to_decimal(binary code):
    decimal = 0
    For i in range(len(binary_code)):
        bit = binary_code[i]
        decimal += int(bit) * (2**(len(binary_code) - i - 1))
    return decimal
OUTPUT

```

4.1.1.2 Discrete Wavelet Transformation

DWT is employed to break down the input brain MRI image into various sub-bands. These sub-bands comprise an approximation sub-band isolating low-frequency data, along with diagonal, vertical, and horizontal sub-bands. In the initial decomposition stage, the input brain MRI image is divided into four sub-bands: LL (Low-Low approximation), LH (Low-High horizontal), HL (High-Low vertical), and HH (High-High diagonal). In the second level of decomposition, a Discrete Wavelet Transform (DWT) is applied to the LL sub-band, leading to the generation of HH2, HL2, LH2, and LL2 sub-bands, equation (4.1). function $\phi(x)$ with respect to the wavelet function $\phi(sx - k)$, where "s" and "k" are parameters that control the scale and translation of the wavelet function While, at third level DWT transformation, LL2 is decomposed into four bands to produce third level sub bands HH3, HL3, LH3, and LL3 equation (4.2). Furthermore, fourth level DWT decomposition is applied over LL3. A four-level decomposition was applied to the brain MRI images, and the resulting extracted features were used to classify them as either malignant or benign, equation (4.3).

$$\varphi(x) = \sum_{k=-\infty}^{\infty} a_k \varphi(sx - k) \quad (4.1)$$

$$\text{Integral} \int_{-\infty}^{\infty} \varphi(x) \varphi(x + 1) dx = \delta_0, l \quad (4.2)$$

$$x = \sum_{k=-\infty}^{\infty} (1)^k [aN - 1 - k(2x - k)] \quad (4.3)$$

Figure 4.2 displays the sub-band images obtained from applying the DWT to the brain MR images at a four-level decomposition.



Figure 4.2: DWT sub-band images are in shows the decomposition of brain MR images using DWT at level 4

4.1.1.3 GLCM Features

GLCM is a statistical approach for feature extraction. GCLM features map is produced using pixels' orientations at 0° , 45° , 90° , and 135° . The pixel orientation at 45° is used for constructing the matrices. The process is presented in Equation (4.4) and Equation (4.5). The Gray Level Co-occurrence Matrix (GLCM) is a matrix where $P(i, j)$ represents the number of times the i th pixel with value i occurs in a specific orientation 45° and is adjacent to the j th pixel with value j . pixel (i, j) in the image $P(i, j)$, calculate the squared difference $[(i - j)]^2$ between the intensities of neighboring pixels. From this matrix, relevant features such as correlation, contrast, entropy, and energy are extracted for use in the classification of brain MRI.

$$ContracCM = \sum_{j,i=1}^m P(i, j) * [(i - j)]^2 \quad (4.4)$$

$$CorrelationGM = \frac{\sum_{j,i=1}^m P(i - \mu_i) * (i - \mu_j)^2 * P(i, j)}{\sigma_j \sigma_i} \quad (4.5)$$

In this context, μ_i and μ_j represent the means of the GLCM matrix in the x and y directions, respectively, while N denotes the number of rows and columns in the GLCM matrix. When calculating GLCM-based features, σ_i and σ_j stand for the standard deviations of the GLCM matrix in the x and y directions, respectively.

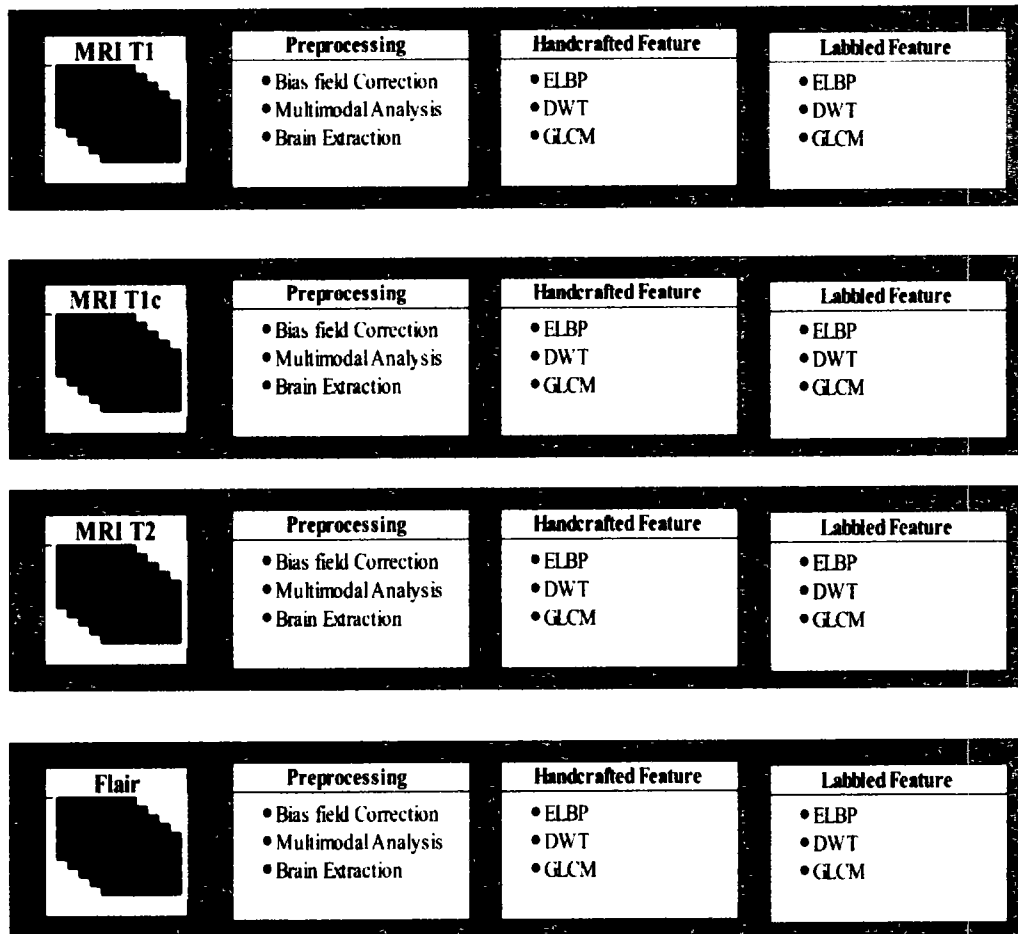


Figure 4.3: Illustrates the feature labeling process

4.1.2 Feature Labeling

In this phase, we labeled feature vectors regarding the provided ground truth. Figure 4.3 illustrates the feature labeling process. Feature labeling represents a crucial phase in the pipeline of machine learning and pattern recognition tasks within medical imaging. In the context of brain tumor segmentation, labeling involves assigning a class or category to each feature vector extracted from the MRI images. This is founded on the ground truth, which usually comes from expert annotations signifying whether tumors are present or absent in different areas of the brain. In this phase, our primary goal is to ensure that each feature vector accurately reflects the underlying pathology as delineated in the ground truth data. The feature vectors generated from the handcrafted feature extraction process, encompassing techniques like Extended Local

Binary Patterns (ELBP), Discrete Wavelet Transforms (DWT), and Gray Level Co-occurrence Matrix (GLCM), undergo a meticulous labeling process. These labels are binary or multiclass, indicating whether the corresponding pixel belongs to a tumor or non-tumor region or to different tumor sub-regions such as necrotic core, edema, or enhancing tumor.

The reliability of the feature labeling directly impacts the accuracy of subsequent machine learning models. Mislabeling features can lead to poor model performance and inaccuracies in tumor segmentation, which can adversely affect clinical decision-making. Thus, we employ a rigorous validation process to verify the correctness of the feature labels against the ground truth provided by medical experts.

4.1.3 Confidence Surface Generation

Finally, the generated feature vectors are mapped as additional MRI modalities. Which is named Confidence Surface (CS) illustrated in Figure 4.4.

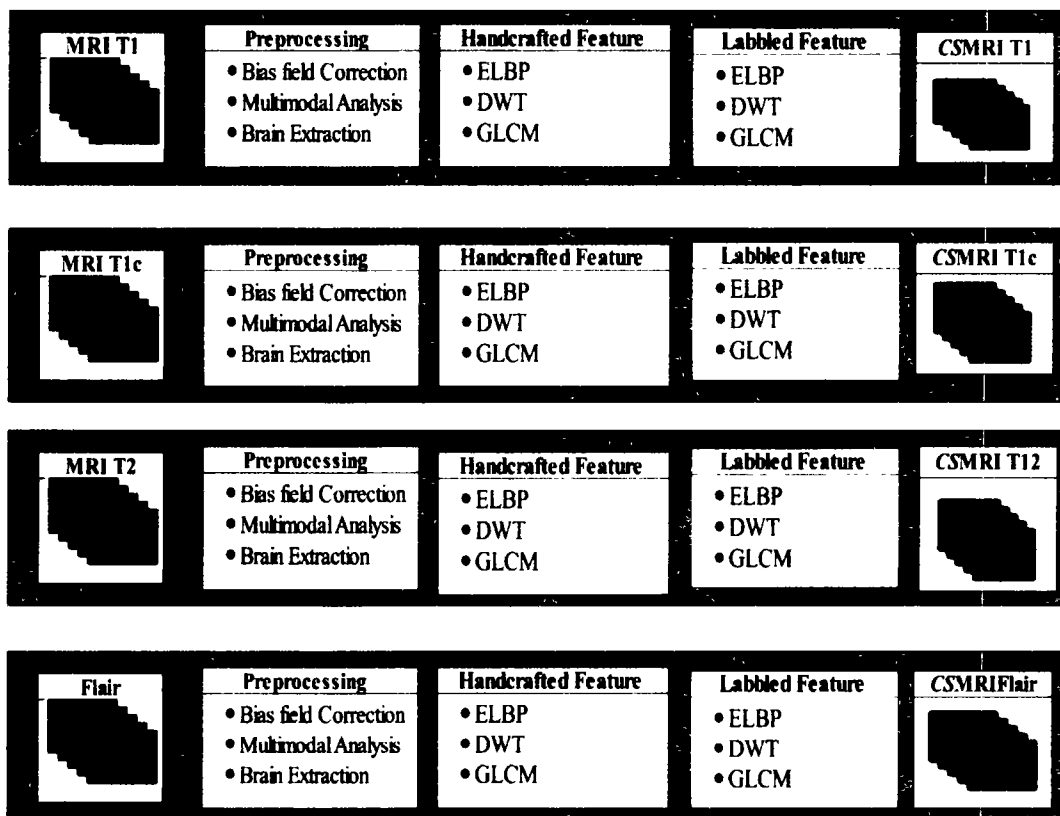


Figure 4.4: Illustrates the Confidence Surface generation process

4.1.4 Dataset

Focusing on gliomas, which are the predominant form of primary brain tumors, the Brain Tumor BraTS [100] challenge explores methods for segmenting brain tumors.

The dataset consists of $240 \times 240 \times 155$ -mm MRI volumes with four different contrast modalities: T1, T1c, T2, and FLAIR. Five different tumor sub-region labels, including necrosis (NCR), edema (ED), non-enhancing tumor (NET), enhancing/active tumor (AT), and all other classifications, are labeled for each voxel. The BraTS 2018 dataset consists of 75 MRI scans for Low Grade Gliomas (LGG) and 210 scans for High Grade Gliomas (HGG).

4.1.5 Data Augmentation

We are using the BraTS dataset for our experiments, that consists of a small number of images. On the contrary, CNN requires a high number of training samples to learn high dimension features. Otherwise, there is a considerable risk of overfitting. In order to mitigate the risk of overfitting, many authors have used data augmentation techniques [102]. Data augmentation increases the number of samples by taking copies using flipping, rotation, and mirroring dimensions. We utilized a blend of these data augmentation strategies to expand our training dataset.

4.1.6 CNN Architecture

After the successful generation of the CSmodalities with handcrafted features, our proposed global CNN (GCNN) architecture is comprised of two parallel CNNs. Each CNN uses two pathways (i.e., local, and global pathways) illustrated in Figure 4.5.

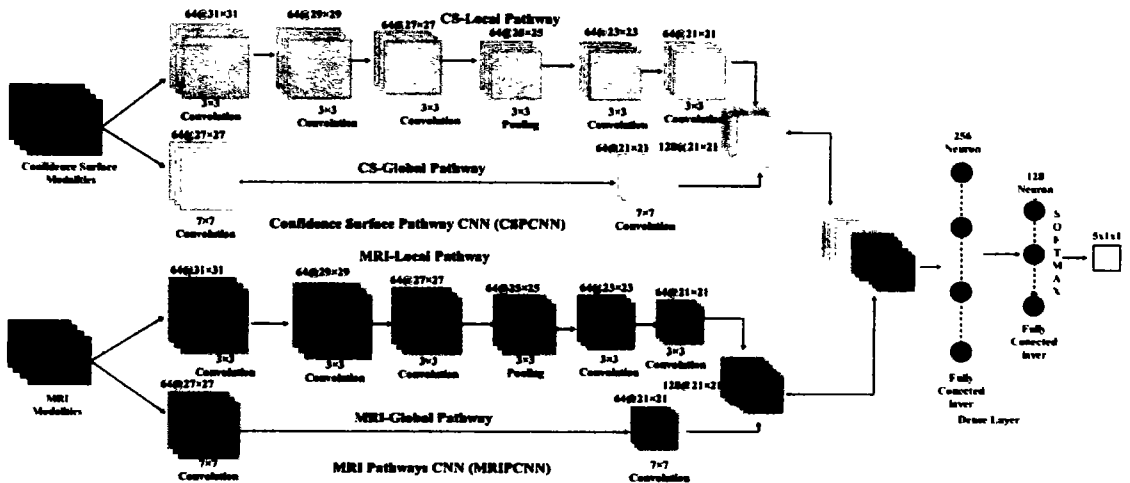


Figure 4.5: Proposed CNN Architecture

The first CNN is called CSPCNN. The CSmodalities, along with the given manual ground truth are processed. The second CNN is called MRI Pathways CNN (MRIPCNN). Along with the provided manual ground truth, the MRI imaging

techniques undergo processing. Both the CSPCNN and MRIPCNN models feature local pathways comprising five convolutional layers, each with a 3×3 convolutional kernel operating at a stride of 1, and a single pooling layer that also uses a 3×3 kernel but varies the stride across 1, 3, 4, and 5. This configuration is detailed in Table 4.1.

Table 4.1: Architectural detail of CSPCNN Local Pathway

Layer	Type	Filter size	Strides	Filters	FC unit	Input	Output
Layer1	Convolution	3×3	1×1	64	-	$4 \times 33 \times 33$	$64 \times 31 \times 31$
Layer2	Convolution	3×3	1×1	64	-	$64 \times 31 \times 31$	$64 \times 29 \times 29$
Layer3	Convolution	3×3	1×1	64	-	$64 \times 29 \times 29$	$64 \times 27 \times 27$
Layer4	Max-pool	3×3	1×1	-	-	$64 \times 27 \times 27$	$64 \times 25 \times 25$
Layer5	Convolution	3×3	1×1	64	-	$64 \times 25 \times 25$	$64 \times 23 \times 23$
Layer6	Convolution	3×3	1×1	64	-	$64 \times 23 \times 23$	$64 \times 21 \times 21$

Table 4.2: Architectural detail of CSPCNN global Pathway

Layer	Type	Filter size	Strides	Filters	FC unit	Input	Output
Layer1	Convolution	7×7	1×1	128	-	$4 \times 33 \times 33$	$128 \times 27 \times 27$
Layer2	Convolution	7×7	1×1	128	-	$128 \times 27 \times 27$	$128 \times 21 \times 21$

The first CNN is called CSPCNN. The CSmodalities, along with the given manual ground truth are processed. The second CNN is called MRIPCNN. The MRI modalities, along with the provided manual ground truth, are processed. Both CSPCNN and MRIPCNN have local pathways consisting of five convolutional layers with a 3×3 convolutional kernel at stride 1 and one pooling layer with a kernel size of 3×3 at strides 1, 3, 4, and 5.

Similarly, the global pathways of both CSPCNN and MRIPCNN are comprised of two convolution layers with convolutional kernels of size 7×7 at stride 1 see Table 4.2.

Table 4.3: Architectural detail of Global CNN

Type	Filter size	Strides	Filters	FC unit	Input	Output
FC	256				$256 \times 21 \times 21$	14,450,688
FC	128			-		
Softmax	5			-		

The architectures of the two CNNs are integrated by merging their respective feature maps. These combined feature maps are subsequently processed through two closely

connected layers. Softmax activation is used for the final segmentation. The ReLU loss function is employed to evaluate the model's performance.

4.2 Experiments

The research implementation process is divided into two stages. The first stage involves the implementation of handcrafted features, such as ELBP, DWT, and GLCM) at each pixel neighborhood. The second phase consists of the performance of GCNN (i.e., CSPCNN and MRIPCNN).

In the phase, three handcrafted features, i.e., ELBP, DWT, and GCLM, are computed in a local neighborhood at each pixel location shown in Figure 4.6.

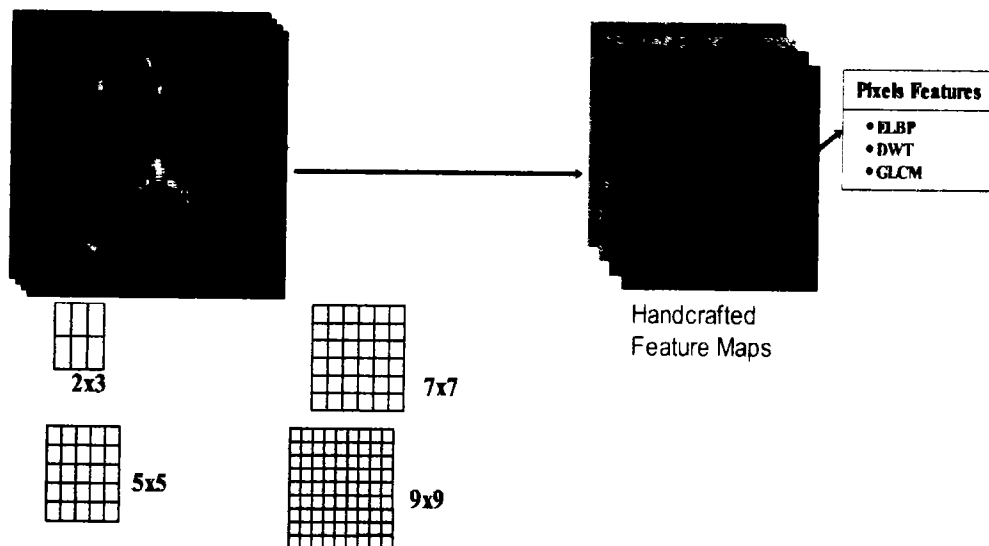


Figure 4.6: Pixel Level Neighborhood with Kernel Sizes of 3,5,7, and 9

The computed features are combined to construct a single feature vector, and subsequently, each pixel is labeled as either healthy or tumorous, as shown in Figure 4.7.

In the dataset, each MRI modality is assigned a unique contrast signature to the same tumor pixel location. Taking inspiration from this observation, a separate modality has been created from handcrafted features.

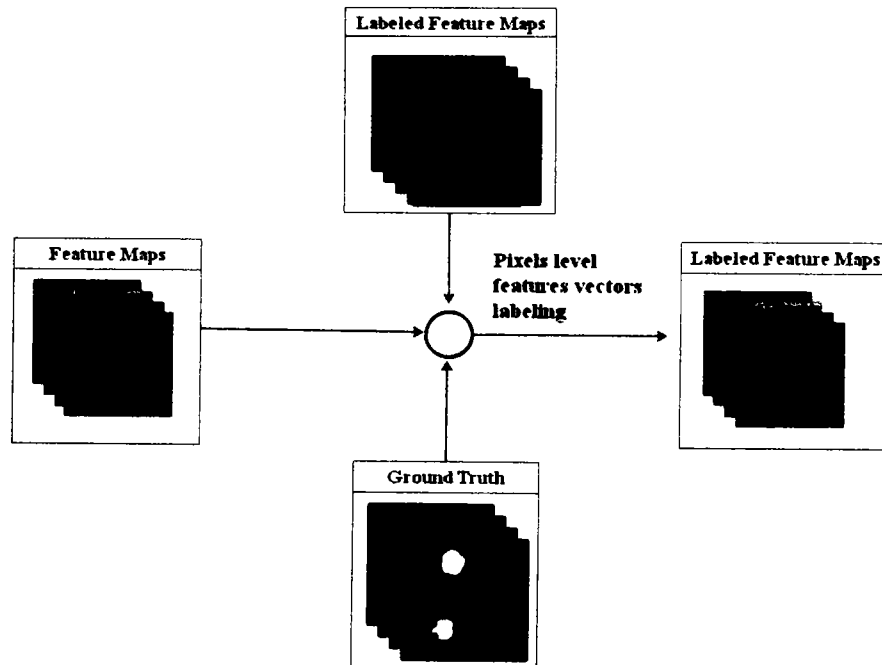


Figure 4.7: Pixel Level Example Labeling

This pixel classification generates four CSmodalities shown in Figure 4.8, Figure 4.9, Figure 4.10 and Figure 4.11. We kept three horizontal and vertical strides in the healthy region and one horizontal and vertical stride in the tumor region. Due to the class imbalance issue, the results of handcrafted techniques are positively biased.

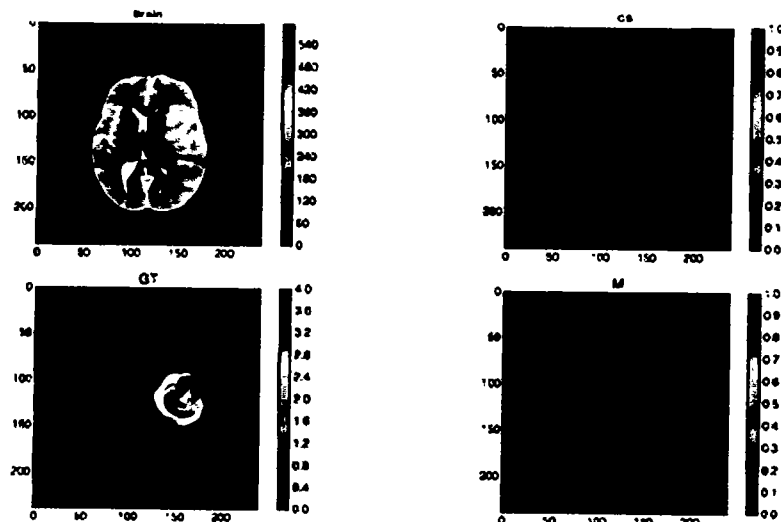


Figure 4.8: T1-weighted MRI confidence surface

As a result, this leads to improved quality in CSmodalities, directly impacting the final brain tumor segmentation. The output of the first phase, CSmodalities, serves as input to CSPCNN during the second phase of implementation. CSPCNN processes the output

of handcrafted features based on traditional ML, which function as estimated prior knowledge in GCNN.

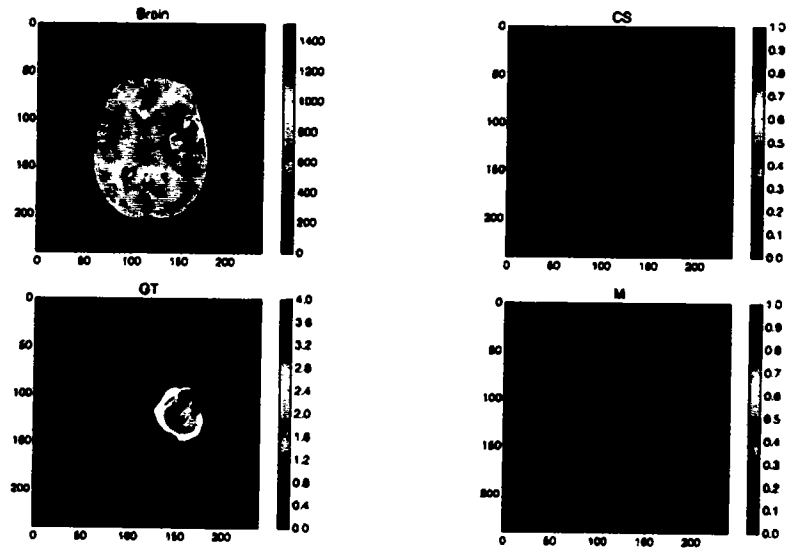


Figure 4.9: T1c-weighted MRI confidence surface

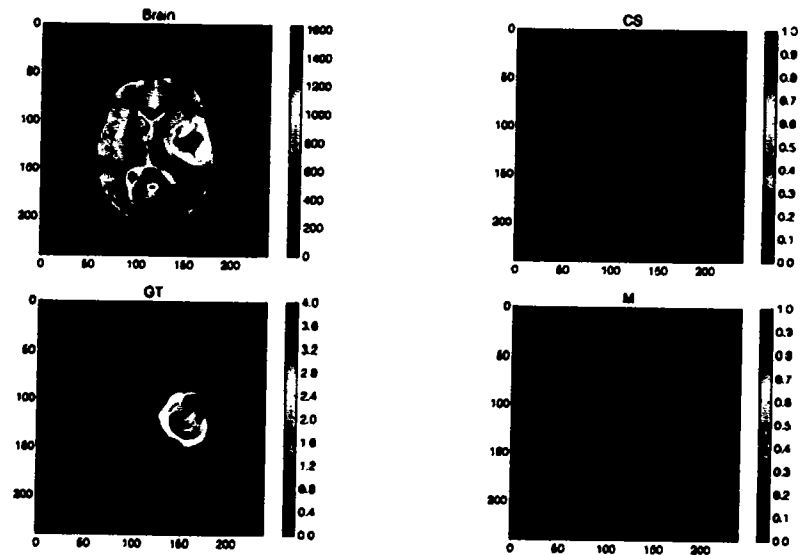


Figure 4.10: T2-weighted MRI confidence surface

During the second phase of the implementation process, the output of the first phase (i.e., CS-modalities), along with the given ground truth is provided to CSPCNN as input. Similarly, four MRI modalities (i.e., T1, T1c, T2, FLAIR) along with ground truth are also provided to MRIPCNN as input. The detailed information on CSPCNN, MRIPCNN, and GCNN can be seen in Figure 4.11.

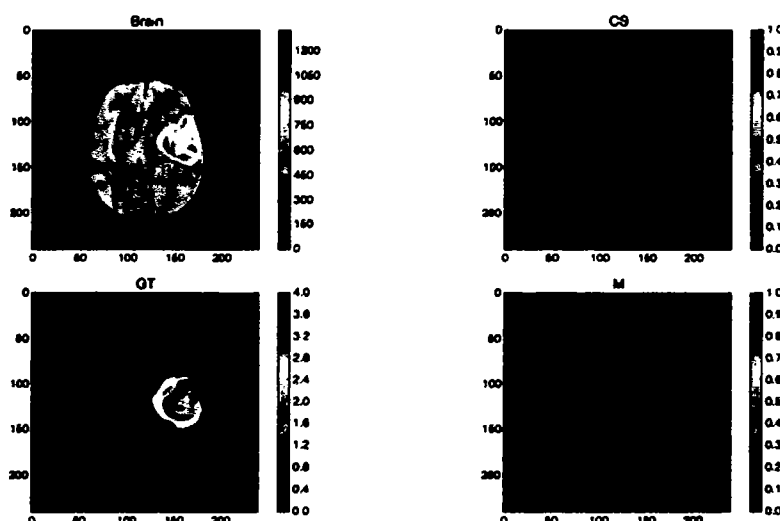


Figure 4.11: FLAIR MRI confidence surface

To evaluate the efficacy of our proposed model, we conducted a thorough analysis employing various widely accepted metrics such as the Dice score. Additionally, as demonstrated in Figure 4.12.

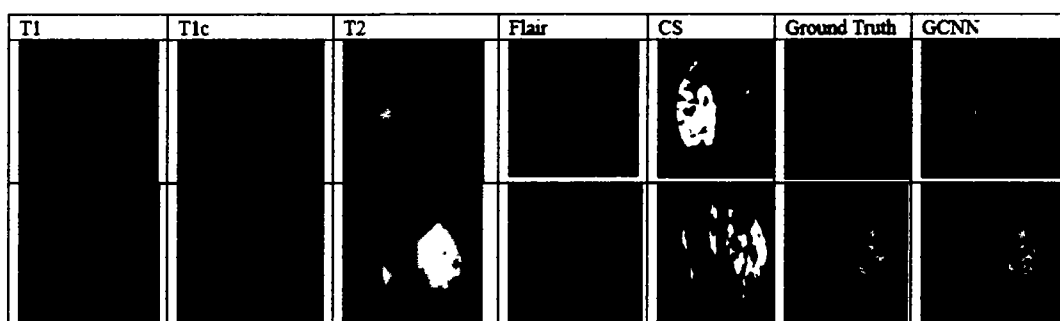


Figure 4.12: predated MRI model

Table 4.4 presents a comparative analysis between the traditional CNN approach and the suggested GCNN method, highlighting the improvement in performance metrics achieved by incorporating handcrafted features into the brain tumor segmentation process.

Table 4.4: Performance Evaluation of Brain Tumor Segmentation Using CNN and GCNN Approaches

Method	Whole Tumor	Core Tumor	Active Tumor
Pure CNN Approach	0.77	0.69	0.65
Proposed GCNN	0.87	0.79	0.75

The training and validation loss Figure 4.13 illustrates the gradual decrease in loss throughout the training process. This loss reduction signifies that the model is

effectively learning and improving its predictive capabilities as it iterates over the training data.

Figure 4.14 illustrates the training and validation loss over 100 epochs, indicating improvements in the model's performance and its increasing accuracy in making predictions over time.

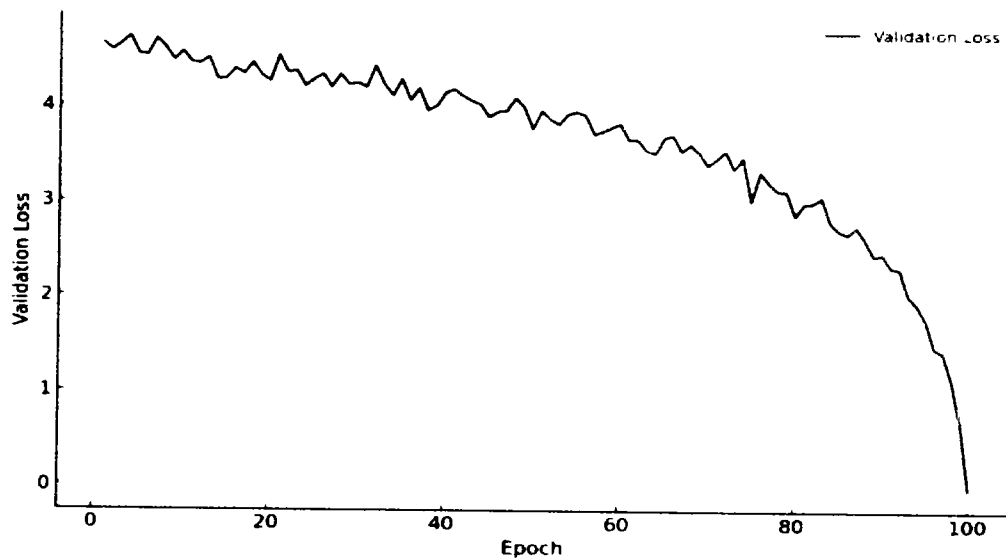


Figure 4.13: Training Loss of the Proposed Model

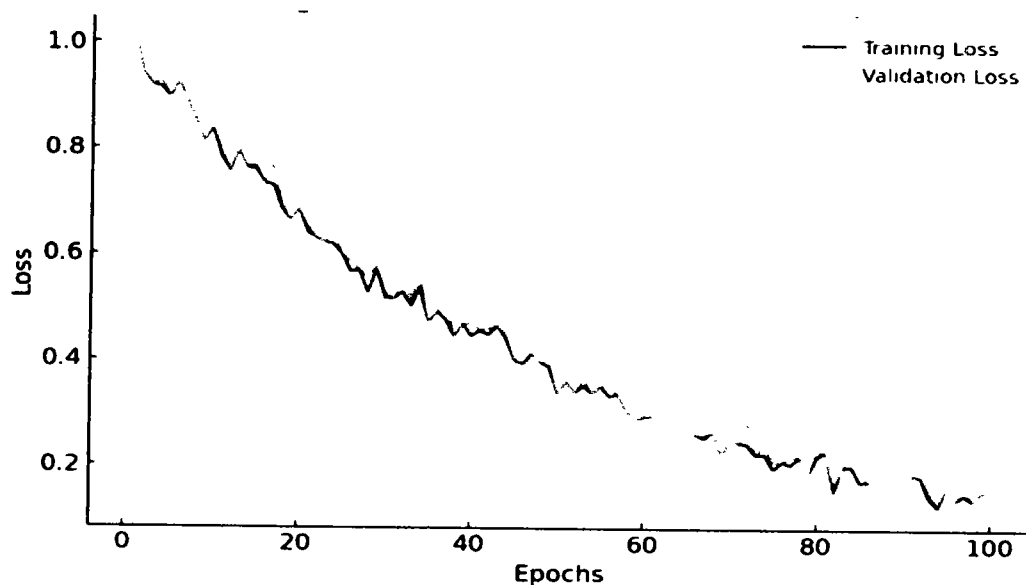


Figure 4.14: Training and Validation Loss over 100 Epochs

To evaluate the efficiency of our hybrid approach, which merges manually designed features with CNN, we conducted a comparative analysis with state-of-the-art methodologies documented in recent research.

Table 4.5: Performance evaluation of the proposed model vs state of the art.

Ref.	Method	Whole Tumor	Core Tumor	Active Tumor
[25]	Divide-wise 2D-patches extracted by 2D-CNN	0.83	0.73	0.69
[28]	3D-patches extracted by using 3D-CNN	0.86	0.74	0.71
[26]	Global and local 2D patches with cascaded 2D-CNNs	0.86	0.79	0.73
[29]	Extract multi 2D patches using pixel level	0.67	Not reported	Not reported
[23]	2D-CNNs	0.76	0.81	0.73
Proposed System	Handcrafted Features and Global Pathway	0.87	0.79	0.75

Table 4.5 presents the performance comparison. The outcomes show that GCNN's overall performance is accurate. With a momentum of 0.9, a weight decay of 0.1, a learning rate of 0.005, and stochastic gradient descent, these results were produced.

4.3 Chapter Summary

This chapter discusses the prevailing methods for segmenting brain tumors primarily depending on manually designed characteristics (such as symmetry analysis, alignment-based feature analysis, or textural properties) or deep CNN. Handcrafted features aim to incorporate domain knowledge, while CNN approaches focus on unsupervised feature generation. Integrating these techniques in a sequential cascade could potentially exceed the performance of other feature-based or data-driven techniques individually. The present study involved the development of a GCNN consisting of CNN for CS Pathways to manage CS modalities in conjunction with the given ground truth, and another CNN for MRI Pathways. The objective of this study is to construct a proficient deep convolutional architecture supplemented with manually designed features capable of effectively managing various categories of tumors. This study highlights the potential of concatenating traditional feature-based approaches with deep learning methods to improve the accuracy of brain tumor segmentation. The proposed GCNN can be further refined and optimized to achieve even higher segmentation accuracy. Additionally, the approach can be extended to other medical imaging applications, such as the detection and segmentation of other types of tumors or lesions, to aid in diagnosis and treatment planning.

CHAPTER 5

MULTIMODAL LIGHTWEIGHT APPROACH FOR BRAIN TUMOR GRADE PREDICTION

Chapter 5

Multimodal Lightweight Approach for Brain Tumor Grade Prediction

On a worldwide scale, Brain tumors, a potentially lethal condition, impact millions of individuals. They inflict harm upon healthy brain tissue and have the potential to elevate intracranial pressure, leading to potentially fatal consequences in numerous instances. Early identification and accurate classification of brain tumors are crucial for optimal treatment planning and effective patient management. This section suggests utilizing the multimodal lightweight Gradient Boosting Technique (MM-XGB) to predict the grade of brain tumors. Brain tumors are categorized based on their grades using an ensemble machine learning technique. This method involves preprocessing MRI data to extract features based on intensity, texture, and shape. The analysis is performed on 285 MRI scans of patients diagnosed with gliomas from the BraTS 2020 dataset.

The proposed lightweight method demonstrates high performance in classifying brain tumors, with an accuracy of 93.0%, precision of 0.94, recall of 0.93, and F1 score of 0.94. The results underscore the potential of the proposed strategy as a valuable instrument for early detection and strategic formulation of treatments for brain tumors. The study findings demonstrate the potential of the proposed MM-XGB methodology as an effective and convenient approach for accurately classifying brain tumors. This strategy holds the capacity to facilitate the timely identification and formulation of treatment plans, ultimately augmenting the quality of patient care and outcomes.

5.1 Introduction

Primary brain tumors are a major worldwide health issue, leading to a significant number of cancer-related deaths. The ABTA reports that there are approximately 700,000 individuals in the United States who are impacted by brain tumors, and around 88,000 new cases are diagnosed annually [103]. Given the increasing prevalence of brain tumors, it is crucial to promptly and efficiently diagnose and treat them in order to improve patient outcomes. Brain tumors are usually classified according to their

histopathological characteristics, which determine their grading and prognosis. The ICD-10, which is the result of international collaboration, employs three-digit numeric codes for the classification of diseases [104].

The traditional approach to grading brain tumors necessitates pathologists to manually assess histological characteristics, which is both time-consuming and subjective [105]. This methodology frequently results in significant discrepancies among observers, leading to inconsistent choices in treatment and potentially less than optimal results for patients [106]. It is essential to develop objective and automated techniques for grading and classifying brain tumors in order to overcome these limitations. ML techniques have become influential tools in the field of medical image analysis, showcasing the exceptional capacity for assessing and categorizing brain tumors [107]. ML algorithms possess the capability to autonomously detect and analyze patterns and characteristics within medical images, thereby enabling a more impartial and uniform assessment and categorization of tumors. Moreover, these algorithms possess the capability to efficiently handle immense volumes of data, rendering them highly adaptable and appropriate for extensive applications [108]. Integrating machine learning algorithms into brain tumor grading classification processes can greatly enhance patient outcomes by offering more accurate and consistent grading [109]. This enables healthcare practitioners to formulate personalized treatment strategies and accurately monitor the progression of illnesses. ML algorithms can reduce the burden on pathologists and radiologists by automating the grading and analysis of medical images, which are typically time-consuming tasks [110]. ML techniques have significantly transformed medical image analysis, leading to improved precision and effectiveness in diagnosing, treating, and monitoring a wide range of diseases [111].

Medical image analysis is an essential component of clinical practice as it offers vital insights into the structure and functioning of different organs and tissues. Various machine learning techniques, such as supervised learning, unsupervised learning, semi-supervised learning, and reinforcement learning, are employed in the analysis of medical images. These techniques are crucial in extracting significant data from the extensive range of medical imaging data, assisting in the process of diagnosing, planning treatment, and managing patients [112]. Each of these techniques is customized for particular tasks, and their application in medical image analysis is anticipated to grow, resulting in enhanced patient outcomes and decreased burden on

healthcare providers. This study seeks to deepen the comprehension of machine learning techniques used in the analysis of medical images, particularly focusing on the classification of brain tumor grades. The text emphasizes the advantages of employing ML algorithms to enhance the accuracy and dependability of tumor grading. This advancement possesses the capability to improve patient results and diminish the workload for medical professionals. ML approaches have demonstrated significant potential in transforming medical image analysis, especially in the classification and grading of brain tumors. The utilization of ML algorithms offers several advantages, including the ability to tailor treatment plans to individual patients, enhance patient outcomes, and effectively monitor the progression of illnesses. The increasing utilization of machine learning (ML) techniques in medical image analysis is expected to improve patient care and alleviate the burden on healthcare professionals. The use of machine learning techniques in medical image analysis is expected to continue growing, resulting in improved patient outcomes and reduced burden on healthcare professionals.

The gradient-boosting algorithm is suggested for constructing a compact machine learning model that accurately determines the grade of a brain tumor.

The integration of an ensemble learning model with multiple gradient boosting techniques enhances accuracy and mitigates overfitting.

A refined regularization technique to augment the precision of tumor detection and mitigate overfitting, thereby enhancing accuracy.

The proposed work is motivated by the pressing necessity to accurately and efficiently classify brain tumor grades. This approach seeks to enhance patient care and outcomes by utilizing machine learning and multimodal features extracted from MRI data to improve early diagnosis and treatment planning. The ramifications of utilizing machine learning for brain tumor grading are advantageous in tailoring treatment plans to individual patients. Additionally, it aids in enhancing disease progression and alleviating the workload on healthcare providers.

5.2 Methodology

This section introduces the proposed system for autonomously evaluating brain tumors. The approach involves utilizing diverse sets of data and employing an optimized

methodology centered around XGBoost. This procedure entails several sequential steps: initially, data preparation is conducted, followed by the extraction of salient features, and ultimately, the integration of all components utilizing a specialized form of classification known as ensemble classification as in Figure 5.1.

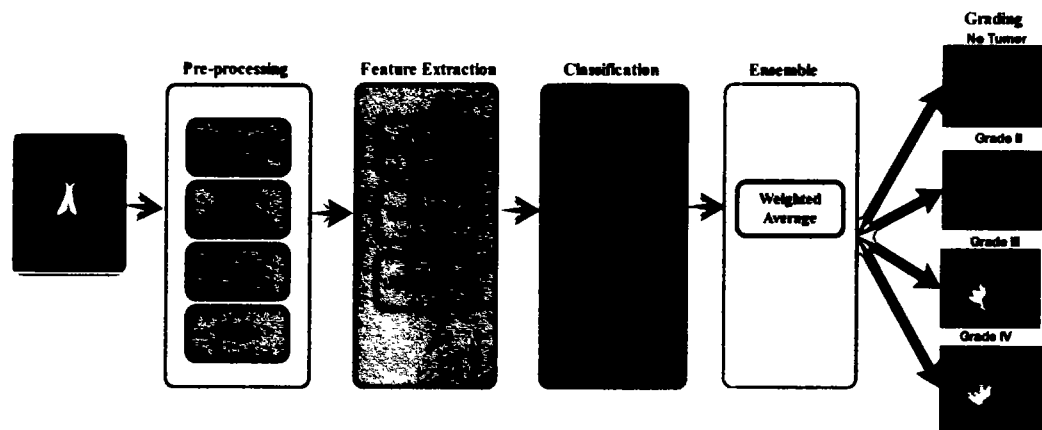


Figure 5.1: An efficient method for classifying brain tumors based on their severity

Data was acquired from the BraTS for 2020 [101] and the Local hospital under the supervision of a Radiologist. The BraTS dataset is readily accessible for research purposes and is commonly employed as a reference for segmentation tasks. The dataset comprises 285 and 59 scans conducted on patients with gliomas using various imaging techniques, such as T1-weighted, T2-weighted, contrast-enhanced T1-weighted, and FLAIR sequences. The scans were carefully analyzed by skilled radiologists to determine the tumor grade according to the WHO categorization system. Subsequently, a training set comprising 70% of the data and a testing set comprising 30% were generated.

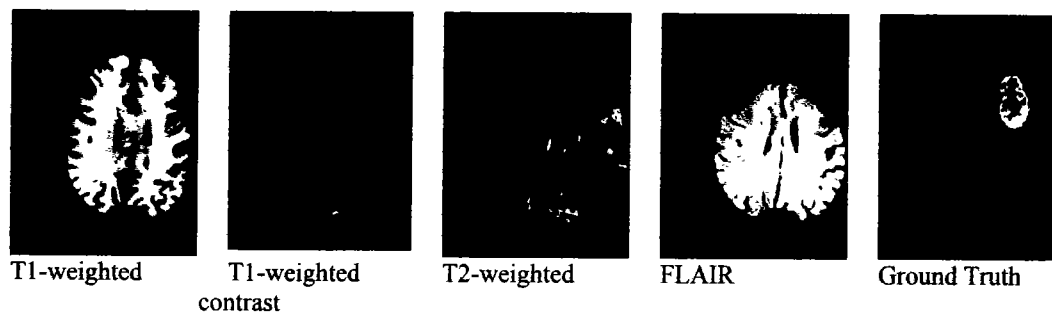


Figure 5.2: Various Modalities of a Brain Tumor in BraTS

Figure 5.2 exhibits an MRI specimen obtained from the BraTS dataset. The scan comprises T1-weighted, contrast-enhanced, T2-weighted, and FLAIR sequences. The T1-weighted sequence provides a clear distinction between the tumor and cerebral tissue. The T1-weighted contrast-enhanced sequence yields additional data on tumor

vascularity. The T2-weighted and FLAIR sequences reveal the presence of tumor edema and infiltration into surrounding tissues. Table 5.1 displays the distribution of tumor grades in the BraTS dataset. The dataset comprises tumor Grades II, III, IV, and non-tumor. Tumors classified as Grade-III and Grade-IV have a more unfavorable prognosis compared to tumors classified as Grade-II. Non-tumor scans enable the model to differentiate between brain tissue and tumor tissue.

Table 5.1: Tumor grades in the BraTS dataset distribution.

Tumor Grade	Number of Scans	Private
Grade-II	118	26
Grade-III	121	14
Grade-IV	46	9
No Tumor	0	10
Total	285	59

Skull segmentation, standardization of intensity levels, and alignment of images were performed to enhance the quality of the dataset. Skull stripping is a process that eliminates non-brain tissue from MRIs. Scan intensity values were standardized across modalities through intensity normalization. Image registration is the process of aligning scans from different modalities. The training, validation, and testing sets are generated randomly from the dataset. The validation set is employed to select the appropriate hyperparameters, the testing set is utilized to assess the performance of the model, and the training set is employed to train the machine learning model. This study utilized the BraTS (Brain Tumor Segmentation) dataset to outline the process of preparing the dataset. The dataset includes information on the grades of tumors and the quality assurance measures taken.

5.2.1 Preprocessing

Preprocessing is an essential stage in converting unprocessed data into a format that is better suited for analysis. It often involves multiple procedures. Preprocessing of MRI scans typically involves multiple procedures aimed at removing unnecessary brain tissues, adjusting image intensities, and reducing the size of the images.

The MRI preprocessing procedures are presented in Table 5.2; image registration is commonly the first step in the preprocessing of MRI data. Image alignment refers to the process of arranging multiple images, whether they depict the same object or different objects, in a common coordinate system. Skull stripping involves removing all non-brain tissues from the images. It is crucial to perform this step because the

presence of non-brain tissues can impact the accuracy of the analysis. Skull stripping was performed using the Brain Extraction Tool (BET) in this case.

Table 5.2: Preprocessing procedures for MRI imaging

Preprocessing Step	Method
Image Registration	Elastix library in Python
Skull Stripping	BET
Intensity	Z-score normalization method
Normalization	--
Resampling	Voxel size of 1mm x 1mm x 1mm

Ultimately, the images were adjusted to a consistent size of 240×240 pixels. Resizing the images is essential to standardize their sizes for analysis, as different images may have varying dimensions. The selection of a fixed size of 240×240 pixels may have been influenced by considerations such as the resolution of the original images and the computational resources accessible for analysis. The preprocessing steps were essential to ensure that the MRI scans were in a suitable format for analysis using machine learning models.

5.2.2 Feature Extraction and Selection

Intensity- and texture-based features were utilized to extract characteristics from MRI scans. Within MRI scans, intensity-based features gather the numerical values of each pixel's intensity, whereas texture-based features document the spatial organization of pixels. The summary of extracted features is displayed in Table 5.3.

Table 5.3: Overview of Extracted Features

Feature Type	Features Extracted
Intensity-based	Different brain areas' means, standard deviations, skewness, and kurtosis
Texture-based	Using GLCM, contrast, energy, homogeneity, and entropy
Shape-based	Area, Perimeter, Circularity, Solidity, and Eccentricity of tumor regions

Intensity-based features are mathematical descriptors that represent the numerical values of intensity within an MRI image. These characteristics are frequently calculated from distinct regions of interest (ROIs) within the MRI image that correspond to various types of tissue, such as healthy brain, tumor, or necrotic tissues. Several intensity-based

features have been devised for brain tumor grading, such as mean intensity, standard deviation, skewness, kurtosis, histogram features, and texture features.

The mean intensity function calculates the average intensity of a region of interest (ROI). The mean intensity values of tumor tissue are higher than those of normal brain tissue. The standard deviation measures the variability of ROI intensity. Higher-grade cancers often exhibit heterogeneous tissue. Skewness and kurtosis evaluate the distribution of ROI intensity. Kurtosis evaluates the degree of peakedness or flatness in a distribution, whereas skewness quantifies the extent of asymmetry. Elevated skewness and kurtosis values may indicate the presence of unhealthy tissue.

$$MRI\ Mean = \left(\frac{1}{n}\right) \times \sum_{i=Li}^{i=1} \quad (5.1)$$

Where Li is the intensity value of pixel i and n is the total number of pixels in the ROI.

$$SD = \sqrt{\left(\frac{1}{n}\right) \times \sum_{i=1}^n (Li - MRI\ Mean)^2} \quad (5.2)$$

where n is the ROI's pixel, Li is the pixel's intensity value, and mean is the ROI's mean intensity value.

$$Skewness = \left(\frac{1}{n}\right) \times \sum_{i=1}^n \left[\frac{Li - MRI\ Mean}{SD} \right]^3 \quad (5.3)$$

In this context, " n " denotes the number of pixels within the region of interest (ROI). The term " Li " represents the intensity value of pixel " i " located within the region of interest (ROI). The term "mean" denotes the average intensity value of the region of interest (ROI), while "SD" stands for its standard deviation.

$$Entropy = \sum_{i=1}^L (pi \times \log_2(pi)) \quad (5.4)$$

The equation involves the variable L , which represents the number of gray levels in the region of interest (ROI). Additionally, pi represents the probability of gray level i occurring, and \log_2 refers to the logarithm with base 2.

Kurtosis is a statistical metric that quantifies the degree of "peakedness" or "flatness" of a distribution. Kurtosis is a useful measure for characterizing brain images in the analysis of MRI images.

$$K = \frac{1}{N} \sum \frac{(x_i - \bar{x})^4}{\sigma^4} \quad (5.5)$$

Where K is the image's kurtosis, N is the number of voxels, x_i is the i th voxel's intensity, and \bar{x} is the image's mean intensity. The image intensity standard deviation is sigma.

Histogram features are obtained by analyzing the distribution of intensity values within a Region of Interest (ROI). Some examples of histogram features are the percentiles, which quantify the intensity values that are below a specific percentage of the pixels. Entropy quantifies the level of randomness or lack of organization in the intensity values. The utilization of intensity-based features has the potential to enhance the accuracy of MRI brain tumor grading, either independently or in conjunction with shape or texture features. Additionally, they have the ability to track changes in tumor characteristics over a period of time in order to assess the effectiveness of treatment and the overall condition of the patient. Overall, the utilization of intensity-based MRI features enhances the accuracy of brain tumor diagnosis and treatment. Texture-based attributes are employed in the fields of image processing and computer vision. GLCM quantifies the statistical distribution of gray levels in an image. The process entails constructing a matrix that evaluates the spatial correlation between pixels exhibiting particular gray-level values. Texture-based characteristics indicate the presence of image texture. GLCM is capable of extracting texture-related measures such as contrast, energy, homogeneity, and entropy. Contrast quantifies the local variations in pixel intensity of an image. Homogeneity quantifies the spatial separation of pixels that have the same gray-level values, whereas energy evaluates the level of uniformity in an image. Entropy quantifies the level of disorder in an image.

$$Contrast = \sum_{i,j=0}^{n-1} (i - j)^2 \times p(i, j) \quad (5.6)$$

$P(i,j)$ is the normalized frequency of occurrence of pixel pairings with gray levels i and j , where i and j are the gray-level values of two nearby pixels.

$$Energy = \sum_{i,j=0}^{n-1} p(i, j)^2 \quad (5.7)$$

where n is the gray levels in the image and $P(i,j)$ is the normalized frequency of pixel pairs with i and j .

$$Homogeneity = \sum_{i,j=0}^{n-1} \left(\frac{p(i,j)}{1+|i-j|} \right) \quad (5.8)$$

where N is the number of gray levels in the image, $p(i,j)$ is the normalized frequency of pixel pairs with gray levels i and j , and $|i-j|$ is the absolute difference.

$$Entropy = -energy = \sum_{i,j=0}^{n-1} (p(i,j) \times \log_2(p(i,j) + \epsilon)) \quad (5.9)$$

Let N represent the number of gray levels in the image. $P(i,j)$ denotes the normalized frequency of pixel pairs with gray levels i and j . To avoid undefined logarithm values for probabilities of 0, a small value is added. Texture features derived from GLCM (Gray-Level Co-occurrence Matrix) can augment image processing tasks such as segmentation, recognition, and classification by offering valuable insights that lead to enhanced accuracy and performance.

Shape-based characteristics are essential in the analysis of MRI brain tumor images. The aforementioned features offer quantitative metrics such as area, perimeter, circularity, solidity, eccentricity, convexity, compactness, and symmetry of the tumor region. These metrics can be employed to differentiate among various kinds of brain tumors, monitor the progression of tumor growth, and assess the effectiveness of treatments. Furthermore, these features can be used as inputs for machine learning algorithms to develop predictive models for diagnosing and treating brain tumors. From a mathematical standpoint, it can be expressed as.

$$A = \sum p(x_i, y_i) \quad (5.10)$$

The pixel intensity value of each region of the tumor is denoted as $P(x_i, y_i)$. Determine the perimeter of the tumor region by measuring the length of its boundary. The procedure can be expressed as:

$$P = \sum p(x_i + 1, y_i) = p(x_i, y_i) \quad (5.11)$$

The expression $P(x_i, y_i)$ denotes the intensity value of a pixel located on the boundary of the tumor region. The sum of all boundary pixels is calculated. The circularity of the tumor region is defined as the ratio of its perimeter to its area. Mathematically, it can be expressed as shown in Equation 12.

$$C = \frac{(4\pi A)}{P^2} \quad (5.12)$$

P represents the perimeter of the tumor, while A represents its area. The eccentricity of the tumor region is mathematically expressed by the ratio of the length of the major axis to the distance between the foci of the best-fitting ellipse.

$$E = \sqrt{\frac{(1-b)^2}{a^2}} \quad (5.13)$$

The lengths of the best-fitting ellipse's major and minor axes are a and b .

5.2.3 Multimodal Lightweight XGBoost

The Multimodal Lightweight XGBoost approach is a machine learning technique used to predict the grade of brain tumors. It employs a combination of XGBoost classifiers to form an ensemble. This method entails the amalgamation of various modalities of MRI scans to forecast the severity level of brain tumors.

XGBoost is a gradient boosting framework that uses decision trees to model the relationships between features and the target outcome. The model constructs an ensemble of decision trees in an iterative manner, employing gradient descent to minimize the loss function. The XGBoost algorithm, which is lightweight, accesses features from MRI data with n samples and m dimensions.

$$f(x) = \sum_{k=1}^K f_k(x) \quad (5.14)$$

$F(x)$ is used to forecast the labels of new samples. The function $f_k(x)$ denotes the collective sum of K regression trees ranging from 1 to k . Every regression tree is trained to minimize the value of L , which signifies the difference between the predicted and actual values. The loss function L can be represented by any differentiable function, such as mean squared error for regression tasks or binary cross-entropy for

classification tasks. XGBoost finds the regression trees $\{fk\}$ from $k=1$ to K that minimize the following objective function.

$$l(\{fk\}k) = 1K = \sum_{i=1}^n L(y_i, F(x_i)) + \sum_{k=1}^K \Omega(fk) \quad (5.15)$$

The term $\Omega(f_k)$ represents a regularization term that penalizes intricate trees in order to avoid overfitting. The regularization term commonly adopts the structure.

$$\Omega(fk) = \gamma T + 1/2 \mu \sum_{j=1}^T w_j^2 \quad (5.16)$$

T represents the number of leaves in the tree, w_j represents the weight of the j^{th} leaf, and gamma and lambda are hyperparameters that control the level of regularization. The XGBoost algorithm employs a gradient-boosting technique to train the trees. At every iteration t , the algorithm incorporates a new tree f_t into the ensemble by training it on the negative gradient of the current forecasts' loss function.

$$-\frac{l(y_i, f_{t-1}(x_i))}{f_{t-1}(x_i)} \quad (5.17)$$

Subsequently, the weight that governs the learning rate is combined with the ensemble, along with the addition of the new tree.

$$F_t(x) = F_{t-1}(x) + \theta \times f_t(x) \quad (5.18)$$

The suggested efficient approach repeats this procedure until the loss function reaches convergence or the maximum number of trees K is attained. The ultimate forecast is derived by aggregating the predictions from each individual tree within the ensemble.

5.2.4 Lightweight Ensemble

The proposed Lightweight model utilizes an ensemble of multiple XGBoost decision trees to generate predictions. Every individual decision tree in XGBoost yields a prediction that is relatively weak, but these predictions are subsequently aggregated with the predictions of other trees to generate a final prediction. The ultimate forecast is a calculated combination of the forecasts generated by each individual tree, with each tree being assigned a weight according to its performance. To grade brain tumors, one can train multiple instances of the XGBoost algorithm using various subsets of multimodal data. Each occurrence can undergo training using distinct hyperparameters, including the learning rate, the quantity of trees, the maximum depth for each tree, and the minimum count of instances needed for splitting a node, as detailed in Table 5.4.

This facilitates the generation of varied instances of the algorithm that can effectively complement each other's respective advantages and disadvantages.

After training each iteration of the algorithm, their predictions can be aggregated to generate a conclusive prediction for the tumor grade. A weighted average approach is employed to merge predictions. The ultimate prediction is determined by the formula: where Y_i represents the prediction of the i th instance of the algorithm, W_i denotes the weight assigned to the i th instance, and $\sum W_i$ represents the sum of weights. The weights can be ascertained by evaluating the performance of each instance on a validation set. The weight assigned to each grade can be computed using the formula that follows: (Weight for grade i) = (Accuracy for grade i on the validation set) / (Total accuracy on the validation set):

$$W_i = \frac{1}{(1 + \exp(-\lambda \times \text{error_}i))} \quad (5.19)$$

The variable $\text{error_}i$ represents the validation error of the i th instance, while λ is a tuning parameter that determines the significance of the validation error in the weight calculation.

Table 5.4: Overview of the Ensemble hyperparameters

	Learning Rate	Number of Trees	Maximum Depth	Minimum Instances	Validation Error	Weight
XGBoost1	0.1	100	6	10	0.2	0.47
XGBoost2	0.05	200	4	20	0.18	0.53
XGBoost3	0.2	50	8	5	0.24	0.43

The hyperparameters used for training three instances of the XGBoost algorithm for brain tumor grading are displayed in Table 5.4. Every occurrence is trained on a distinct subset of the multimodal data, utilizing distinct hyperparameters. The validation error and weight for each instance are displayed as well.

5.3 Results and Discussion

The BraTS 2020 dataset was employed, and stratified sampling was implemented during the training process to tackle the issue of class imbalance. The preprocessing of the MRI images involved three steps: scaling, intensity normalization, and skull extraction. The dataset is primarily composed of Grade-II cancers, with Grade-III and Grade-IV tumors being significantly underrepresented, resulting in a severe imbalance.

The imbalance in the dataset may adversely affect the performance of the ML models, leading to potentially inaccurate results.

Stratified sampling is employed to tackle the problem of class imbalance in model training and testing. Stratified sampling ensures that the distribution of samples from each class in the training and testing sets is proportional to the distribution of samples in the entire dataset. The preprocessing of medical images, specifically MRI scans, is an essential phase in the analysis process. Preprocessing is performed to enhance the quality of images and reduce the effects of noise and artifacts. The MRI images in the dataset were subjected to preprocessing prior to training the machine learning models on them. Skull normalization, resizing, and stripping were all steps involved in the preprocessing procedure. The BET method was employed to conduct skull stripping, which involves the removal of non-brain elements. The images' intensity levels were adjusted through normalization to achieve a mean of zero and a standard deviation of one. The images were subsequently resized to a definitive dimension of 240×240 pixels.

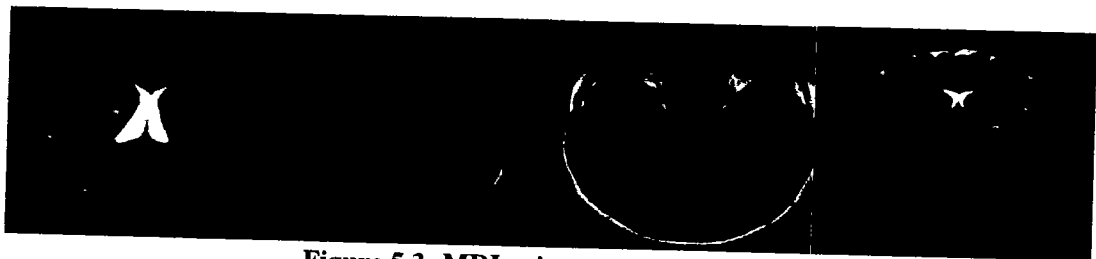


Figure 5.3: MRI prior to preprocessing

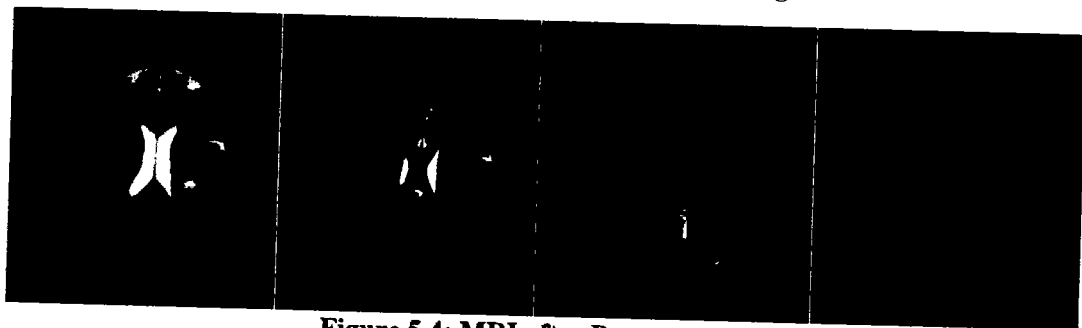


Figure 5.4: MRI after Preprocessing

The MRI scans undergo image registration, skull stripping, intensity normalization, and resampling to improve their quality and minimize the impact of noise and artifacts. These processes are detailed in Table 5.3 and Table 5.4.

Subsequently, the subsequent step involves extracting distinctive features from the preprocessed MRI scans. Feature extraction refers to the process of extracting valuable information from images that can be used as inputs for machine learning algorithms.

The study involved extracting the features from the preprocessed MRI scans, as indicated in Table 5.5.

Table 5.5: Features extracted for various grades of brain tumors.

Feature Type	Grade-II	Grade-III	Grade-IV
Intensity-based	Mean	Mean	Mean
	Std Dev	Std Dev	Std Dev
	Skewness	Skewness	Skewness
	Kurtosis	Kurtosis	Kurtosis
Texture-based	Contrast	Contrast	Contrast
	Energy	Energy	Energy
	Homogeneity	Homogeneity	Homogeneity
	Entropy	Entropy	Entropy
Shape-based	Area	Area	Area
	Perimeter	Perimeter	Perimeter
	Circularity	Circularity	Circularity
	Solidity	Solidity	Solidity
	Eccentricity	Eccentricity	Eccentricity

Table 5.6 lists the results of feature extraction for each grade of brain tumor. The retrieved features are categorized into three groups: intensity-based, texture-based, and shape-based features. Several characteristics were obtained for each category, and the average values of those characteristics were computed for each tumor grade. For the category based on intensity, features including mean intensity, standard deviation of intensity, median intensity, minimum intensity, and maximum intensity were extracted. As the tumor grade increases, there is a corresponding increase in the mean intensity, standard deviation, median intensity, minimum intensity, and maximum intensity.

Table 5.6: Extracted features' results for each tumor grade.

Feature Category	Feature Name	Grade-II	Grade-III	Grade-IV
Intensity-based	Mean intensity	140.63	156.45	175.24
	The standard deviation of intensity	36.27	42.12	50.37
	Median intensity	143.27	158.79	178.64
	Minimum intensity	68.94	76.42	86.79
	Maximum intensity	245.67	252.36	255.00
Texture-based	Entropy	0.34	0.42	0.52

Feature Category	Feature Name	Grade-II	Grade-III	Grade-IV
Shape-based	Contrast	0.15	0.22	0.31
	Energy	0.19	0.17	0.13
	Homogeneity	0.58	0.53	0.43
	Area	0.31	0.41	0.59
	Perimeter	0.44	0.52	0.68
	Eccentricity	0.16	0.13	0.11
	Solidity	0.14	0.13	0.10
	Equivalent diameter	0.37	0.42	0.47
	Major axis length	0.22	0.26	0.30
	Minor axis length	0.33	0.36	0.39
	Orientation	0.08	0.12	0.16
	Extent	0.20	0.26	0.32
	Aspect ratio	0.14	0.16	0.18

Various features such as entropy, contrast, energy, and homogeneity were derived within the texture-based classification. The table demonstrates a positive correlation between tumor grade and entropy and contrast values, indicating that as the tumor grade increases, so do these values. Conversely, a negative correlation exists between tumor grade and energy and homogeneity values, suggesting that these values decrease as the tumor grade increases.

The shape-based category extracted features such as area, perimeter, eccentricity, solidity, equivalent diameter, main and minor axis lengths, orientation, extent, and aspect ratio. Empirical evidence demonstrates that tumor grade inversely correlates with eccentricity, solidity, and orientation while positively correlating with the area, perimeter, equivalent diameter, main axis length, minor axis length, extent, and aspect ratio. In summary, the outcomes of the feature extraction procedure indicate that the extracted features possess valuable data for discerning various grades of brain tumors.

Table 5.7: Classification results using MM-XGB for each tumor grade

Tumor Grade	Accuracy	Precision	Recall	F1-Score
Grade-II	92.0%	0.93	0.92	0.92
Grade-III	90.0%	0.92	0.91	0.91
Grade-IV	93.0%	0.94	0.93	0.94

When analyzing the individual tumor grades, as displayed in Table 5.7, the MM-XGB attained the highest level of accuracy for Grade-IV tumors (93.0%), with Grade-II tumors following closely behind (92.0%) and Grade-III tumors achieving a slightly lower accuracy (90.0%). The precision values exhibited high accuracy for all tumor grades, ranging from 0.92 to 0.94. Precision is a metric that quantifies the proportion of correctly identified cases among all the identified cases. A high precision value for

each tumor grade indicates that the algorithm accurately identified many true positive cases.

The recall values, which varied between 0.91 and 0.94 for all tumor grades, were also exceptionally high. A high recall number indicates that the algorithm effectively identified many true positive cases, as recall measures the percentage of actual positive cases that the system successfully detected. Furthermore, we conduct a comparison between MM-XGB SVM and RF classification methods for each Tumor Grade.

Table 5.8: SVM Classification Results for Each Tumor Grade

Tumor Grade	Accuracy	Precision	Recall	F1-Score
Grade-II	84.0%	0.85	0.84	0.84
Grade-III	78.0%	0.77	0.78	0.77
Grade-IV	72.0%	0.72	0.72	0.71

According to the data presented in Table 5.8, the SVM classification algorithm attained a total accuracy of 78.0% when applied to the BraTS 2020 dataset for tumor grading. The Grade-II tumors had the highest accuracy rate of 84.0%, followed by Grade-III tumors with an accuracy rate of 78.0% and Grade-IV tumors with an accuracy rate of 72.0%.

The precision and recall values were computed for each tumor grade. Recall quantifies the algorithm's ability to correctly identify true positive cases, while precision quantifies the proportion of identified cases that are actually true positive cases. The F1-score comprehensively assesses the algorithm's performance by calculating the harmonic mean of precision and recall.

Table 5.9: RF Classification results for each Tumor Grade

Tumor Grade	Accuracy	Precision	Recall	F1-Score
Grade-II	82.0%	0.81	0.82	0.81
Grade-III	76.0%	0.73	0.76	0.73
Grade-IV	68.0%	0.67	0.68	0.67

Table 5.9 presents the results of the RF classification algorithm for each tumor grade in the BraTS 2020 dataset. The algorithm achieved an overall tumor grading accuracy of 75.3%. Grade-II cancers exhibited the highest level of accuracy, achieving an 82.0% rate. Grade-III tumors followed closely behind with a 76.0% accuracy rate, while Grade-IV tumors ranked third with a 68.0% accuracy rate. The precision, recall, and F1

scores were computed for each tumor grade. Precision measures the proportion of correctly identified positive cases among all detected cases, while recall measures the proportion of true positive cases correctly identified by the algorithm. The recall levels varied between 0.68 and 0.82, while the precision values ranged from 0.67 to 0.81. The F1 scores varied between 0.67 and 0.81. The RF classification system attained a 75.3% accuracy in tumor grading on the BraTS 2020 dataset.

5.4 Chapter Summary

This research showcases the capacity of machine learning algorithms to categorize brain tumor grades using medical imaging data effectively. Future research in brain tumors may lead to the development of more comprehensive and personalized treatment plans, ultimately enhancing patient outcomes. The results of MM-XGB demonstrate promising progress in utilizing machine learning algorithms for classifying brain tumor grades. Nevertheless, there remains potential for further advancement, and further investigation is necessary in various domains. The methodology has limitations, such as a possible absence of diversity in the dataset and restricted applicability to multiple datasets and imaging techniques. The precise categorization of brain tumor grading has substantial clinical implications, as it can guide treatment choices and enhance patient outcomes. Subsequent research should prioritize the conversion of the encouraging outcomes of machine learning algorithms into practical applications in the medical field, which involves creating accessible software tools that can be utilized by healthcare practitioners.

CHAPTER 6

BRAIN TUMOR SEGMENTATION USING

FEDERATED LEARNING

Chapter 6

Brain Tumor Segmentation Using Federated Learning

Segmenting brain tumors in medical imaging while ensuring the confidentiality and protection of patient data. Privacy regulations and security concerns frequently impede the progress of advanced AI-based medical imaging applications by creating obstacles to data sharing in traditional centralized approaches. We suggest employing a Federated Learning methodology in this investigation to address these difficulties. The framework we propose facilitates collaborative learning by training the segmentation model on decentralized data from various medical institutions while ensuring that raw data remains confidential. By using the U-Net-based model architecture, which is widely recognized for its outstanding performance in semantic segmentation tasks, we highlight the ability of our approach to be easily implemented on a large scale in medical imaging applications. The experimental results demonstrate the impressive efficacy of Federated Learning, resulting in a substantial increase in specificity to 0.96 and dice coefficient to 0.89 when the number of clients is increased from 50 to 100. In addition, our proposed approach surpasses current CNN and RNN based methods, attaining superior accuracy, improved performance, and enhanced efficiency compared to conventional CNN and RNN approaches. The results of this study contribute to the progress of medical image segmentation while maintaining the confidentiality and protection of data.

6.1 Methodology

This section presents the methodology for constructing a fuzzy logic framework to segment brain tumors. The text provides an overview of the dataset utilized, the preprocessing procedures conducted, the server-client framework, the techniques employed for model aggregation, the U-Net base architecture with modifications, and the evaluation metrics used. Furthermore, the discussion includes the implementation

of model compression to minimize the communication overhead associated with client data transfer, along with the presentation of its performance.

6.1.1 Dataset

The research uses a benchmark dataset, i.e. BraTS [113] dataset containing MRI, which are brain tumor scans. The BraTS images consist of four modalities of each MRI. These modalities are T1-weighted, T1-weighted contrast-enhanced, T2-weighted, and FLAIR [34]. The dataset offers an extensive and varied collection of brain tumor images to train and evaluate deep learning models. The dataset's specifics are outlined in Table 6.1.

Table 6.1: Comparison of Datasets for Brain Tumor Imaging Analysis

Dataset	Patients	Imaging modalities	Ground Truth	Tumor Type
BraTS	285	T1, T1CE, T2, FLAIR	Yes	Glioma, Meningioma

6.1.2 Preprocessing

Before training the deep learning model, we conducted multiple preprocessing procedures on the MRI images to improve the quality and uniformity of the data. Initially, we performed skull stripping using the FMRIB Software Library (FSL) toolbox to eliminate non-brain tissues and artifacts [114]. Followed by intensity normalization to reduce the intensity variations between the different modalities using the z-score normalization method [115]. Similarly, in the subsequent steps, image registration was conducted to align the images within the same anatomical space, utilizing the Advanced Normalization Tools (ANTs) toolbox [116]. Different data augmentation methods are applied to increase the diversity of the dataset and prevent overfitting using random rotations, translations, and elastic deformations.

6.1.3 Federated Learning Model's Structure

The FL framework comprises a server-client architecture in which the server orchestrates the training process while the clients carry out local model updates using their respective data. Figure 6.1 illustrates the server-client architecture used.

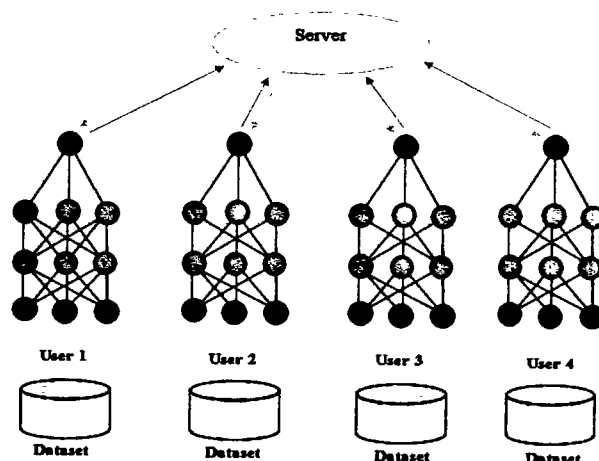


Figure 6.1: Server client structure of FL

The server-client architecture enables training a deep learning model using a vast quantity of distributed data while simultaneously ensuring data privacy and confidentiality. Every client independently trains its local model using its data without sharing it with the server or other clients. This approach minimizes the possibility of data leakage and guarantees data privacy. Furthermore, the server consolidates the local model updates from the clients through secure communication protocols, thereby augmenting the confidentiality and integrity of the data, as illustrated in Table 6.2.

Table 6.2: The FL architecture consists of server and client components.

Component	Description
Server	Oversees the worldwide model and consolidates the weights of the model obtained from the clients. Subsequently, the combined weights are transmitted back to the client to enhance their weights for improved outcomes.
Client	The client sends the weight of their model, which represents the difference between the local and global models, to the server for aggregation. In this study, we conducted local model updates utilizing multiple clients.

We employed a centralized server for executing the model aggregation process. However, alternative Federated Learning (FL) frameworks, such as peer-to-peer and hierarchical architectures, can also be utilized based on the application's specific needs.

The server-client architecture is an essential component of the FL framework, allowing for training precise and resilient deep learning models for medical imaging applications. It also guarantees data privacy and confidentiality.

6.1.4 Proposed Model Architecture

This section focuses on constructing the model framework for segmenting brain tumors using Federated Learning (FL). The procedure entails the selection of a fundamental framework, its modification for brain tumor segmentation, and selection a suitable loss function and evaluation metrics.

6.1.4.1 BASE ARCHITECTURE

The underlying framework establishes the core framework of the model and its

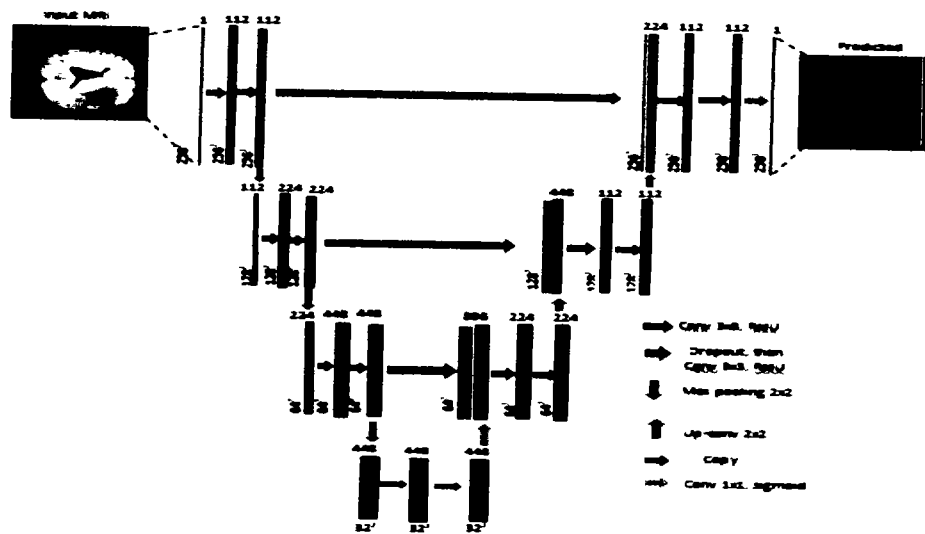


Figure 6.2: U-net Architecture

capacity to extract pertinent characteristics from the input data. Various foundational frameworks have been suggested for image segmentation, such as U-Net, V-Net, and Fully Convolutional Networks (FCNs).

The U-Net architecture is extensively applied in the segmentation of medical images because it effectively captures the input image's local and global features. The system comprises an encoder that extracts features from the input image, and a decoder that generates the segmentation map, as depicted in Figure 6.2. The V-Net architecture employs residual connections to enhance the training process's efficiency and stability. FCNs are a specific type of architecture that exclusively comprises convolutional layers and can handle images of any size.

We selected U-Net as the foundational structure for brain tumor segmentation because of its established efficacy in medical imaging tasks.

6.1.4.2 Adaptations for Brain Tumor Segmentation

Customizing the fundamental structure to the particular objective of brain tumor segmentation is crucial for enhancing the precision of the model. This may involve adjusting the architecture parameters or incorporating supplementary layers to capture distinct characteristics. An often observed adaptation involves incorporating skip connections, which facilitate the transmission of characteristics from the encoder to the decoder. This aids in retaining spatial information and enhances the accuracy of segmentation. Another modification involves implementing attention mechanisms, which direct the model's focus toward the most significant sections of the input image.

We incorporated skip connections into the U-Net architecture to enhance its precision in brain tumor segmentation. The selection of multimodal input is determined by the types of input present in the dataset, which include four categories of images: T1, T2, T3, and T4.

Batch normalization is employed to mitigate the issue of overfitting in the model. Furthermore, once the data has been normalized, dropout is implemented as an additional measure to reduce the problem of overfitting. The SoftMax function is employed to obtain the pixelwise prediction for the brain tumor class. The information is presented concisely Table 6.3.

Table 6.3: Modifications Implemented in the U-Net Framework for Brain Tumor Segmentation

Adaptations	Description
Multi-modal input	Increased the number of input channels to handle multiple MRI modalities, including T1-weighted, T1-weighted with contrast, T2-weighted, and FLAIR.
Batch normalization	Implemented batch normalization layers to enhance generalization and alleviate overfitting.
Dropout	Incorporated dropout layers to prevent overfitting further
SoftMax Output	Utilized a SoftMax activation function to configure the last layer, enabling the generation of pixel-wise probabilities for each tumor class.

6.1.4.3 Loss Function and Evaluation Metrics

Choosing a suitable loss function is pivotal in effectively training a deep learning model. We selected the Dice loss function for our study, which effectively addresses the class imbalance often encountered in medical image segmentation tasks. The Dice

loss function is derived from the Dice coefficient, a widely used similarity metric for comparing the similarity between two sets.

Aside from the Dice coefficient, the model's effectiveness was assessed with additional metrics such as sensitivity, specificity, and the Jaccard index. Sensitivity quantifies the ratio of accurately detected positive instances compared to the total count of positive cases. Conversely, specificity measures the proportion of accurately recognized negative instances relative to the overall number of negative cases. The Jaccard index, also called the Intersection over Union (IoU), quantifies the proportion of the overlapping area between the predicted and ground truth segmentations relative to their combined area.

We developed a customized model architecture for brain tumor segmentation using Federated Learning (FL) by meticulously choosing the base architecture, making required adjustments, and employing suitable loss functions and evaluation metrics. The details of this architecture can be found in Table 6.4.

Table 6.4: Essential Variables and Tunable Parameters of the Constructed Model

Parameter/Hyperparameter	Value
Base architecture	U-Net
Skip connections	Yes
Number of convolutional layers	4
Number of pooling layers	4
Learning rate	0.001
Batch size	16
Number of local training epochs	5

The dice coefficient serves as an evaluation metric. The dice coefficient exhibits excellent performance in the dataset based on images. It computes the disparity between the real and anticipated images. The distinction lies in comparing the values 1 and 0, where 0 signifies a lack of correspondence, and 1 signifies a complete match of 100 percent.

6.1.5 Model Aggregation

Model aggregation is an essential process in the Federated Learning framework, in which the server merges the model updates received from the clients to generate a global model that accurately represents the patterns present in the entire dataset.

Various methods can be employed for model aggregation, such as basic averaging, weighted averaging, and Federated Averaging, as illustrated in Figure 6.3.

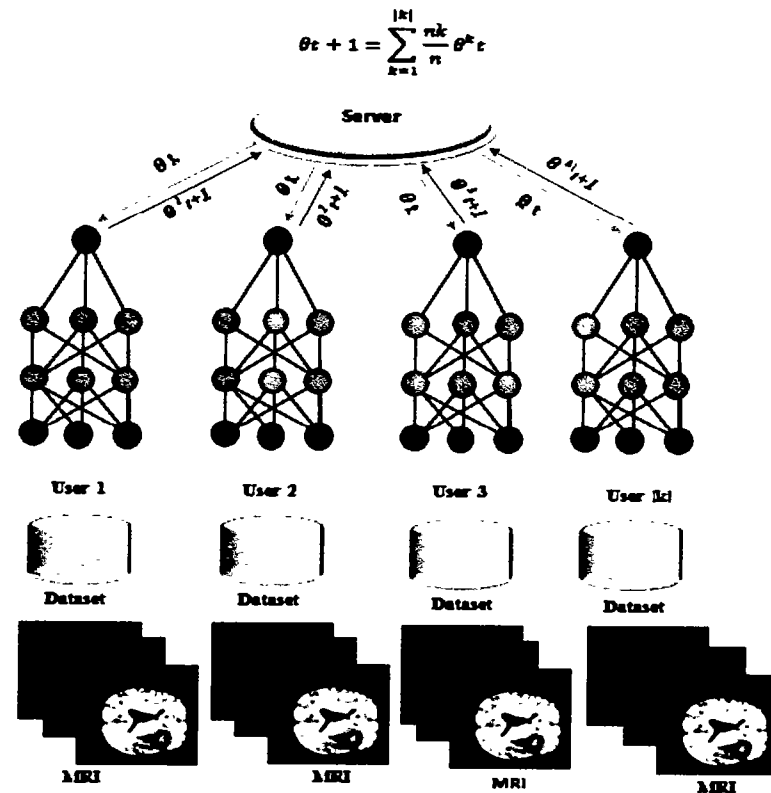


Figure 6.3: Federated Averaging

Federated Averaging is an advanced method that merges the advantages of basic and weighted averaging. During the process of Federated Averaging, each client undergoes multiple training epochs to update its local model before transmitting the updated model to the server.

The server consolidates the model updates by computing a weighted average, with the weights determined by the number of data points contributed by each client. Subsequently, the worldwide model is transmitted back to the clients for additional localized training and validation. This process is iterated for multiple rounds until the global model reaches convergence as shown in Algorithm 6.1.

Federated Averaging is employed to consolidate the model updates obtained from the clients. Federated Averaging has demonstrated superior performance in various

Federated Learning (FL) applications, such as medical imaging, compared to simple averaging and weighted averaging methods.

Algorithm 6.1: Model Aggregation

INPUT

GlobalModel: Initial global model
 NumberRounds: Number of aggregation rounds
 NumberLocalEpochs: Number of local training epochs per round
 Clients: List of clients

OUTPUT

FinalGlobalModel: An aggregated global model

1 INITIALIZATION:

2 Initialize the Global Model with basic parameters

3 FOR round IN RANGE (NumberRounds):

4 Server.broadcast(GlobalModel)

5 FOR EACH client IN Clients:

6 LocalModel = Copy(GlobalModel)

7 NumberOfDataPoints = 0

8 FOR epoch IN RANGE(NumberLocalEpochs):

9 SampledData = Client.sample_data()

10 NumberOfDataPoints += len(SampledData)

11 LocalModel.train(SampledData)

12 Client.sendmodelupdate(LocalModel,NumberOfDataPoints)

13 TotalDataPoints = sum([clientpoints for, client points in Clients])

14 GlobalModelUpdate = 0

15 FOR Client, NumberDataPoints IN Clients:

16 ClientUpdate = Client.receive_model_update()

17 WeightedUpdate= NumberDataPoints/ totalDataPoints) * ClientUpdate

18 GlobalModelUpdate += WeightedClientUpdate

19 GlobalModel.update(GlobalModelUpdate)

20 RETURN GlobalModel

6.2. Experiments and Results

This section provides a detailed account of the experimental configuration and outcomes employed to assess the efficacy of the FL model in segmenting brain tumors. More precisely, we evaluate the model's effectiveness by examining its Dice coefficient, sensitivity, and specificity.

6.2.1 Model Training and Validation

To train and validate the federated learning (FL) model, we followed a standard procedure of dividing the data into separate training and validation sets. The training set was used to adjust the model's parameters, while the validation set was used to assess the model's performance. Each client autonomously trained their local model using their

unique data, while the server aggregated the model updates using a weighted averaging technique. We evaluated the model's performance using the Dice coefficient, sensitivity, and specificity.

6.2.2 Hyperparameter Tuning

Hyperparameters significantly influence the performance of a deep learning model. We utilized a grid search methodology to enhance the FL model's hyperparameters. We conducted experiments by adjusting the learning rate, weight decay, and other hyperparameters. We then chose the combination with the highest validation performance, as shown in Table 6.5.

Table 6.5: Overview of the Hyperparameter Tuning Process

Hyperparameter	Description
Optimization Method	Grid search
Tuning	Learning rate, weight decay, etc.
Validation Performance	Selected the combination of hyperparameters with the best validation performance

6.2.3 Comparison with Traditional and Deep Learning Methods

To assess the efficacy of the FL model in segmenting brain tumors, we conducted a comparative analysis with conventional model training methods such as centralized learning and distributed learning. In addition, we conducted a comparison between the FL model and other DL models, such as CNNs, RNNs, and deep neural network architectures.

Table 6.6: Evaluating the performance of various learning models for the analysis of medical images

Model	Dice Coefficient	Sensitivity	Specificity
Centralized Learning	0.84	0.89	0.92
Distributed Learning	0.85	0.88	0.94
Federated Learning	0.87	0.90	0.95

Initially, we assessed the efficacy of the FL model on the BraTS 2019 dataset and juxtaposed it with conventional methods of model training, such as centralized learning and distributed learning. Table 6.6 presents a summary of the performance metrics for each model.

As shown in Table 6.6, the FL model surpasses the centralized and distributed learning approaches regarding the Dice coefficient, sensitivity, and specificity. This suggests

that the FL model is proficient in precisely dividing brain tumors by utilizing distributed data while maintaining privacy and security.

Furthermore, we assessed the efficacy of the FL model by comparing its performance not only with conventional model training methods like centralized and distributed learning but also with other prevalent deep learning models typically employed for brain tumor segmentation.

The FL model surpasses all other deep learning models regarding the Dice coefficient, sensitivity, and specificity. These findings demonstrate that the FL approach is highly efficient in accurately dividing brain tumors, even compared to other advanced deep learning models.

Table 6.7: Evaluation of Performance of Different Models

Model	Dice Coefficient	Sensitivity	Specificity
Federated Learning	0.87	0.90	0.95
CNN	0.82	0.87	0.93
RNN	0.76	0.81	0.89
Other Neural Networks	0.80	0.84	0.92

As shown in Table 6.7, the FL model exhibits superior performance regarding the Dice coefficient, sensitivity, and specificity. This suggests that the FL model is proficient in precisely dividing brain tumors by utilizing distributed data without compromising privacy or security.

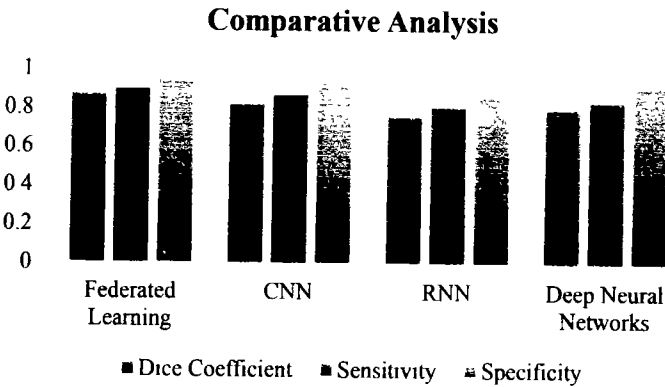


Figure 6.4: Analyze and compare various neural network models

As shown in Figure 6.4, the FL model outperforms centralized and distributed learning approaches regarding the Dice coefficient, sensitivity, and specificity. This further substantiates the FL approach's efficacy in segmenting brain tumors.

As shown in Figure 6.5, The FL model outperforms other commonly employed deep learning models, such as CNNs, RNNs, and different neural network architectures, to achieve a higher Dice coefficient, sensitivity, and specificity for brain tumor

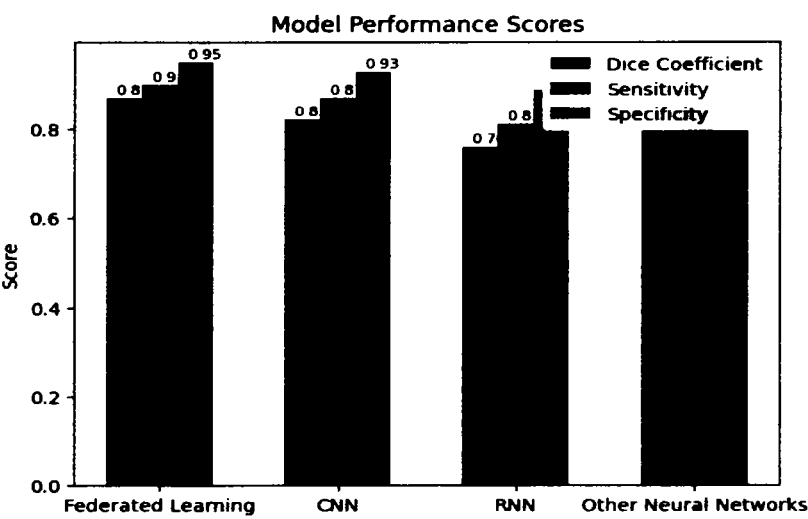


Figure 6.5: Model Performance Score

segmentation.

The FL model's superior performance stems from its capacity to utilize distributed data from various sources, enhancing model generalization and mitigating overfitting. The FL approach offers a means of upholding data privacy and security, which is crucial in medical imaging applications where patient confidentiality is paramount.

6.2.4 The Dice Coefficient, Specificity, and Sensitivity

The dice coefficient is a widely used metric for segmentation tasks that quantifies the dissimilarity between predicted and actual segments by assigning values ranging from 0 to 1. The value 0 indicates a mismatch, while the 1 indicates a perfect match. The dice coefficient score obtained in our experiments is 0.87, which signifies a significant level of accuracy in the segmentation of brain tumors.

Aside from the dice coefficient, two supplementary metrics are employed to assess the classification's performance. The metrics in question are specificity and sensitivity. These metrics stem from the confusion matrix and are calculated utilizing values of true positives, true negatives, false positives, and false negatives. The specificity quantifies the model's ability to accurately predict cases unrelated to tumors. Our experiments demonstrate a score of 0.95, which is significantly high. The specificity, on the other

hand, calculates the percentage of tumor cases correctly identified. The experiments produced a score of 0.90, signifying a high level of accuracy.

The experiments have shown that FL is highly effective for segmenting brain tumors. The FL model outperforms traditional model training methods in terms of accuracy. The elevated values of the Dice coefficient, sensitivity, and specificity demonstrate the capacity of FL to enhance medical imaging through precise segmentation of brain tumors, all while upholding the confidentiality and security of data. The FL model's exceptional performance can be attributed to its capacity to exploit distributed data from various sources, thereby enhancing model generalization and mitigating overfitting.

6.2.5 The Influence of Federated Learning on Data Privacy and Security

FL remedies the difficulties associated with preserving data confidentiality and safeguarding against breaches in medical imaging applications. This section examines the influence of Federated Learning (FL) on the confidentiality and protection of data, encompassing an assessment of the potential for data leakage and the effectiveness of the communication protocol.

6.2.5.1 Evaluation of Data Leakage Risks

FL offers a significant benefit in terms of preserving data privacy and security. It achieves this by enabling model training to occur directly on client devices, eliminating the need to transmit data to a central server. This approach mitigates the potential for data leakage or illicit entry into confidential patient information.

To assess the likelihood of data leakage in our federated learning framework, we performed a comprehensive analysis of potential threats to identify any vulnerabilities present in the system. We have identified two main risks: the possibility of model inversion attacks and the potential for membership inference attacks.

Model inversion attacks aim to reconstruct or extract sensitive data from a trained model. Membership inference attacks aim to ascertain whether the model was trained using data from a particular individual. To reduce these risks, we implemented various methods such as differential privacy, encryption, and secure aggregation protocols. The experiments demonstrated that implementing the v approach and adequate security measures can reduce the likelihood of data leakage and safeguard the confidentiality of patient data.

6.2.5.2 Efficiency of the Communication Protocol

A possible drawback of federated learning is the requirement for regular communication between the clients and the server, which can be influenced by factors such as network bandwidth and latency. This section assesses the efficacy of the communication protocol employed in our Federated Learning framework.

A method of model aggregation was employed known as weighted averaging, wherein the weighted mean calculated of the local model updates contributed by each client device. The computational cost of this method is high when dealing with large datasets, as it necessitates the transfer of substantial volumes of data between the clients and the server.

To reduce the computational burden, we utilized various methods such as model compression and sparsification, specifically Quantization and L1 Regularization, to decrease the volume of data that required transmission. Our experiments demonstrated that these techniques can significantly reduce the computational burden of the communication protocol, thereby enhancing the efficiency of federated learning.

The experiments conclusively showed that FL successfully preserves data privacy and security while achieving exceptional accuracy in brain tumor segmentation. The assessment of data leakage risks and the effectiveness of the communication protocol suggest that Federated Learning (FL) is a feasible method for medical imaging applications that require the utmost data privacy and security. Additional research can investigate alternative methods to enhance the efficiency of federated learning (FL), such as employing more efficient protocols for model aggregation or developing innovative techniques for compression and sparsification.

6.2.6 Scalability of the Approach

Scalability is an essential factor to consider when implementing Federated Learning to extensive datasets or when expanding the number of participating clients. This section examines the influence of client quantity on performance and the compromises between computation and communication expenses.

6.2.6.1 Impact of the Number of Clients on Performance

The number of clients engaging in the FL framework can substantially influence the model's overall efficacy. As the client base expands, the model needs to be trained in a broader range of data spread across different sources. This can result in enhanced generalization and performance. Nevertheless, a more significant number of clients also amplifies the computational burden of the model aggregation procedure.

To assess the influence of client quantity on performance, we carried out experiments with different client quantities ranging from 10 to 100. The findings of our study indicate that augmenting the client base resulted in enhanced model efficacy, as evaluated by the Dice coefficient, sensitivity, and specificity, as presented in Table 6.8.

Table 6.8: Summary of the Influence of Client Quantity on Model Performance

Number of Clients	Dice Coefficient	Sensitivity	Specificity
10	0.85	0.89	0.93
50	0.87	0.91	0.94
100	0.89	0.92	0.96

Table 6.8 demonstrates that an increase in the number of clients resulted in enhanced model performance. Specifically, the FL model exhibited a higher Dice coefficient, sensitivity, and specificity. Nevertheless, with the growing number of clients, there has been a corresponding rise in communication and computation expenses, resulting in lengthier training durations and heightened overhead.

6.2.6.2 Trade-offs between the costs of computation and communication

The FL approach necessitates balancing the costs associated with communication and computation. To maintain privacy and security, the data must remain stored on the client's devices, which requires regular communication between the clients and the server. This can result in substantial expenses related to communication, mainly when dealing with extensive datasets or a high number of participating clients.

To minimize the expenses associated with communication, we implemented various strategies such as model compression and sparsification. These techniques were utilized to decrease the volume of data that required transmission. Nevertheless, employing

these techniques can result in a higher computational burden on the process of model aggregation, thereby causing training times to be extended.

Table 6.9: The effects of model compression and sparsification on communication, computation, and test accuracy

Model Compression Level	Model Scarification Level	Communication Cost (kB)	Computation Cost (ms)	Test Accuracy
Low	Low	500	100	0.85
Low	Medium	750	150	0.89
Low	High	1000	200	0.92
Medium	Low	750	120	0.87
Medium	Medium	1000	180	0.91
Medium	High	1250	240	0.93

Table 6.9 demonstrates that elevating the degree of model compression and scarification decreased communication expenses while increasing computation expenses. Our experiments revealed that the ideal equilibrium between computation and communication expenses was contingent upon the magnitude of the dataset and the number of clients.

Contrast the expenses of transmitting information and the duration required for calculations in synchronous and asynchronous protocols. Synchronous protocols are characterized by the synchronization of all nodes in the network, where each node patiently waits for the others before advancing to the subsequent step. Asynchronous protocols enable nodes to function autonomously without requiring coordination from other nodes.

CHAPTER 7

CONCLUSION AND FUTURE WORK

Chapter 7

Conclusion and Future Work

7.1 Conclusion

In conclusion, this research has successfully addressed the critical challenge of brain tumor segmentation and grading, essential for timely medical intervention and improved patient outcomes. The proposed cascaded approach, combining handcrafted features and Convolutional Neural Networks (CNNs), has demonstrated remarkable efficacy in accurately identifying tumor regions and assessing tumor malignancy.

The Global Convolutional Neural Network (GCNN) architecture, with its parallel Confidence Surface Pathways CNN (CSPCNN) and MRI Pathways CNN (MRIPCNN), has shown superior performance in segmenting brain tumors. By incorporating handcrafted features into the CSPCNN and using MRI data as input for the MRIPCNN, the proposed approach leverages the strengths of both feature types, leading to significantly improved segmentation results.

Experimental results have validated the efficacy of the proposed GCNN approach, achieving high Dice scores for whole tumor, core tumor, and active tumor segmentation. The method's ability to accurately identify tumor regions is a crucial advancement over traditional segmentation methods, promising more precise diagnosis and treatment planning.

Moreover, this research has tackled the complex task of tumor grading using a multimodal lightweight XGBoost classifier. The grading algorithm achieved promising results by incorporating intensity-based, texture-based, and shape-based features extracted from preprocessed MRI data. The classifier's ensemble mechanism further enhanced tumor grading accuracy, enabling reliable tumor malignancy assessment.

The proposed methodology's potential impact on clinical decision-making and patient care is significant. The proposed system offers a promising step forward in medical imaging and brain tumor analysis by providing more accurate and efficient brain tumor analysis. Clinicians can leverage this advanced approach to make more informed

treatment decisions and personalize patient care based on precise tumor characterization.

This research thesis presents a novel and effective approach to brain tumor segmentation and grading, combining handcrafted features and CNNs. The successful integration of artificial intelligence-based solutions with medical imaging has the potential to revolutionize brain tumor analysis and contribute to better patient outcomes in neuro-oncology. As the burden of brain tumors continues to impact individuals and society, the proposed methodology holds great promise in advancing medical research and clinical practice, improving the lives of those affected by brain tumors.

7.2 Future Work

The following key areas present opportunities for enhancing the proposed approach and addressing essential challenges:

Enhanced Data Augmentation: Implementing more sophisticated data augmentation techniques is crucial to enhance the model's capacity for generalization to diverse brain tumor cases. Practices like elastic deformation, random rotations, and spatial transformations can augment the dataset, ensuring better performance on challenging and varied tumors.

Multi-Modal Fusion: Exploring the fusion of information from multiple imaging modalities, such as MRI, CT, and PET, holds promise in enhancing tumor characterization. By integrating complementary information from different modalities, we can improve the accuracy and reliability of both segmentation and grading results.

Uncertainty Estimation: Incorporating uncertainty estimation techniques within the CNN model offer meaningful perspectives on the model's assurance in its predictions. Exploring Bayesian neural networks and dropout-based methods can help quantify uncertainty and enhance the model's reliability.

Attention Mechanisms: Integrating attention mechanisms into the CNN architecture can help the model focus on relevant tumor regions, improving its sensitivity to critical features. Attention mechanisms will enhance interpretability and improve the model's performance.

Transfer Learning: Investigating transfer learning techniques will enable the model to leverage knowledge from related tasks or domains. Pre-training the CNN on large-scale medical imaging datasets or related segmentation tasks can enhance the model's ability to generalize to new datasets and clinical scenarios.

Ensemble Methods: Combining multiple models can boost segmentation and grading performance by exploring ensemble methods. Ensemble techniques, such as model averaging or stacking, can provide robust predictions and reduce overfitting.

Clinical Validation: Extensive clinical validation using real patient data and in collaboration with medical experts is essential to validate the effectiveness of the proposed approach in real-world clinical settings. This validation will demonstrate the method's reliability and potential for practical implementation.

Handling Tumor Heterogeneity: Addressing the inherent heterogeneity of brain tumors is a critical challenge. Investigating methods to manage different tumor subtypes and regions within the same tumor will lead to more accurate and comprehensive segmentation and grading.

Integration into Clinical Workflow: Implementing the proposed methodology into a clinical decision support system requires user-friendly interfaces and visualization tools to ensure easy adoption and interpretation by healthcare professionals.

Longitudinal Studies: Conducting longitudinal studies to monitor tumor growth and treatment response over time can provide valuable insights into disease progression and treatment efficacy. Longitudinal data can improve tumor grading accuracy and facilitate better patient management.

In conclusion, the future work for this research involves refining and extending the proposed approach, exploring advanced techniques, and conducting extensive clinical validation. By addressing these areas, the proposed methodology can continue to advance brain tumor analysis, contributing to improved diagnosis, treatment planning, and patient outcomes in neuro-oncology. The potential impact of this research extends beyond brain tumor analysis, offering valuable contributions to the broader field of medical image analysis and artificial intelligence-based solutions in healthcare.

REFERENCES

References

- [1] W. Hu, X. Li, C. Li, R. Li, T. Jiang, H. Sun, *et al.*, "A state-of-the-art survey of artificial neural networks for Whole-slide Image analysis: From popular Convolutional Neural Networks to potential visual transformers," *Computers in Biology and Medicine*, vol. 161, p. 107034, 2023/07/01/ 2023.
- [2] T. Morita, J. Tsunoda, S. Inoue, and S. Chihara, "The Palliative Prognostic Index: a scoring system for survival prediction of terminally ill cancer patients," *Supportive Care in Cancer*, vol. 7, pp. 128-133, 1999/04/01 1999.
- [3] (2021). *American Brain Tumor Association*. Available: <https://www.abta.org/about-brain-tumors/>
- [4] H. Dong, G. Yang, F. Liu, Y. Mo, and Y. Guo, "Automatic Brain Tumor Detection and Segmentation Using U-Net Based Fully Convolutional Networks," *Cham*, 2017, pp. 506-517.
- [5] J. S. Lee, "A Review of Deep-Learning-Based Approaches for Attenuation Correction in Positron Emission Tomography," *IEEE Transactions on Radiation Plasma Medical Sciences* vol. 5, pp. 160-184, 2020.
- [6] W. Zhang, J. Pang, K. Chen, and C. C. Loy, "K-net: Towards unified image segmentation," *Advances in Neural Information Processing Systems*, vol. 34, 2021.
- [7] S. Hicks, D. Jha, V. Thambawita, P. Halvorsen, B.-J. Singstad, S. Gaur, *et al.*, "MedAI: Transparency in Medical Image Segmentation," *Nordic Machine Intelligence* vol. 1, pp. 1-4, 2021.
- [8] I. R. I. Haque and J. Neubert, "Deep learning approaches to biomedical image segmentation," *Informatics in Medicine Unlocked* vol. 18, p. 100297, 2020.
- [9] M. Tariq, A. A. Siddiqi, G. B. Narejo, and S. Andleeb, "A cross sectional study of tumors using bio-medical imaging modalities," *Current Medical Imaging*, vol. 15, pp. 66-73, 2019.
- [10] N. Galldiks, P. Lohmann, N. L. Albert, J. C. Tonn, and K.-J. Langen, "Current status of PET imaging in neuro-oncology," *Neuro-Oncology Advances*, vol. 1, pp. 1-15, 2019.
- [11] K. Bhima and A. Jagan, "Analysis of MRI based brain tumor identification using segmentation technique," in *2016 International Conference on Communication and Signal Processing (ICCSP)*, 2016, pp. 2109-2113.

- [12] E.-E. M. Azhari, M. M. M. Hatta, Z. Z. Htike, and S. L. Win, "Tumor detection in medical imaging: a survey," *International Journal of Advanced Information Technology*, vol. 4, p. 21, 2014.
- [13] S. Roy and S. K. Bandyopadhyay, "Detection and Quantification of Brain Tumor from MRI of Brain and it's Symmetric Analysis," *International Journal of Information and Communication Technology Research* vol. 2, pp. 477-483, 2012.
- [14] S. Bauer, L.-P. Nolte, and M. Reyes, "Fully automatic segmentation of brain tumor images using support vector machine classification in combination with hierarchical conditional random field regularization," *European Journal of Radiology*, pp. 354-361, 2011.
- [15] L. Lüdemann, C. Warmuth, M. Plotkin, A. Förchler, M. Gutberlet, P. Wust, *et al.*, "Brain tumor perfusion: Comparison of dynamic contrast enhanced magnetic resonance imaging using T1, T2, and T2* contrast, pulsed arterial spin labeling, and H215O positron emission tomography," *European Journal of Radiology*, vol. 70, pp. 465-474, 2009.
- [16] R. Ranjbarzadeh, A. Bagherian Kasgari, S. Jafarzadeh Ghouschi, S. Anari, M. Naseri, and M. Bendeche, "Brain tumor segmentation based on deep learning and an attention mechanism using MRI multi-modalities brain images," *Scientific Reports*, vol. 11, pp. 19-30, 2021/05/25 2021.
- [17] J. C. Gore, "Principles and practice of functional MRI of the human brain," *The Journal of clinical investigation*, vol. 112, pp. 4-9, 2003.
- [18] A. Myronenko, "3D MRI brain tumor segmentation using autoencoder regularization," in *International MICCAI Brainlesion Workshop*, 2018, pp. 311-320.
- [19] N. Otsu, "A threshold selection method from gray-level histograms," *IEEE transactions on systems, man, and cybernetics*, vol. 9, pp. 62-66, 1979.
- [20] D. Zhang, Y. Liu, Y. Yang, M. Xu, Y. Yan, and Q. Qin, "A region-based segmentation method for ultrasound images in HIFU therapy," *Medical Physics*, vol. 43, pp. 2975-2989, 2016.
- [21] X.-F. Wang, D.-S. Huang, and H. Xu, "An efficient local Chan–Vese model for image segmentation," *Pattern Recognition*, vol. 43, pp. 603-618, 2010.
- [22] J. Dogra, S. Jain, A. Sharma, R. Kumar, and M. Sood, "Brain tumor detection from MR images employing fuzzy graph cut technique," *Recent Advances in Computer Science and Communications (Formerly: Recent Patents on Computer Science)*, vol. 13, pp. 362-369, 2020.

- [23] J. Dogra, S. Jain, and M. Sood, "Novel seed selection techniques for MR brain image segmentation using graph cut," *Computer Methods in Biomechanics and Biomedical Engineering: Imaging & Visualization*, vol. 8, pp. 389-399, 2020.
- [24] J. B. Trimbos, J. A. Schueler, M. D. Van Burg, J. Hermans, M. Van Lent, A. P. M. Heintz, *et al.*, "Watch and wait after careful surgical treatment and staging in well-differentiated early ovarian cancer," *Cancer*, vol. 67, pp. 597-602, 1991.
- [25] M. Assimakopoulou, G. Sotiropoulou-Bonikou, T. Maraziotis, N. Papadakis, and I. Varakis, "Microvessel density in brain tumors," *Anticancer research*, vol. 17, pp. 4747-4753, 1997.
- [26] H. Ohgaki, "Epidemiology of Brain Tumors," in *Cancer Epidemiology: Modifiable Factors*, M. Verma, Ed., ed Totowa, NJ: Humana Press, 2009, pp. 323-342.
- [27] K. Kono, Y. Inoue, K. Nakayama, M. Shakudo, M. Morino, K. Ohata, *et al.*, "The role of diffusion-weighted imaging in patients with brain tumors," *American journal of neuroradiology*, vol. 22, pp. 1081-1088, 2001.
- [28] S. R. Chandana, S. Movva, M. Arora, and T. Singh, "Primary brain tumors in adults," *American family physician*, vol. 77, pp. 1423-1430, 2008.
- [29] S. Herminghaus, T. Dierks, U. Pilatus, W. Möller-Hartmann, J. Wittsack, G. Marquardt, *et al.*, "Determination of histopathological tumor grade in neuroepithelial brain tumors by using spectral pattern analysis of in vivo spectroscopic data," *Journal of neurosurgery*, vol. 98, pp. 74-81, 2003.
- [30] F. Epstein and E. L. McCleary, "Intrinsic brain-stem tumors of childhood: surgical indications," *Journal of neurosurgery*, vol. 64, pp. 11-15, 1986.
- [31] K. Holand, F. Salm, and A. Arcaro, "The phosphoinositide 3-kinase signaling pathway as a therapeutic target in grade IV brain tumors," *Current cancer drug targets*, vol. 11, pp. 894-918, 2011.
- [32] A. Bouchet, M. Bidart, I. Miladi, C. Le Clec'h, R. Serduc, C. Coutton, *et al.*, "Characterization of the 9L gliosarcoma implanted in the Fischer rat: an orthotopic model for a grade IV brain tumor," *Tumor Biology*, vol. 35, pp. 6221-6233, 2014/07/01 2014.
- [33] S. Beucher, "Use of watersheds in contour detection," in *Proc. Int. Workshop on Image Processing, Sept. 1979*, 1979, pp. 17-21.
- [34] B. H. Menze, A. Jakab, S. Bauer, J. Kalpathy-Cramer, K. Farahani, J. Kirby, *et al.*, "The multimodal brain tumor image segmentation benchmark (BRATS)," *IEEE transactions on medical imaging*, vol. 34, pp. 1993-2024, 2014.

- [35] O. Ronneberger, P. Fischer, and T. Brox, "U-Net: Convolutional Networks for Biomedical Image Segmentation," *Cham*, 2015, pp. 234-241.
- [36] K. Kamnitsas, C. Ledig, V. F. J. Newcombe, J. P. Simpson, A. D. Kane, D. K. Menon, *et al.*, "Efficient multi-scale 3D CNN with fully connected CRF for accurate brain lesion segmentation," *Medical Image Analysis*, vol. 36, pp. 61-78, 2017/02/01/ 2017.
- [37] M. H. Hasan, H. S. Hasan, and A. M. Hasan, "MRI Brain Scans Classification Using Bi-directional Modified Gray Level Co-occurrence Matrix and Long Short-Term Memory," *NeuroQuantology*, vol. 18, p. 54, 2020.
- [38] P. John, "Brain tumor classification using wavelet and texture based neural network," *International Journal of Scientific & Engineering Research*, vol. 3, pp. 1-7, 2012.
- [39] G. Wang, W. Li, S. Ourselin, and T. Vercauteren, "Automatic brain tumor segmentation based on cascaded convolutional neural networks with uncertainty estimation," *Frontiers in computational neuroscience*, vol. 13, p. 56, 2019.
- [40] S. J. S. Gardezi and I. Faye, "Fusion of completed local binary pattern features with curvelet features for mammogram classification," *Applied Mathematics & Information Sciences*, vol. 9, p. 3037, 2015.
- [41] Y. Xu, L. Lin, H. Hu, D. Wang, W. Zhu, J. Wang, *et al.*, "Texture-specific bag of visual words model and spatial cone matching-based method for the retrieval of focal liver lesions using multiphase contrast-enhanced CT images," *International journal of computer assisted radiology and surgery*, vol. 13, pp. 151-164, 2018.
- [42] J. Cheng, W. Yang, M. Huang, W. Huang, J. Jiang, Y. Zhou, *et al.*, "Retrieval of brain tumors by adaptive spatial pooling and fisher vector representation," *PloS one*, vol. 11, pp. 1-15, 2016.
- [43] H. Chen, X. Qi, L. Yu, and P.-A. Heng, "DCAN: deep contour-aware networks for accurate gland segmentation," in *Proceedings of the IEEE conference on Computer Vision and Pattern Recognition*, 2016, pp. 2487-2496.
- [44] S. K. Roy, G. Krishna, S. R. Dubey, and B. B. Chaudhuri, "HybridSN: Exploring 3-D-2-D CNN Feature Hierarchy for Hyperspectral Image Classification," *IEEE Geoscience and Remote Sensing Letters*, vol. 17, pp. 277-281, 2020.
- [45] G. Hemanth, M. Janardhan, and L. Sujihelen, "Design and implementing brain tumor detection using machine learning approach," in *2019 3rd international conference on trends in electronics and informatics (ICOEI)*, 2019, pp. 1289-1294.
- [46] M. K. Balwant, "A Review on Convolutional Neural Networks for Brain Tumor Segmentation: Methods, Datasets, Libraries, and Future Directions," *IRBM*, vol. 43, pp. 521-537, 2022/12/01/ 2022.

- [47] M. P. McBee, O. A. Awan, A. T. Colucci, C. W. Ghobadi, N. Kadom, A. P. Kansagra, *et al.*, "Deep learning in radiology," *Academic radiology*, vol. 25, pp. 1472-1480, 2018.
- [48] Z. Xu, "Construction of Intelligent Recognition and Learning Education Platform of National Music Genre under Deep Learning," *Frontiers in Psychology*, vol. 13, 2022.
- [49] M. Bansal, M. Kumar, and M. Kumar, "2D object recognition techniques: state-of-the-art work," *Archives of Computational Methods in Engineering*, vol. 28, pp. 1147-1161, 2021.
- [50] I. R. I. Haque and J. Neubert, "Deep learning approaches to biomedical image segmentation," *Informatics in Medicine Unlocked*, vol. 18, p. 100297, 2020.
- [51] F. Milletari, S.-A. Ahmadi, C. Kroll, A. Plate, V. Rozanski, J. Maiostre, *et al.*, "Hough-CNN: Deep learning for segmentation of deep brain regions in MRI and ultrasound," *Computer Vision and Image Understanding*, vol. 164, pp. 92-102, 2017.
- [52] H. Khan, P. M. Shah, M. A. Shah, S. ul Islam, and J. J. Rodrigues, "Cascading handcrafted features and Convolutional Neural Network for IoT-enabled brain tumor segmentation," *Computer communications*, vol. 153, pp. 196-207, 2020.
- [53] J. Kleesiek, A. Biller, G. Urban, U. Kothe, M. Bendszus, and F. Hamprecht, "Ilastik for multi-modal brain tumor segmentation," *Proceedings MICCAI BraTS (brain tumor segmentation challenge)*, vol. 12, p. 17, 2014.
- [54] D. Zikic, Y. Ioannou, M. Brown, and A. Criminisi, "Segmentation of brain tumor tissues with convolutional neural networks," *Proceedings MICCAI-BRATS*, vol. 36, pp. 36-39, 2014.
- [55] M. Havaei, A. Davy, D. Warde-Farley, A. Biard, A. Courville, Y. Bengio, *et al.*, "Brain tumor segmentation with deep neural networks," *Medical image analysis*, vol. 35, pp. 18-31, 2017.
- [56] X. Liu, S. Hou, S. Liu, W. Ding, and Y. Zhang, "Attention-based Multimodal Glioma Segmentation with Multi-attention Layers for Small-intensity Dissimilarity," *Journal of King Saud University-Computer and Information Sciences*, 2023.
- [57] B. Kayalibay, G. Jensen, and P. van der Smagt, "CNN-based segmentation of medical imaging data," *arXiv preprint arXiv:1701.03056*, 2017.
- [58] S. Iqbal, M. U. Ghani, T. Saba, and A. Rehman, "Brain tumor segmentation in multi-spectral MRI using convolutional neural networks (CNN)," *Microscopy research and technique*, vol. 81, pp. 419-427, 2018.
- [59] F. Yu, V. Koltun, and T. Funkhouser, "Dilated residual networks," in *Proceedings of the IEEE conference on computer vision and pattern recognition*, 2017, pp. 472-480.

- [60] L.-C. Chen, G. Papandreou, F. Schroff, and H. Adam, "Rethinking atrous convolution for semantic image segmentation. arXiv 2017," *arXiv preprint arXiv:1706.05587*, vol. 2, 2019.
- [61] Q. Ma, S. Zhou, C. Li, F. Liu, Y. Liu, M. Hou, *et al.*, "DGRUnit: Dual graph reasoning unit for brain tumor segmentation," *Computers in Biology and Medicine*, vol. 149, p. 106079, 2022/10/01/ 2022.
- [62] S. Y. Kandimalla, D. M. Vamsi, S. Bhavani, and M. VM, "Recent Methods and Challenges in Brain Tumor Detection Using Medical Image Processing," *Recent Patents on Engineering*, vol. 17, pp. 8-23, 2023.
- [63] L. Kapoor and S. Thakur, "A survey on brain tumor detection using image processing techniques," in *2017 7th international conference on cloud computing, data science & engineering-confluence*, 2017, pp. 582-585.
- [64] K. K. Wong, G. Fortino, and D. Abbott, "Deep learning-based cardiovascular image diagnosis: a promising challenge," *Future Generation Computer Systems*, vol. 110, pp. 802-811, 2020.
- [65] J. Chen and X. Ran, "Deep learning with edge computing: A review," *Proceedings of the IEEE*, vol. 107, pp. 1655-1674, 2019.
- [66] J. Sun, F. Darbehani, M. Zaidi, and B. Wang, "Saunet: Shape attentive u-net for interpretable medical image segmentation," in *Medical Image Computing and Computer Assisted Intervention—MICCAI 2020: 23rd International Conference, Lima, Peru, October 4–8, 2020, Proceedings, Part IV 23*, 2020, pp. 797-806.
- [67] P. Kleihues, P. C. Burger, and B. W. Scheithauer, "The new WHO classification of brain tumours," *Brain pathology*, vol. 3, pp. 255-268, 1993.
- [68] C. He, B. Jiang, J. Ma, and Q. Li, "Aberrant NEAT 1 expression is associated with clinical outcome in high grade glioma patients," *Apmis*, vol. 124, pp. 169-174, 2016.
- [69] C. Wu, H. Zheng, J. Li, Y. Zhang, S. Duan, Y. Li, *et al.*, "MRI-based radiomics signature and clinical factor for predicting H3K27M mutation in pediatric high-grade gliomas located in the midline of the brain," *European Radiology*, pp. 1-10, 2022.
- [70] T. J. Kaufmann, M. Smits, J. Boxerman, R. Huang, D. P. Barboriak, M. Weller, *et al.*, "Consensus recommendations for a standardized brain tumor imaging protocol for clinical trials in brain metastases," *Neuro-oncology*, vol. 22, pp. 757-772, 2020.
- [71] J. S. Lam, O. Shvarts, J. W. Said, A. J. Pantuck, D. B. Seligson, M. E. Aldridge, *et al.*, "Clinicopathologic and molecular correlations of necrosis in the primary tumor of patients with renal cell carcinoma," *Cancer*, vol. 103, pp. 2517-2525, 2005.

- [72] R. Jain, L. M. Poisson, D. Gutman, L. Scarpace, S. N. Hwang, C. A. Holder, *et al.*, "Outcome prediction in patients with glioblastoma by using imaging, clinical, and genomic biomarkers: focus on the nonenhancing component of the tumor," *Radiology*, vol. 272, pp. 484-493, 2014.
- [73] N. M. Dipu, S. A. Shohan, and K. Salam, "Deep learning based brain tumor detection and classification," in *2021 International conference on intelligent technologies (CONIT)*, 2021, pp. 1-6.
- [74] A. N. Khan, H. Nazarian, N. A. Golilarz, A. Addeh, J. P. Li, and G. A. Khan, "Brain tumor classification using efficient deep features of MRI scans and support vector machine," in *2020 17th International computer conference on wavelet active media technology and information processing (ICCWAMTIP)*, 2020, pp. 314-318.
- [75] S. Bauer, L.-P. Nolte, and M. Reyes, "Fully automatic segmentation of brain tumor images using support vector machine classification in combination with hierarchical conditional random field regularization," in *Medical Image Computing and Computer-Assisted Intervention—MICCAI 2011: 14th International Conference, Toronto, Canada, September 18-22, 2011, Proceedings, Part III 14*, 2011, pp. 354-361.
- [76] R. Rajagopal, "Glioma brain tumor detection and segmentation using weighting random forest classifier with optimized ant colony features," *International Journal of imaging systems and technology*, vol. 29, pp. 353-359, 2019.
- [77] C. K. Sohn and S. Bisdas, "Diagnostic accuracy of machine learning-based radiomics in grading gliomas: systematic review and meta-analysis," *Contrast Media & Molecular Imaging*, vol. 2020, pp. 1-12, 2020.
- [78] H. Mzoughi, I. Njeh, A. Wali, M. B. Slima, A. BenHamida, C. Mhiri, *et al.*, "Deep multi-scale 3D convolutional neural network (CNN) for MRI gliomas brain tumor classification," *Journal of Digital Imaging*, vol. 33, pp. 903-915, 2020.
- [79] D. N. Louis, A. Perry, G. Reifenberger, A. Von Deimling, D. Figarella-Branger, W. K. Cavenee, *et al.*, "The 2016 World Health Organization classification of tumors of the central nervous system: a summary," *Acta neuropathologica*, vol. 131, pp. 803-820, 2016.
- [80] A. Cruz-Roa, A. Basavanthally, F. González, H. Gilmore, M. Feldman, S. Ganesan. *et al.*, "Automatic detection of invasive ductal carcinoma in whole slide images with convolutional neural networks," in *Medical Imaging 2014: Digital Pathology*, 2014, p. 904103.

- [81] Z. Akkus, I. Ali, J. Sedlář, J. P. Agrawal, I. F. Parney, C. Giannini, *et al.*, "Predicting deletion of chromosomal arms 1p/19q in low-grade gliomas from MR images using machine intelligence," *Journal of digital imaging*, vol. 30, pp. 469-476, 2017.
- [82] C. Chen, X. Guo, J. Wang, W. Guo, X. Ma, and J. Xu, "The diagnostic value of radiomics-based machine learning in predicting the grade of meningiomas using conventional magnetic resonance imaging: a preliminary study," *Frontiers in Oncology*, vol. 9, p. 1338, 2019.
- [83] Q. U. Ain, I. Duaa, K. Haroon, F. Amin, and M. Z. ur Rehman, "MRI Based Glioma Detection and Classification into Low-grade and High-Grade Gliomas," in *2021 15th International Conference on Open Source Systems and Technologies (ICOSST)*, 2021, pp. 1-5.
- [84] S. Ahuja, B. Panigrahi, and T. Gandhi, "Transfer learning based brain tumor detection and segmentation using superpixel technique," in *2020 International Conference on Contemporary Computing and Applications (IC3A)*, 2020, pp. 244-249.
- [85] Y. W. Park, J. Oh, S. C. You, K. Han, S. S. Ahn, Y. S. Choi, *et al.*, "Radiomics and machine learning may accurately predict the grade and histological subtype in meningiomas using conventional and diffusion tensor imaging," *European radiology*, vol. 29, pp. 4068-4076, 2019.
- [86] M. Sollini, L. Antunovic, A. Chiti, and M. Kirienko, "Towards clinical application of image mining: a systematic review on artificial intelligence and radiomics," *European journal of nuclear medicine and molecular imaging*, vol. 46, pp. 2656-2672, 2019.
- [87] K. Kamnitsas, C. Ledig, V. F. Newcombe, J. P. Simpson, A. D. Kane, D. K. Menon, *et al.*, "Efficient multi-scale 3D CNN with fully connected CRF for accurate brain lesion segmentation," *Medical image analysis*, vol. 36, pp. 61-78, 2017.
- [88] S. Gull, S. Akbar, and I. A. Shoukat, "A deep transfer learning approach for automated detection of brain tumor through magnetic resonance imaging," in *2021 International Conference on Innovative Computing (ICIC)*, 2021, pp. 1-6.
- [89] V. Wasule and P. Sonar, "Classification of brain MRI using SVM and KNN classifier," in *2017 Third International Conference on Sensing, Signal Processing and Security (ICSSS)*, 2017, pp. 218-223.
- [90] R.-C. Chen, C. Dewi, S.-W. Huang, and R. E. Caraka, "Selecting critical features for data classification based on machine learning methods," *Journal of Big Data*, vol. 7, p. 52, 2020.
- [91] Y. Pan, W. Huang, Z. Lin, W. Zhu, J. Zhou, J. Wong, *et al.*, "Brain tumor grading based on neural networks and convolutional neural networks," in *2015 37th annual*

- international conference of the IEEE engineering in medicine and biology society (EMBC)*, 2015, pp. 699-702.
- [92] C. Chen, X. Ou, J. Wang, W. Guo, and X. Ma, "Radiomics-based machine learning in differentiation between glioblastoma and metastatic brain tumors," *Frontiers in oncology*, vol. 9, p. 806, 2019.
 - [93] O. Kouli, A. Hassane, D. Badran, T. Kouli, K. Hossain-Ibrahim, and J. D. Steele, "Automated brain tumor identification using magnetic resonance imaging: A systematic review and meta-analysis," *Neuro-oncology advances*, vol. 4, p. vda081, 2022.
 - [94] A. Rehman, S. Naz, M. I. Razzak, F. Akram, and M. Imran, "A deep learning-based framework for automatic brain tumors classification using transfer learning," *Circuits, Systems, and Signal Processing*, vol. 39, pp. 757-775, 2020.
 - [95] O. Fasihi Shirehjini, F. Babapour Mofrad, M. Shahmohammadi, and F. Karami, "Grading of gliomas using transfer learning on MRI images," *Magnetic Resonance Materials in Physics, Biology and Medicine*, vol. 36, pp. 43-53, 2023.
 - [96] Y.-q. Huang, C.-h. Liang, L. He, J. Tian, C.-s. Liang, X. Chen, *et al.*, "Development and validation of a radiomics nomogram for preoperative prediction of lymph node metastasis in colorectal cancer," *Journal of clinical oncology*, vol. 34, pp. 2157-2164, 2016.
 - [97] Z. Zhang, J. Xiao, S. Wu, F. Lv, J. Gong, L. Jiang, *et al.*, "Deep convolutional radiomic features on diffusion tensor images for classification of glioma grades," *Journal of Digital Imaging*, vol. 33, pp. 826-837, 2020.
 - [98] Y. Hayashi, "New unified insights on deep learning in radiological and pathological images: Beyond quantitative performances to qualitative interpretation," *Informatics in Medicine Unlocked*, vol. 19, p. 100329, 2020.
 - [99] M. M. Zahoor, S. A. Qureshi, S. Bibi, S. H. Khan, A. Khan, U. Ghafoor, *et al.*, "A new deep hybrid boosted and ensemble learning-based brain tumor analysis using MRI," *Sensors*, vol. 22, p. 2726, 2022.
 - [100] "Multimodal Brain Tumor Segmentation Challenge 2018," ed, 2018.
 - [101] M. B. T. S. Challenge, "BraTS," ed, 2020.
 - [102] S. Bagyaraj, R. Tamilselvi, P. B. Mohamed Gani, and D. Sabarinathan, "Brain tumour cell segmentation and detection using deep learning networks," *IET Image Processing*, vol. 15, pp. 2363-2371, 2021.
 - [103] S. J. Pan and Q. Yang, "A survey on transfer learning," *IEEE Transactions on knowledge and data engineering*, vol. 22, pp. 1345-1359, 2010.

-
- [104] T. Morita, J. Tsunoda, S. Inoue, and S. Chihara, "The Palliative Prognostic Index: a scoring system for survival prediction of terminally ill cancer patients," *Supportive care in cancer*, vol. 7, pp. 128-133, 1999.
 - [105] P. M. Shah, F. Ullah, D. Shah, A. Gani, C. Maple, Y. Wang, *et al.*, "Deep GRU-CNN model for COVID-19 detection from chest X-rays data," *Ieee Access*, vol. 10, pp. 35094-35105, 2021.
 - [106] H. Dong, G. Yang, F. Liu, Y. Mo, and Y. Guo, "Automatic brain tumor detection and segmentation using U-Net based fully convolutional networks," in *Medical Image Understanding and Analysis: 21st Annual Conference, MIUA 2017, Edinburgh, UK, July 11–13, 2017, Proceedings 21*, 2017, pp. 506-517.
 - [107] F. Ullah, A. Salam, M. Abrar, and F. Amin, "Brain Tumor Segmentation Using a Patch-Based Convolutional Neural Network: A Big Data Analysis Approach," *Mathematics*, vol. 11, p. 1635, 2023.
 - [108] M. De Bruijne, "Machine learning approaches in medical image analysis: From detection to diagnosis," vol. 33, ed: Elsevier, 2016, pp. 94-97.
 - [109] M. Zoli, V. E. Staartjes, F. Guaraldi, F. Friso, A. Rustici, S. Asioli, *et al.*, "Machine learning-based prediction of outcomes of the endoscopic endonasal approach in Cushing disease: is the future coming?," *Neurosurgical focus*, vol. 48, p. E5, 2020.
 - [110] M. W. Nadeem, M. A. A. Ghamdi, M. Hussain, M. A. Khan, K. M. Khan, S. H. Almotiri, *et al.*, "Brain tumor analysis empowered with deep learning: A review, taxonomy, and future challenges," *Brain sciences*, vol. 10, p. 118, 2020.
 - [111] L. G. K. T. B. BE, "Setio AAA Ciompi F Ghafoorian M van der Laak JA van Ginneken B Sánchez CI A survey on deep learning in medical image analysis," *Med Image Anal*, vol. 42, p. 60, 2017.
 - [112] B. Shen, W. Hou, Z. Jiang, H. Li, A. J. Singer, M. Hoshmand-Kochi, *et al.*, "Longitudinal Chest X-ray Scores and their Relations with Clinical Variables and Outcomes in COVID-19 Patients," *Diagnostics*, vol. 13, p. 1107, 2023.
 - [113] "Multimodal Brain Tumor Segmentation Challenge," ed, 2018.
 - [114] S. M. Smith, M. Jenkinson, M. W. Woolrich, C. F. Beckmann, T. E. Behrens, H. Johansen-Berg, *et al.*, "Advances in functional and structural MR image analysis and implementation as FSL," *Neuroimage*, vol. 23, pp. S208-S219, 2004.
 - [115] G. Zeng, X. Yang, J. Li, L. Yu, P.-A. Heng, and G. Zheng, "3D U-net with multi-level deep supervision: fully automatic segmentation of proximal femur in 3D MR images," in *Machine Learning in Medical Imaging: 8th International Workshop, MLMI 2017*,

Held in Conjunction with MICCAI 2017, Quebec City, QC, Canada, September 10, 2017, Proceedings 8, 2017, pp. 274-282.

- [116] B. B. Avants, N. Tustison, and G. Song, "Advanced normalization tools (ANTS)," *Insight j*, vol. 2, pp. 1-35, 2009.

